NTNU

Norwegian University of
Science and Technology

# Power Production from Low Temperature Heat Sources

**Michael Pfaff**

Master of Science in Energy and Environment
Submission date: October 2010
Supervisor: Trygve Magne Eikevik, EPT

Norwegian University of Science and Technology
Department of Energy and Process Engineering

# Problem Description

Background and objective. Sintef Energy Research As is involved in a KMB project 162617/i40 Resource Optimization and recovery in the MAterials industry.

We are involved in the Energy Recovery part of this project. A new technology for power production from low to medium temperature heat sources will be developed. Application to power production from exhaust of electrolysis cells in the aluminium industry will be investigated. This technology will be based on the use of CO2 as a working fluid. CO2 is non flammable non toxic and is environmental friendly. Preliminary calculations showed an important potential for performance improvement compared to existing technologies.

A prototype was built in our laboratory early in 2009. The student will perform experimental investigations. Results will be analysed and improvements should be foud for the test facility. Simulations (Pro/II) should be performend in order to establish optimizations. The following questions should be considered in the project work:

1. Literature power production from low temperature heat sources

2. Perform experimental investigations

3. Summary of the experimental results

4. Build power production cycle model with Pro/II to find improvements

5. Compare experimental results

6. Summary, draft version of a scientific paper

Assignment given: 01. March 2010
Supervisor: Trygve Magne Eikevik, EPT

EPT-M-2010-83

**MASTER THESIS**

for
Michael Pfaff
Spring 2010

***Power production from low temperature heat sources***

**Background and objective**

In the process industry and in particularly in aluminium production, large amount of waste heat is produced. Conversion of this heat to electrical power is a very attractive alternative for energy recovery.

SINTEF is developing a new technology for power production from low temperature heat sources, for example the gas coming out of electrolysis cell for aluminium production. This technology is based on $CO_2$ as working fluid. $CO_2$ is environment friendly, non toxic, non flammable and has a potential for high efficiency power generation.

A test rig has been built in the laboratory in order to test different control strategies. The student will run experiments investigating systematically effect of various parameters. Results will be compared with a Modelica based model that the student will develop with the help of our partners at Braunschweig University. This Master Thesis is financed by the project 182617/i40 Resource Optimization and Recovery in the Material industry, where the main metal producers in Norway participate.

**The following questions should be considered in the work:**

1. Literature power production from low temperature heat sources
2. Establish a systematic plan for the experimental investigation
3. Perform experimental investigations
4. Summary of the experimental results
5. Build power production cycle model with Modelica
6. Compare experimental and simulation results
7. Summary, draft version of a scientific paper
8. Further work

Within 14 days of receiving the written text on the diploma thesis, the candidate shall submit a research plan for his project to the department.

When the thesis is evaluated, emphasis is put on processing of the results, and that they are presented in tabular and/or graphic form in a clear manner, and that they are analyzed carefully.

The thesis should be formulated as a research report with summary both in English and Norwegian, conclusion, literature references, table of contents etc. During the preparation of the text, the candidate should make an effort to produce a well-structured and easily readable reportreport. In order to ease the evaluation of the thesis, it is important that the cross-references are correct. In the making of the report, strong emphasis should be placed on both a thorough discussion of the results and an orderly presentation.

The candidate is requested to initiate and keep close contact with his/her academic supervisor(s) throughout the working period. The candidate must follow the rules and regulations of NTNU as well as passive directions given by the Department of Energy and Process Engineering.

Pursuant to "Regulations concerning the supplementary provisions to the technology study program/Master of Science" at NTNU §20, the Department reserves the permission to utilize all the results and data for teaching and research purposes as well as in future publications.

One – 1 complete original of the thesis shall be submitted to the authority that handed out the set subject. (A short summary including the author's name and the title of the thesis should also be submitted, for use as reference in journals (max. 1 page with double spacing)). Two – 2 – copies of the thesis shall be submitted to the Department. Upon request, additional copies shall be submitted directly to research advisors/companies. A CD-ROM (Word format or corresponding) containing the thesis, and including the short summary, must also be submitted to the Department of Energy and Process Engineering

The main report from the work shall be submitted to the Department of Energy and Process Engineering within 30th June 2010.

Department of Energy and Process Engineering, 26. February 2010

Olav Bolland
Departmant Head

Tryve M. Eikevik
Academic Supervisor

Research Advisors: Yves Ladam (SINTEF)
Trond Andersen (SINTEF)

## Task variation

The delivering date was changed from $30^{th}$ June 2010 to the $30^{th}$ September 2010. The reason for this decision was that main device (the expander), it was not running for 3 weeks. The expander was removed and send to Austria to the producer Obrist for repairing it.

The used software was changed from Modelica to Pro/II for the simulations. The reason for this decision was there should be found some improvements for devivces at the test facility. For this task the software Pro/II was better qualified to perform this simulations.

## Declaration

I hereby declare that this submission is my own work and that, to the best of my knowledge and belief, it contains no material previously published or written by another person nor material which to a substantial extent has been accepted for the award of any other degree or diploma of the university or other institute of higher learning, except where due acknowledgment has been made in the text.

Trondheim $30^{th}$ September 2010

Signature

## Problem Description

Background and objective. Sintef Energy Research As is involved in a KMB project 162617/i40 Resource Optimization and recovery in the MAterials industry.

We are involved in the Energy Recovery part of this project. A new technology for power production from low to medium temperature heat sources will be developed. Application to power production from exhaust of electrolysis cells in the aluminium industry will be investigated. This technology will be based on the use of $CO_2$ as a working fluid. $CO_2$ is non flammable non toxic and is environmental friendly. Preliminary calculations showed an important potential for performance improvement compared to existing technologies.

A prototype was built in our laboratory early in 2009. The student will perform experimental investigations. Results will be analysed and improvements should be foud for the test facility. Simulations (Pro/II) should be performend in order to establish improvements. The following questions should be considered in the project work:

1. Literature power production from low temperature heat sources
2. Perform experimental investigations
3. Summary of the experimental results
4. Build power production cycle model with Pro/II to find optimizations
5. Compare experimental results
6. Summary, draft version of a scientific paper

# Preface

This Master's Thesis report is result of Michael Pfaff's work at the Norwegian University of Science and Technology, Faculty of Engineering Science and Technology, Department of Energy and Process Engineering, spring 2010. The subject of the thesis was decided in cooperation with SINTEF Energy Research and is a part of the KMB project Resource Optimization and recovery in the MAterials industry (ROMA).

The work done in my Master thesis has been a combination of practical work in the laboratory, calculations and simulations for optimizations of the prototype rig. This project has greatly increased my interest and motivation within the field of themodynamic and energy utilization. I feel that my knowledge have been tested thoroughly by the different tasks given in the work with this thesis.

In my work with the thesis I've had a lot of helpful guidance and assistance. For this I would like to thank my research advisor Yves Ladam for the fine combination of giving helpful advices and challenging my knowledge. I would like to thank Reidar Tellebon and Gunnar Lohse for the help in the laboratory. Also, I would like to thank the NTNU and Sintef Energy Research for giving me the great opportunity of studing this year in Norway in the fantastic city of Trondheim.

Special thanks go to my family and friends.

Michael Pfaff

Summer 2010

## Summary

This Master Thesis is a conclusion on work done as part of the Resource Optimization and recovery in the Materials industry project (Roma). This project is involved in the development of a new technology for power production from low temperature heat sources for off gases from aluminum production cells. The technology is based on an transcritical Rankine cycle with $CO_2$ as a working fluid, as the work recovery circuit. The center of the test facility is the expander, a prototype provided by Obrist Engineering . 81 tests were perfomed to investigate the behavoir of the expander cycle. Effect of three main parameters were investigated:

- Effect $CO_2$ massflow rate
- Effect of heat source temperature
- Effect of $CO_2$ condensation pressure

For each parameter combination, the high pressure side of the expander cycle was varied in order to find the maximum power output.

This study clearly showed limitation of the turbine which cannot maintain large pressure difference probably due to large internal leakages. As a result, turbine outlet is highly superheated. This superheat is lost energy for the power cycle, and is simply dumped into the heat sink. One possible improvement would be to include a recuperator that recovers superheat after the pump.

The results also indicate that the fan of the air loop is too small: increasing the $CO_2$ flow rate to limit superheat at turbine outlet leads to turbine inlet temperature reduction.

Last, for large $CO_2$ mass flow rate (3.5 $\frac{kg}{min}$) which is required for proper operation of the turbine, the power generated is too large for the generator installed on the loop. Its temperature reached 120 °C for some conditions. A new solution should be seeked.

Based on experimental results, a mode of the power cycle was implemented in Pro/II and simulations were run in order to find an improved design. The main goal is to be able to run the cycle at high $CO_2$ mass flow rate: 3.5 $\frac{kg}{min}$. It was found that the air loop fan should be able to deliver up to 1 260 $\frac{m^3}{h}$. The new generator or braking system should be able to absorb up to 297 W.

## Summary

Denne master avhandling oppsummerer arbeidet utført som en del av prosjektet Resource Optimization and recovery in the Materials industry (Roma). Dette prosjekt går på utvikling av ny teknologi for kraft produskjon fra lav temperature spilvarme tilgjengelig i rå gasen fra aluminium produksjon celler. Teknologien er basert på transkritisk Rankine syklus med $CO_2$ som arbeidsmedium. Hoved komponent i transkritisk syklus i kretsen er den turbine, en prototype levert av Obrist Engineering.

81 forsøk var kjørt for å undersøke denne kraft produksjon syklus. Effekt av tre hoved parameter har vært undersøkt:

- Effekt av $CO_2$ masse strøm
- Effekt av varme kilde temperatur
- Effekt av $CO_2$ kondensering temperatur For hver parameter, flere forsøk med forskjellige høy trykk side av $CO_2$ kretsen var kjørt for å finne maksimum kraft produksjon.

Denne undersøkelse viser noe begrensninger for turbinen som ikke kan holde stor trykk forskjell, antagligvis på grunn av interne lekasjer. Konsekvens av det er att utløpet av turbinen er som regel overhetet. Denne overheting er ren tapt av energi for syklusen, varmen dumpes i varme sluk. En mulig forbedring ville være å bruke en rekuperator for å gjenvinne overheting etter pumpen.

Resultater viser også att viften til varm luft sløyfa er for liten: nor $CO_2$ masse strøm er økt for å begrenser overheting ved turbinen utløpet, innløp temperatur blir lavere.

Sist, for stor $CO_2$ massestrøm (3.5 kg/min) som er nødvendig for optimal drift av turbinen, for mye kraft er produsert for generatoren installert i kretsen. Temperatur til generator har vært målt helt opp til 120 °C. En ny løsning må finnes.

Basert på eksperimentelle data, en modell av kraft produksjon syklus var implementert i Pro/II, og simuleringer var kjørt for å finne ett forbedret design. Hoved mål er å kunne kjører forsøk med høyre $CO_2$ massestrøm:3.5 kg/min. det er beregnet att viften burde kunne levere opp til 1 260 $\frac{m^3}{h}$. den nye generator eller bremse system skal kunne absorbere opp til 297 W.

# Contents

# List of Figures

# List of Tables

# Nomenclature

## Abbrevoiations

| Symbol | Description |
|---|---|
| Al | Aluminium |
| $Al_2O_3$ | Aluminium Oxide |
| C | Carbon |
| C | Condenser |
| CO | Carbon monoxide |
| $CO_2$ | Carbon dioxide |
| CP | Condensate pump |
| CSV | Control and stop valve |
| CT | Cooling tower |
| CWP | Cooling water pump |
| DAQ | Data acquisation |
| DC | Direct current |
| E | Evaporator |
| e | Electron |
| G | Generator |
| $H_2$ | Hydrogen |
| $H_2O$ | Water |
| $H_2O$-$NH_3$ | Water-ammonia mixture |
| He | Helium |
| HX | Heat exchanger |
| IW | Injection well |
| M | Makeup water supply |
| N | Number |
| $Na_3AlF_6$ | Aluminium Cryolite |
| $NH_3$ | Ammonia |
| ORC | Organic Rankine Cycle |
| p | Pump |
| PH | Preheater |

| Symbol | Description |
|---|---|
| PW | Production well |
| R134a | Refrigerant, Tetrafluorethane |
| R744 | Refrigerant, Carbon Dioxide |
| Rec | Recaiver |
| Roma | Resource Optimization and recovery in the Material industry |
| RPH | Recuperative preheater |
| S | Seperator |
| T | Turbine |
| TV | Throttle valve |

## Latin letters

| Symbol | Description | Unit |
|---|---|---|
| h | Entrophy | $\frac{kJ}{kg}$ |
| $h_{exp\,inlet}$ | Entrophy at the expander inlet | $\frac{kJ}{kg}$ |
| $h_{exp\,outlet}$ | Entrophy at the expander outlet | $\frac{kJ}{kg}$ |
| $h_{pump\,inlet}$ | Entrophy at the plunger pump inlet | $\frac{kJ}{kg}$ |
| $h_{pump\,outlet}$ | Entrophy at the plunger pump outlet | $\frac{kJ}{kg}$ |
| I | Current | kA |
| $M_{exp\,tourque}$ | Driving force of the expander | Nm |
| $\dot{m}_{air\,loop}$ | Massflow of air in the air loop | $\frac{kg}{min}$ |
| $\dot{m}_{CO_2}$ | Massflow of $CO_2$ | $\frac{kg}{min}$ |
| P | Pressure | bar |
| $P_{exp\,inlet}$ | Pressure at the inlet of the expander | bar |
| $P_{exp\,outlet}$ | Pressure at the outlet of the expander | bar |
| $P_{exp\,output}$ | Isentropic work output of the expander | W |
| $P_{exp}$ | Work output of the expander | W |
| $P_{HX-2\,inlet}$ | Pressure at the heat exchager 2 inlet | bar |
| $P_{HX-2\,outlet}$ | Pressure at the heat exchager 2 outlet | bar |
| $P_{pump}$ | Work input plunger pump | W |
| $P_{pump\,inlet}$ | Pressure at the plunger pump inlet | bar |
| $P_{pump\,outet}$ | Pressure at the plunger pump outlet | bar |
| $Q_H$ | Heat addition from a heat source | W |
| $Q_{in}$ | Heat input from a heat source | W |
| $Q_L$ | Heat rejection to a heat sink | W |
| $Q_{out}$ | Heat output to a heat sink | W |
| $\dot{q}$ | Heat flow density | $\frac{W}{m^2}$ |
| $\dot{q}_{in}$ | Heat flow density referring to a high temperarture reservoir | $\frac{W}{m^2}$ |
| $\dot{q}_{out}$ | Heat flow density referring to a low temperarture reservoir | $\frac{W}{m^2}$ |
| rpm | Rotations per minute | $\frac{1}{min}$ |
| $rpm_{exp}$ | Rotations per minute of the expander | $\frac{1}{min}$ |
| s | Entropy | $\frac{kJ}{kg \cdot K}$ |
| $s_{exp\,inlet}$ | Entropy at the expander inlet | $\frac{kJ}{kg \cdot K}$ |
| $s_{exp\,outlet}$ | Entropy at the expander outlet | $\frac{kJ}{kg \cdot K}$ |
| $s_{pump\,inlet}$ | Entropy at the plunger pump inlet | $\frac{kJ}{kg \cdot K}$ |

| Symbol | Description | Unit |
|---|---|---|
| $s_{pump\,inlet}$ | Entropy at the plunger pump inlet | $\frac{kJ}{kg \cdot K}$ |
| $s_{pump\,outlet}$ | Entropy at the plunger pump outlet | $\frac{kJ}{kg \cdot K}$ |
| T | Absolute temperature | K |
| $T_H$ | Absolute temperature heat source | K |
| $T_L$ | Absolute temperature heat sink | K |
| T | Absolute temperature | K |
| t | temperature | °C |
| $t_{exp\,inlet}$ | temperature at the expander inlet | °C |
| $t_{exp\,outlet}$ | temperature at the expander outlet | °C |
| $t_{HX-2\,inlet}$ | temperature at the heat exchanger 2 inlet | °C |
| $t_{HX-2\,outlet}$ | temperature at the heat exchanger 2 outlet | °C |
| $t_{pump\,inlet}$ | temperature at the expander inlet | °C |
| $t_{pump\,outlet}$ | temperature at the expander outlet | °C |
| U | Voltage | V |
| UA | Heat transfer coeffcient times area | $\frac{kW}{K}$ |
| v | Specific volume | $\frac{m^3}{kg}$ |
| $W_{net}$ | Work output | W |
| $W_{shaft,in}$ | Mechanical work input at the shaft | W |
| $W_{shaft,out}$ | Mechanical work output at the shaft | W |
| $\overline{X}$ | Arithmetic average | |

## Greek letters

| Symbol | Description |
|---|---|
| $\eta_{th}$ | Theoretic efficiency |
| $\eta_{cycle}$ | Theoretic efficiency of the cycle |
| $\eta_{exp}$ | Theoretic efficiency of the expander |
| $\eta_{pump}$ | Isentropic efficiency of the plunger pump |
| $\Pi_{press\,ratio\,exp}$ | Pressure ratio expander |
| $\Pi_{press\,ratio\,pump}$ | Pressure ratio plunger pump |

# 1 Background

The background of the ROMA (Resource Optimization and recovery in the MAterials industry) project is the energy utilization of waste heat from the production of aluminum. The project is financed by the companies Hydro Aluminium, Elkem / Alcoa and Søral, wich are active in the aluminium production. The following section gives a short resume of the production process of aluminum and the source of waste heat from the aluminum production process.

## 1.1 The aluminium production process

The main theory from the aluminium production is taken from Kammer [1] unless otherwise noted and translated.

The extraction from aluminium is realised by the HALL-HEROULT process, invented in 1886. An aluminium production plant needs in average 13-14 kWh electrical energy per kg aluminium. Figure 1.1 shows a schematic from of an aluminium electrolytic cell. Single electrolysis cells are arranged in series. Aluminium oxide ($Al_2O_3$) has a very high melting point temperature of 2050 °C. When aluminium oxide is mixed with molten cryolite the new melting temperature of this aluminium cryolite ($Na_3AlF_6$) is at the eutectic point at 962.5 °C (with 10.5 % $Al_2O_3$ content in the aluminium production cell). Due to the fact that the aluminium oxide is soluble in the cryolite the electrolysis is actable between 950 °C and 980 °C. The content of aluminium oxide during the process is between 2 % and 5 %.

The Aluminium oxide electrolysis is realised with carbon electrodes. The so generated oxygen is oxidised to carbon dioxide ($CO_2$) and carbon monoxide (CO). These reactions can be described as:

$$2Al_2O_3 + 3C \longrightarrow 4AL + 3CO_2 \tag{1.1}$$

$$Al_2O_3 + 3C \longrightarrow 2Al + 3CO \tag{1.2}$$

The following two main reactions are running at the electrodes:

- Aluminium $2Al^{3+} + 6e^{-} \rightarrow 2Al$ is discharged at the cathode.
- The oxygen ions which are flowing to the anode reacting there to $CO_2$ and CO. The anode is expended from this reaction.

The carbon cathode includes the iron cathode bars and it is at the same time the collecting pan for the molten aluminium, pictured in figure 1.1. The current (I) that flows to the cathodes is between I = 100 kA and 280 kA, with a voltage (U) at circa U = 4.2 V. Some of the electrical energy, which flows to the collection pan, is transferred to heat because of the electrical resistance of the molten aluminium. But, this thermal energy is necessary to fuse the aluminium oxide, and to keep the aluminium and also the flux molten. The $Al_2O_3$ is collected into the alumina hopper pictured in figure 1.1 and is flowing from there to the frozen flux and alumina. The crust breaker is necessary to break the crust from the flux to provide a flow way for the aluminium oxide to the molten flux.

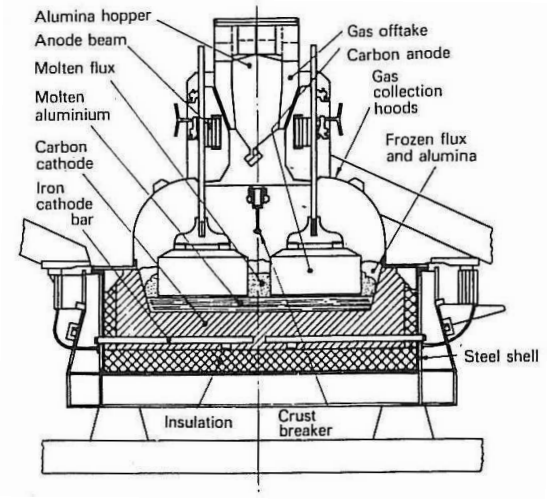


Figure 1.1: Multi-anode electrolytic cell for extracting aluminium from alumina [2]

## 1.2 The offgas of the aluminium production

The collection from the offgas which includes the waste heat for the power production cycle is realized by the gas offtake direct inside the capsuled electrolytic cell pictured in figure 1.1. The single aluminuim production cells are arranged in series. A typical aluminium production plant consists of 400 single aluminium production cells, but there existing plants with up to 1 000 aluminium production cells. The offgas of the single electrolysis

cells is collected into a central offgas collection. The typical offgas temperature of one cell is 120 °C, but in the central offgas collection system the typical offgas temperature is circa 100 °C. The typical offgas massflow rate out of one single cell is 2 $\frac{kg}{s}$.

# 2 Power production from waste heat - State of the art

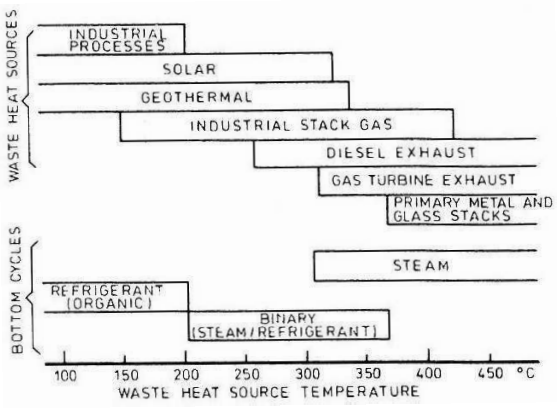


Figure 2.1: Waste heat sources [9]

It is certain that the fossil energy fuels are finite or only producible with a lot more effort and financial costs in the future. The energy wasted in boiler stacks, engine exhausts, cooling towers and other waste exhaust streams can be recovered. The power production from waste heat is a very important topic to utilize more of the energy from the power potential of present available fossil fuels.

There exist a set of technologies to produce electricity from waste heat sources today (figure 2.1). This chapter presents some of the relevant technologies that are available to utilize efficient waste heat potentials from different processes.

## 2.1 The ideal power cycle and its fundamental constraints

The main theory on the Carnot cycle is taken from Chen and Elliot [11] and Hsieh [12] unless otherwise noted.

To be able to compare the usefulness of the different processes to each other, a reference process is needed. When considering a thermodynamic process where work is extracted from heat transferred from a heat source ($T_H$) to a heat sink ($T_L$), the Carnot cycle is a much-used ideal.

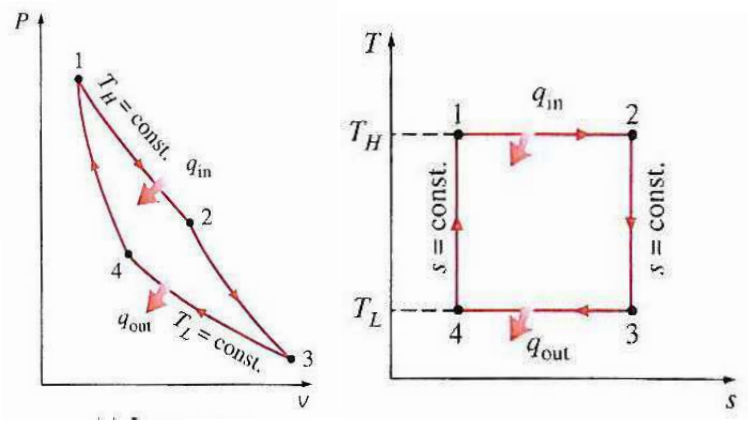


Figure 2.2: The P-v and T-s diagram of the Carnot cycle [10]

This cycle has two isothermal state changes for heat addition and heat rejection to the environment. The other two changes in state are adiabatic and reversible therefore isentropic. So the process is a reversible process shown in (figure 2.2):

- Process step 1-2 is an isothermal expansion at $T_H$, absorbing a quantity of heat ($q_{in}$) from the high energy reservoir.
- Process step 2-3 is an isentropic expansion, lowering temperature from $T_H$ to $T_L$.
- Process step 3-4 is an isothermal compression at $T_L$ rejecting a quantity of heat ($q_{out}$) to the low temperature energy reservoir.
- Process step 4-1 is an isentropic compression, raising temperature from $T_L$ to $T_H$.

Because the process is reversible, the maximum thermal efficiency for a Carnot cycle can be defined strictly by heat source ($T_H$) and heat sink ($T_L$):

Equation :

$$\eta_{th} = 1 - \frac{T_L}{T_H} \tag{2.1}$$

The Carnot cycle is depicted in figure 2.2.

Practical attempts to attain the Carnot cycle in reality failed, predominantly because of finite temperatures differences during the heat transfer processes and fluid friction during the work-transfer processes. As a result, the Carnot cycle has no counterpart in actual practice, but it is often used to compare the efficiency of other cycles with the efficiency of the Carnot cycle (figure 2.1).

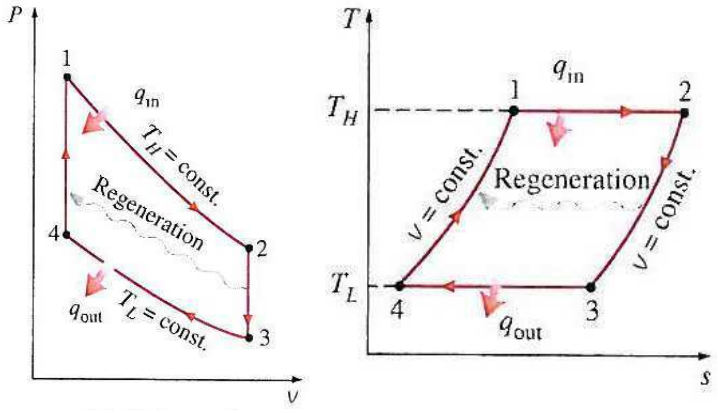


Figure 2.3: The P-v and T-s diagram of the Stirling cycle [10]

## 2.2 Stirling cycle

Another reversible cycle is the ideal Stirling cycle. This Stirling engine consists of a cylinder with two pistons, one piston at each side of the cylinder and a regenerator in the middle. The four working positions of the pistons are illustrated in figure 2.4 and also in the P-v and T-s diagrams in figure 2.3.

- Process step 1-2 is an absolute reversible isothermal expansion at $T_H$, absorbing a quantity of heat ($q_{in}$) from the heat source.
- Process step 2-3 is an absolute reversible heat rejection at constant volume, lowering temperature from $T_H$ to $T_L$.
- Process step 3-4 is an absolute reversible isothermal compression at $T_L$ rejecting a quantity of heat ($q_{out}$) to the low temperature energy reservoir.
- Process step 4-1 is an absolute reversible heat addition at constant volume, raising temperature from $T_L$ to $T_H$.

The thermal efficiencies have been found to be low, but the Stirling engine has potential as an external combustion device. Its capability of using low-grade fuels or external heat sources, keeps the reseach going [24].

The Stirling engine fills a niche for quiet, small engines capable of operating with a wide variety of fuels. Typically, light gases (hydrogen ($H_2$) and helium (He) [3]) are used as working fluid in Stirling engines, but nitrogen or air [21] is possible, too. The Stirling engine is a closed external engine, this avoid contaminations of the working fluid.

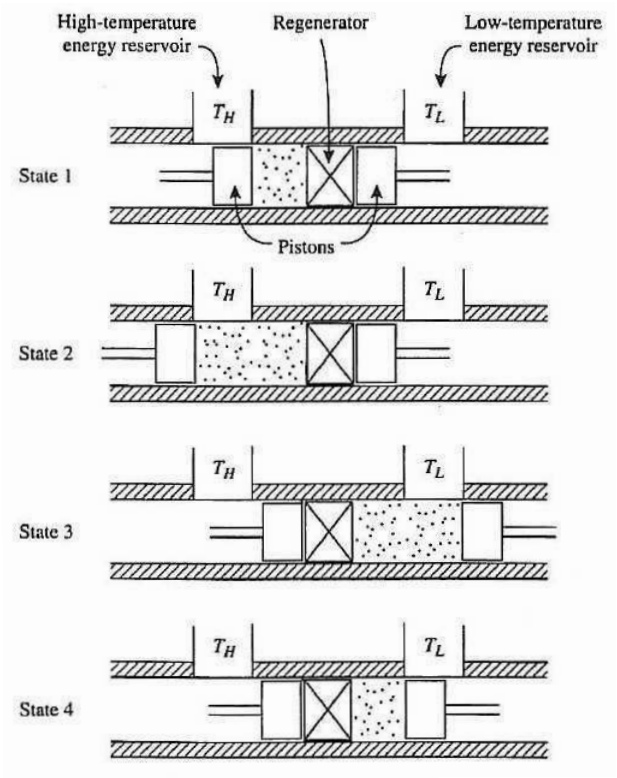


Figure 2.4: The working positions of the pistons at the four states of the Stirling cycle [12]

There exists Stirling engine applications in solar power plants where high temperature is available [4]. But there were also investigations from Chen for low temperature applications (max. working gas temperature 100 °C) with using a solar Stirling engine [21].

There have been also research projects on Stirling engines for applications using the waste heat potential from low-grade exhaust gases from natural-gas heating systems and with bio-fuel fired heating systems for electrical power production [22]. After Kongtragool [5] the key to success of the Stirling engine for low temperature applications are, new materials and good heat transfer to the working fluid.

## 2.3 Brayton cycle

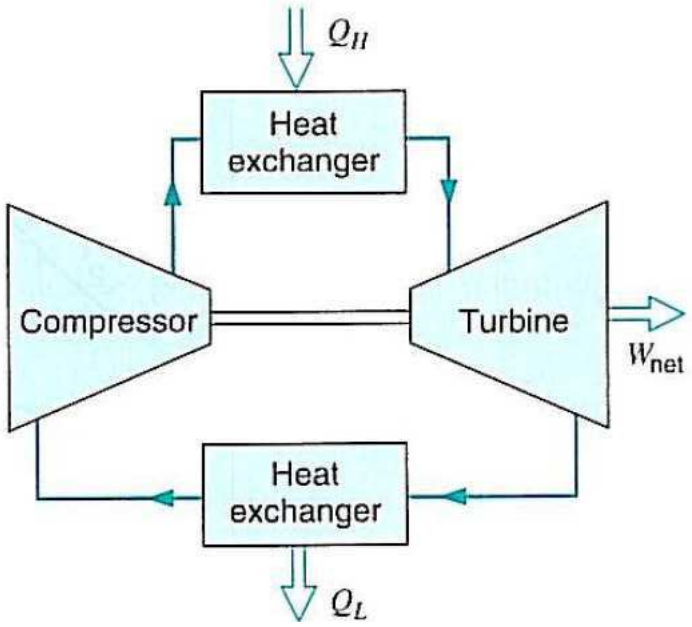


Figure 2.5: The closed Brayton cycle [14]

The Brayton cycle is also known as the closed Joule cycle and consists of the four following process steps:

- Process step 1-2 is an isentropic compression in a compressor.
- Process step 2-3 is an isobar heat addition ($Q_H$) in a heat exchanger.
- Process step 3-4 is an isentropic expansion in a turbine with work output ($W_{net}$) at the shaft.
- Process step 4-1 is an isobar heat rejection ($Q_L$) in a heat exchanger.

The working fluid of the Brayton cycle is a single-phase gas without condensing.

With the advent of nuclear reactors, the closed-cycle gas turbine has become more important. Heat is transferred, either directly or via a second fluid, from the fuel in the nuclear reactor to the working fluid in the gas turbine. Heat is rejected from the working fluid in the gas turbine to the surroundings [14].

There were investigations for using a supercritical $CO_2$ Brayton cycle from Moisseytsev and Sienicki [15] in combination with an intermediate sodium loop in atomic power plants. But there was used a high source temperature of 488 °C.

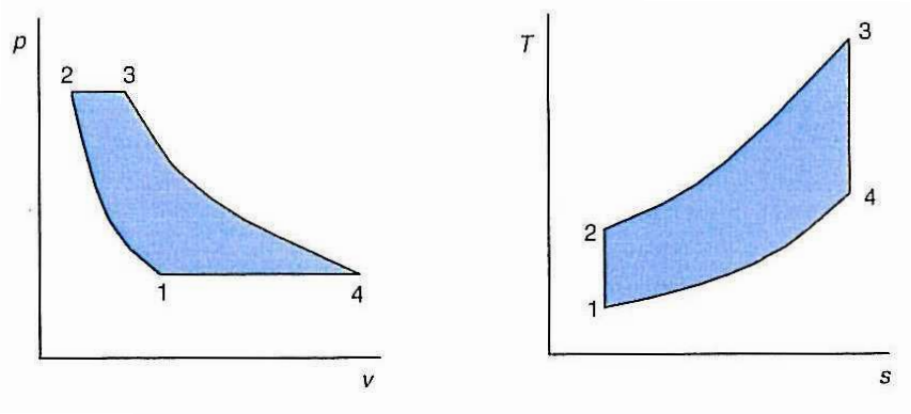


Figure 2.6: The P-v and T-s diagram for the Brayton cycle [13]

As topping cycle in a combination with ambient pressure gas turbine, Xue, Wei and Zhongyue [16] have found potential for using the Brayton cycle for a utilization of exhaust gases.

## 2.4 Water vapour Rankine cycle

The water vapour Rankine cycle is a thermodynamic cycle where water is used as working fluid. The cycle consists of four process steps (1 - 4). Water enters the pump at step 1 as saturated liquid and is compressed to the operating pressure of the steam generator at step 2. At the steam generator all of the liquid is evaporated by a heat source ($Q_{in}$) between step 2 and 3. The steam leaves the vapour generator as superheated vapour at step 3. The superheated vapour at state 3 enters the turbine, where it expands is transfered to mechanical work ($W_{shaft\,out}$) by rotating the shaft connected to an electrical generator. The temperature and pressure of the steam drop during this process to the values at step 4. In these conditions of step 4 (usually as a saturated liquid-vapour mixture) the working fluid enters the condenser. Inside the condenser the working fluid is condensed to liquid by using a cooling fluid. The working fluid is leaving the condenser in conditions of step 1 and flows back to the pump.

The T-s diagram of the Rankine cycle in figure 2.7 show, additional process steps 3' and 4' of a Rankine cycle using superheated steam at the turbine inlet in conditions of step 3'. The superheated steam leaves the expansion process in the prime mover (turbine) in conditions showm in step 4'.

The steam Rankine cycle is best suited for recovery of high-grade waste heat. This is due to the condensing temperature at ambient pressure being 100 ° C and the need for

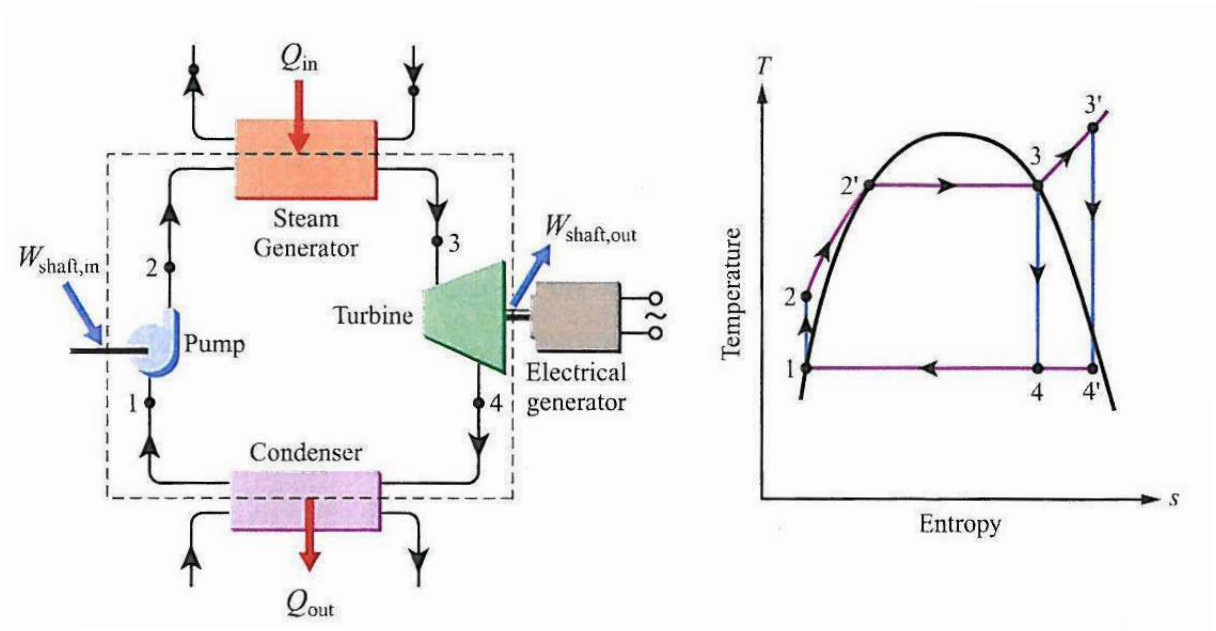


Figure 2.7: Components associated with a simple Rankine cycle and the corresponding T-s diagram for the cycle steps 1-2-3-4-1. The diagram also show Rankine cycle steps with superheated steam: 1-2-3'-4'-1. [3]

superheat of the gas in order to avoid a wet expansion through the expander.

The disadvantage of water as working fluid in a Rankine cycle recovering heat sources below 370 °C is that water is so wet, which means the slope of saturated gas line in the T-s diagram is minus, so a great superheat is needed to avoid a wet process inside the turbine [23]. Another disadvantage of water as working fluid in a Rankine cycle for low temperature heat source is the latent heat. High latent heat means a long evaporating process in the evaporator, which results in large temperature difference between the two sides of the heat exchanger [23]. The temperature of water evaporating inside the evaporator is for some time unchanged (at the two phase area in the T-s diagram) while the temperature of the heat source changes.

## 2.5 Organic Rankine cycle

The Organic Rankine Cycle (ORC) is based upon the water vapour Rankine cycle. The ORC process follows the same four process steps, but the main difference is the used working fluid.

If it is waste heat that has to be converted into mechanical work that is yielding most benefit, the Rankine cycle is most suitable. At lower temperatures, smaller than 400 °C, not the known Rankine-process with water is the most favourable one that is realised in steam power plants, but a similar process with an organic working medium, e.g. a refrigerant (fluorine hydrocarbon) or another hydrocarbon. This ORC shows a higher efficiency at the same low maximum temperature than the Rankine process with water [17].

The ORC has advantages in recovering low-grade heat, such as high efficiency and a one stage turbine (as the reason of low enthalpy drops at the turbine). Thus ORC can be economically feasible when the system is well designed. ORC systems are used in industrial waste heat recovery plants, geothermal plants and solar thermal systems [23]. Preliminary design suggestions for waste heat of industrial processes and combustion engines have been given by Larjola [6].

## 2.6 The $CO_2$ trans-critical Rankine cycle

The trans-critical Rankine cycle with $CO_2$ as working fluid is a variation from the basic Rankine cycle with water as working fluid described in section 2.4. The main difference is the used working fluid $CO_2$, which has a low critical temperature of 31.1 °C and a critical pressure of 73.3 bar. These thermodynamic characteristics can be expedient for low temperature applications in a Rankine cycle. The cycle consists of the same components like the water vapour Rankine cycle.

The $CO_2$ is in subcooled conditions at the pump inlet, because the pressure at room temperature is in a range of circa 60 bar. The $CO_2$ leaves the pump at a pressure level higher then the critical pressure and than enters the evaporator. There, the $CO_2$ is absorbing heat from an external heat source (e.g. waste heat). At the outlet of the heat exchanger is the $CO_2$ in the highest temperature and pressure conditions during the process. After this heat addition the working fluid flows to the expander, where power from the high pressure is transferred to mechanical work. With a pressure drop the $CO_2$ leaves the expander and flows to the condenser, where it is cooled down to subcooled conditions again.

For power production from low temperature heat sources the main advantage from $CO_2$ is pictured in figure 2.8, which compares the temperature enthalpy profile of $CO_2$ with the temperature enthalpy profile of the refrigerant R134a. The blue line illustrates the temperature and entropy characteristics on the flow-way of these two working fluids inside the heat exchanger cooled by the heat sink. The figure 2.8 shows also the temperature and enthalpy trend from the heat source (red line). This illustration shows the possible benefit of using $CO_2$ for low temperature heat sources, because the temperature difference is very small everywhere in the heat exchanger. There is no phase changing of the working fluid during the complete heat exchanging. Also the pinch point is close to the end at the heat exchanger, with $CO_2$ as working fluid.

Heat transfer with this dense $CO_2$ gas is beneficial and volumetric efficiency high, thus avoiding large heat exchanger volumes characterizing usual gas processes. In the vicinity of the critical region the heat transfer is actually better than for the most boiling fluids. The density of the gas at the exit of the turbine (at condensation pressure) is rather large, allowing for the development of very compact equipment [18].

But the use of $CO_2$ has some disadvantages too. The cycle has to work with a high pressure compared with other working fluids at the same temperature range (e.g. R134a at the right diagram in figure 2.8). Thus it is necessary to use pipes which material thickness is designed for such a high pressure. It is also necessary to design sealing gaskets, pumps, heat exchangers and expanders for these conditions. $CO_2$ diffuses also at such a high pressure into gaskets and forms small gas pockets there. When the pressure drops in the system an explosive decompression can happen. The reason for this explosive decompression is that the enclosed gas inside the gas pockets expands, and breaks the sealing gasket. Another disadvantge is that $CO_2$ decreases the viscosity of the lubricant oil, because it has the tendency to dissipate into it. As a result of this it is advisable to use oil which quantities can handle this requirements.

## 2.7 The Kalina cycle

The main theory from the Kalina cycle is taken from DiPippo [7] unless otherwise noted.

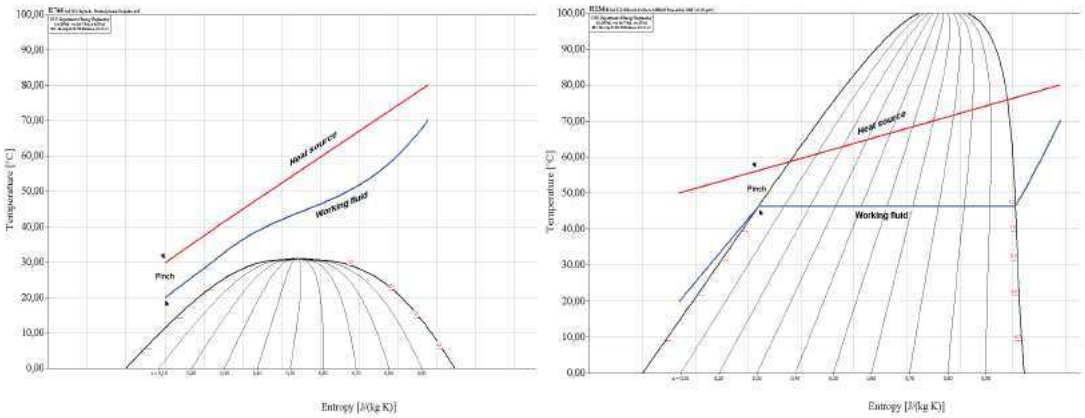


Figure 2.8: T-s diagram to compare R744 with R134a temperature - entropy profile in the evaporator

The Kalina cycle is using water-ammonia mixtures as working fluid used for power generation cycles. The simplest configuration of a Kalina cycle is shown in figure 2.9. The physical plant is more complex than a basic binary plant illustrated in figure 2.9.

The following is a description of the simple basic binary plant of figure 2.9. The separator (S) allows a saturated vapour that is rich in ammonia to flow through the turbine (T). This ammonia-rich fluid drops out on the top outlet of the separator. The water-rich fliud is the second fluid, which leaves the separator on the down side. The water-rich fluid flows though the control and stop valve (CSV) and is after that mixed together again with ammiona rich fluid, which is throttled down inside the turbine. The mixture is then used in a recuperative preheater (RPH) prior to being fully condensed, by the heat sink inside the condenser (C). At the condensate pump (CP) the ammonia-water mixture is pumped to the pressure level of the evaporator (E). Inside the evaporator, the working fluid is vaporized by the temperature input from the heat source and flows then to the separator. A throttle valve (TV) is necessary to regulate the water-rich working fluid on the way from the separator, which flows direct to the preheater (PH), and then to the recuperative preheater. The preheater has the function to precool the separated fluid, which flows from the separator to the recuperative preheater. The other function of the preheater is to preheat the water-ammonia mixture, which flows from the recuperative preheater to the evaporator. The separate cooling loop (heat sink) consists of a cooling tower (CT), a cooling water pump (CWP), and the makeup water supply (M). The heat source consists of production well (PW), pump (P), evaporator (E) and injection well (IW).

A possible difficulty for the Kalina cycle is maintaining very tight pinch-point temperature differences in the heat exchangers (one that is common to all cycles that strive for high

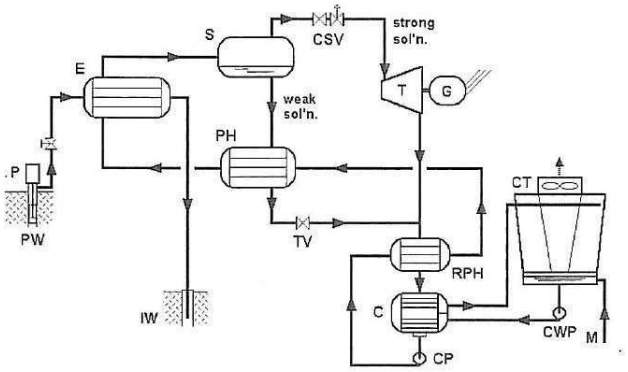


Figure 2.9: Kalina cycle with variable composition of the water-ammonia working fluid [7]

efficiency). Also, the advantage of variable-temperature condensation is reduced because the condensing isobars of the ammonia-rich $H_2O$-$NH_3$ mixtures used in power cycles are concave upward, leading to a pinch-point. Thus, there are relatively large temperature differences at the start and at the end of the condensing process.

The features that distinguish the Kalina cycles (there are several versions) from other binary cycles are these:

- The working fluid is a binary mixture of $H_20$ and $NH_3$.
- Evaporation and condensation occur at variable temperature.
- Cycle incorporates heat recuperation from turbine exhaust.
- Composition of the mixture may be varied during cycle in some lay-out versions.

There is a Kalina plant in operation in Husavik (Iceland) with a heat source temperature at the inlet of the evaporator of 124 °C (result of a test 16th –25th September 2002 [8]). The performance of the Kalina cycle in Husavik shows potential for applications in low-grade heat sources, but the aggressive water-ammonia mixture corroded the turbine, which needed some maintenance after 15 months in operation. In addition a study of DiPippo [8] concluded that broad claims of 15 – 50 % more power output for the same heat input for Kalina cycles relative to binary ORC are not being achieved for plants in operation so far.

# 3 Roma project – The prototype rig

An overview of the laboratory scale prototype rig is given in the following section. For a power producing test system it is important to run very stable tests in order to get reproducible test results. The test facility consists of four different cycles interacting with each other. This is involving some boundary conditions as well. One focus of this thesis is to investigate the limitations of important devices at the rig to achieve further improvements.

## 3.1 The primary process – expander cycle

The central point of the test facility is the expander cycle. This cycle is illustrated with purple lines in figure 3.1. The core of this expander cycle, or work recovery circuit, is the expander. All the other units, which are included this expander cycle, are selected for the requirements of the expander. An important part of the project is to research the behavoir of the expander with focus on conditions for maximal power production. The expander cycle exchanges heat with a heat source (HX-2) and a heat sink (HX-3, HX-8 and HX-10) through several heat exchangers. A plunger pump is installed after the condensation heat exchangers to circulate the working fluid $CO_2$ in the expander circuit. To avoid cavitation inside the plunger pump it is placed at the lowest point of the test facility. These positioning of the plunger pump features the maximum static pressure of the working fluid, and the lowest risk for cavitation inside the plunger pump. To avoid cavitation within the plunger pump, there is placed a receiver and a heat exchanger (HX-10) before the pump. These devices make sure that always sub cooled liquid, and no working fluid which is in the gas phase, flows to the plunger pump inlet.

### 3.1.1 The expander

An expander is a fluid kinetic machine that extracts energy from a fluid flow. With other words the kinetically energy is converted into rotational energy that can be used to drive a generator in the case of the Roma test facility. The used prototype has been fabricated by Obrist engineering. This expander is a classified project, so no additional information was provided.

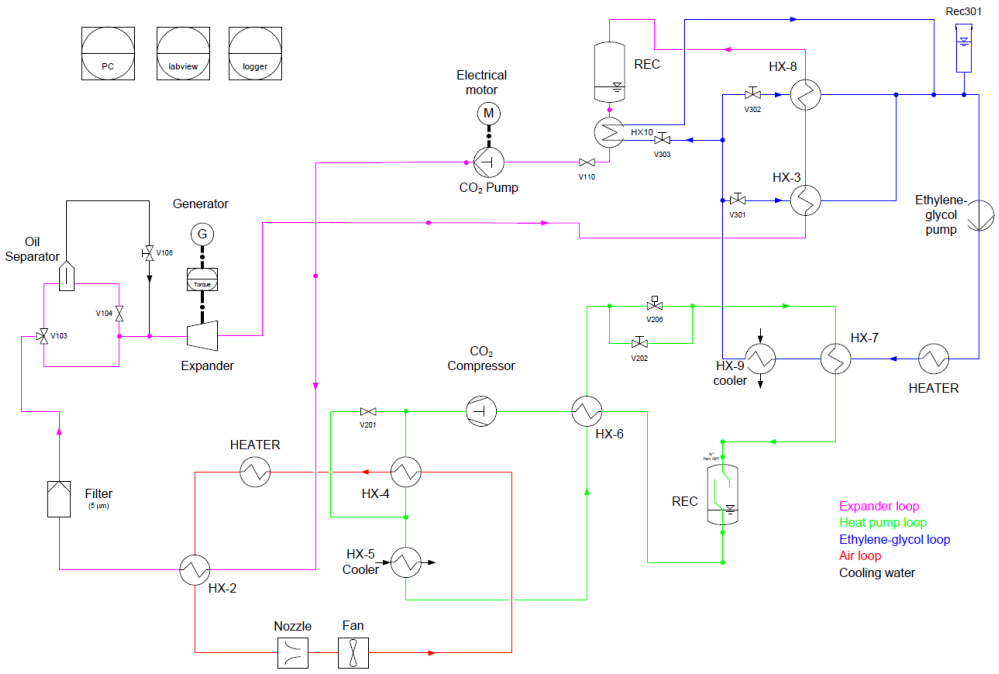


Figure 3.1: Schematic figure of the Roma test facility

| variable | value | unit |
|---|---|---|
| maximal high pressure (inlet) | 133 | bar |
| maximal low pressure (outlet) | 90 | bar |
| minimal low pressure (outlet) | 15 | bar |
| maximal inlet temperature | 160 | °C |
| maximal housing temperature | 80 | °C |
| maximal mass flow | 250 | $\frac{kg}{h}$ |
| maximal driving force (with clutch) | 2 | Nm |
| rpm | 1 500 - 10 000 | $\frac{1}{min}$ |

Table 3.1: Technical data sheet of the expander unit [19]

The expander is designed for only $CO_2$ as working fluid. Due to the high revolutions this machine is very sensitive for axial forces on the shaft. An adjustment plate were installed to avoid possible damages of the safety coupling (max. driving torque $\leq$ 2 Nm, table 3.1). Furthermore a burst plate system was installed to protect the expander from inlet pressures $\geq$ 133 bar (table 3.1). To launch the expander, a amount of 5 - 10 ml oil has to be accumulated on the inlet of the expander. To respect this point it was necessary to built-in an oil separator (illustrated in the loop with black lines in figure 3.1). The separator accumulates the needed amount of oil for an expander start-up. The oil has not only a lubrication function. It also has a sealing function too.

### 3.1.2 The generator

The used generator is a direct current dynamo machine, which had been used as a dynamo in Volkswagen cars in the late 60's. Unfortunately no data sheet for the dynamo was available. For the installed expander it was necessary to find a solution to start it with a motor, because the minimum rotation speed is at 1 500 rpm, see table 3.1. The used generator is a DC (direct current) machine which is able to run in motor mode and providing the necessary rpm to start the expander. When the expander has reached the minimum rotation speed and pressure difference, the operation mode of the DC machine can switched from motor to generator mode for electrical power production. A simplified illustration of the motor and generator mode of a DC machine is illustrated in figure 3.3.

To run the turbine with the DC motor, a battery has to be connected to provide magnetising current for the copper winding and the magnetic field inside of the DC machine has to be activated. In generator mode the battery only supplies the power for the switches and relays. The battery delivers the electrical power for the DC machine to run as a motor and the load is realized by an external device. This installation was necessary to protect the battery from a harmfull back flowing current (battery can be

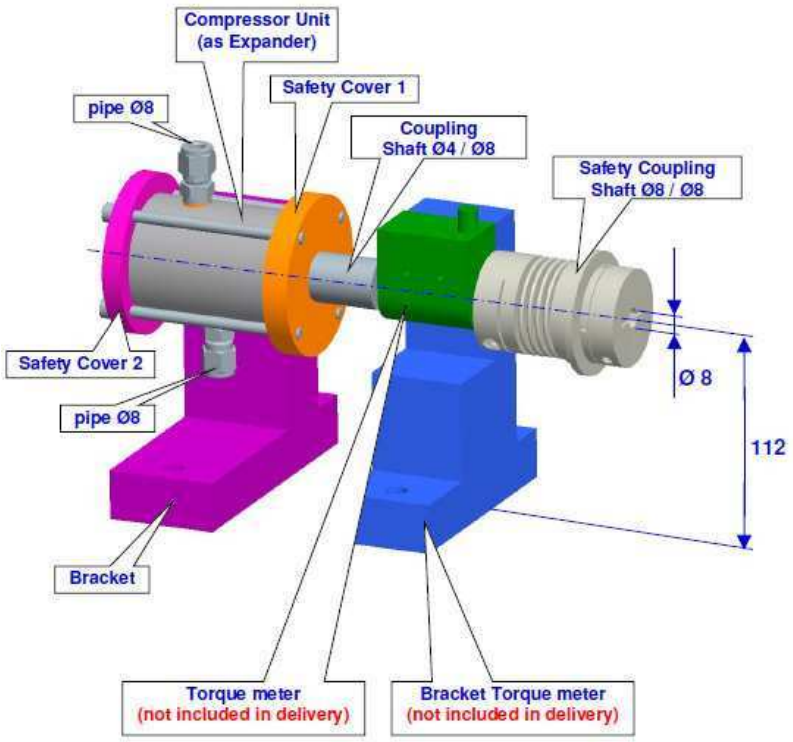


Figure 3.2: Obrist expander system set-up with torque meter and clutch [19]

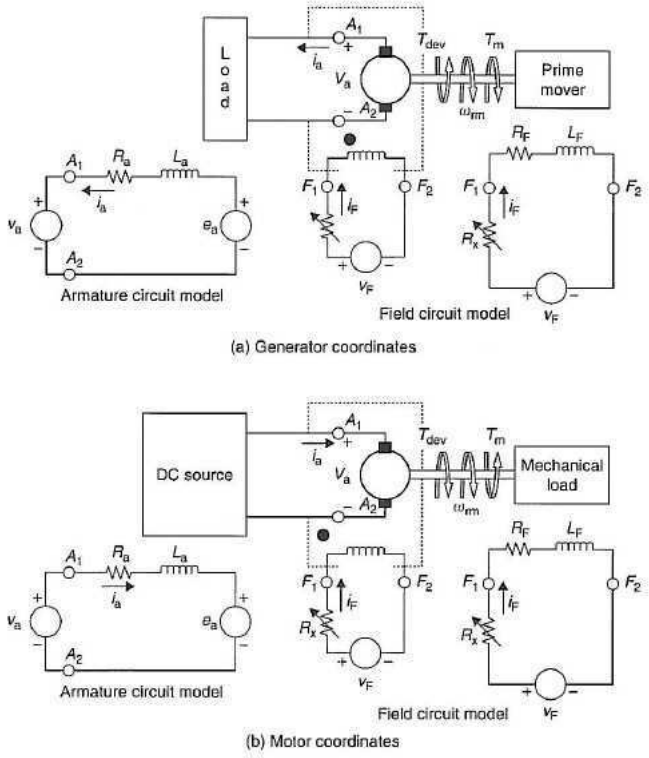


Figure 3.3: Simplified DC machine model illustrating motor and generator mode [25]

polarized or overloaded). So the produced power cannot flow back to the battery. There are 3 lamps (each with 55 W power) and a heater installed to convert the produced power to light and heat energy. The magnetising force in motor and generator mode can be regulated with an external device.

### 3.1.3 Torque and rotation speed

The torque (top screen in figure 3.4) and the rotation speed (bottom screen in figure 3.4) are the two variables that characterize the expander. The torque is expressed in Newton meter (Nm) and the rotation speed in revolutions per minute ("U/min" figure 3.4). The display is an important device to check the rotation speed and torque at the shaft between expander and generator, during a test to avoid dangerous levels of speed and force. The minimum working conditions for the expander inlet and outlet can be controlled, on the display during the power producing mode.


Figure 3.4: Torque meter and rotation speed sensor with digital display [20]

## 3.2 The heat source - The air loop

The air loop is an important part of the test facility, because it is to simulate the offgas from the aluminium production cells, which includes the waste heat. This cycle is illustrated with red lines in figure 3.1. The heat exchanging with the expander cycle is done with the HX-2 heat exchanger. When the $CO_2$ heat pump is running, using HX-4 as condenser, the air is warmed up by this heat exchanger (HX-4). In case, when there is need of some supplementary heating to obtain the desired temperature of the air, the electric heater provides the rest of the heat needed. After the first expander tests the heat exchanger HX-4 was removed from the air loop (this data are not used for the results in this thesis). In this case it was required to provide all of the heat, which was needed for the tests, with the heater. The reason for the dislodged HX-4 was to get more stable air temperature conditions for the tests. This modification had a positive effect, because the temperature profile was more stable during all the tests afterwards. The circulation of the air is provided by an air fan, installed right in front of the position of HX-4.

## 3.3 The heat sink - The ethylene-glycol loop

The ethylene-glycol loop, which works on the low-pressure side of the expander loop is represented with blue lines in figure 3.1. The working fluid at the beginning of the tests, was water inside the ethylene glycol loop. But for tests with a lower condensation

pressure the cooling fluid was replaced for a ethylene-glycol mixture with an freezing point of -19.5 °C, because the heat sink was provided then from the heat pump loop with HX-7 as heat exchanger. For the tests with water as cooling fluid the cooler HX-9 was used as heat sink, which was cooled with fresh water from the drinking-water pipeline or an external tank with regenerated water from the laboratory. The major goal of this loop is to subcool the $CO_2$ which is the working fluid at the expander loop down (circa 10 °C) below saturation temperature. This is necessary to avoid cavitation at the plunger pump of the expander loop. Two different constructions of heat exchangers (HX) are at the ethylene-glycol loop installed. HX-3 is a typical counter flow heat exchanger, whereas HX-8 and HX-10 are so-called tubular internal heat exchangers. The heat exchangers operate in parallel in relative to the cooling cycle and in series relative to the expander circuit (figure 3.1). The cooling performance of these two heat exchangers is controlled manually by changing the massflow of the cooling fluid, which is distributed between the heat exchangers. A single pump is used to provide the necessary circulation of the cooling fluid, which can be controlled by the speed of the electrical motor of the ethylene-glycol pump.

## 3.4 Supplementary circuit – heat pump loop

The main reason for constructing this cycle, which is illustrated with green lines in figure 3.1, was to recycle as much as possible of the condensation heat of the expander cycle. The main working components of a heat pump are the evaporator, the condensers, the compressor and an expansion device. In this circuit the HX-7 heat exchanger works as an evaporator, which exchanges the heat from the ethylene-glycol loop to evaporate the $CO_2$, which is the working fluid at the heat pump loop. The condensation of the $CO_2$ was provided in HX-4 heat exchanger where $CO_2$ was cooled by air from the warm air loop, and in the additional heat exchanger (HX-5) the $CO_2$ was cooled even further (when necessary) by fresh water from the drinking water pipeline. But since the heat exchanger HX-4 is removed, the heat exchanger HX-5 is the only condenser of the heat pump loop. So the function of the heat pump loop at the moment is to provide cooling for the ethylene-glycol loop when needed.

The compressor unit used is a semi-hermetic radial piston compressor with fixed displacement. The expansion device is a manual expansion valve. Furthermore an internal heat exchanger (HX-6) is installed, to increase the performance of the heat pump and to provide dry $CO_2$ gas entering the compressor. There is also a receiver in place between the evaporator and the internal heat exchanger, to provide saturated gas to the internal heat exchanger, and to contribute to changes of the conditions at the low-pressure side of the heat pump.

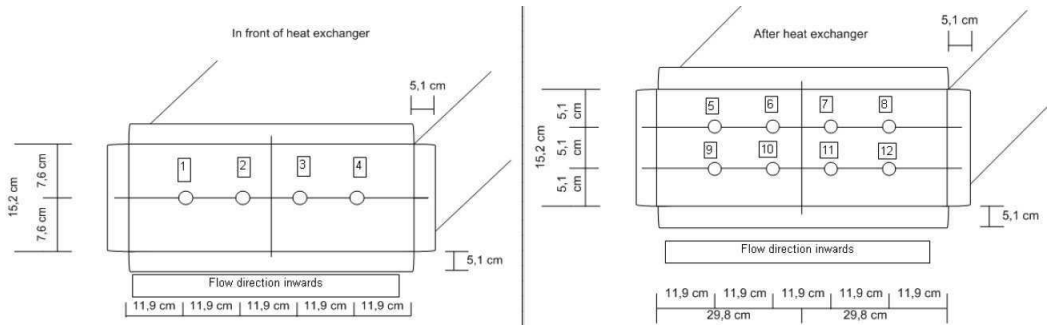


Figure 3.5: Fitting position of the thermocouples in the air loop before and after HX-2

## 3.5 Instrumentation

### 3.5.1 Thermocouples

The thermocouples used in the test facility were made out of material that could stand temperatures up to 200 °C. This was seen as necessary since the temperatures of the air coming out of the heater (heater 401 in figure A.1) were planned to operate at temperatures close to that region. The fitting position of the thermocouples inside the air loop on the positions before and after HX-2 is illustrated in figure 3.5. The design of thermocouples measuring temperatures inside tubes (figure 3.6) consists of putting the thin needle into the tube where liquid or gas flows. A short length of a small tube, which is closed at one end, holds the thermocouple inside the tube where the fluid streaming. These thermocouples are used to measure the temperature of the $CO_2$, the ethylene-glycol water mixture, the warm air and the water. Every thermocouple is connected to a data acquisition (DAQ). In that way, the temperatures will be logged into a data file on a computer.

### 3.5.2 Pressure sensors and massflow meters

As well as the thermocouples, the pressure sensors and massflow meters have to be connected to the DAQ. The massflow meters (figure 3.7) which are installed at the heat pump loop, the expander loop and the ethylene-glycol loop measuring self-contained the parameters for calculating the mass flow and transmit the values to the DAQ. The range of the final signal given by the pressure sensors and massflowmeters is 4 to 20 mA.

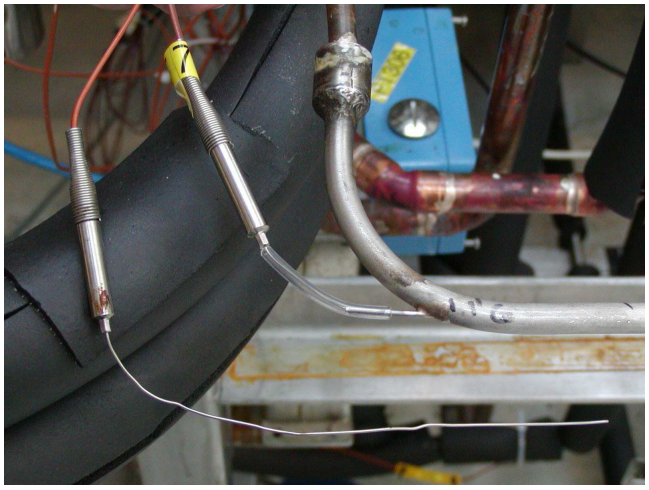

Figure 3.6: Thermocouple installed in the expander loop

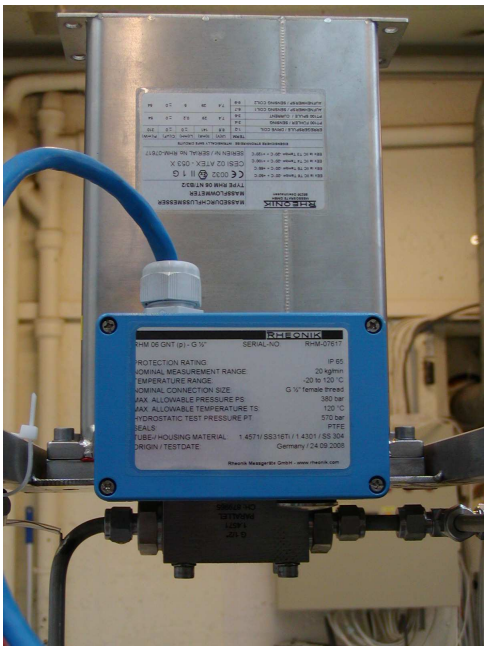


Figure 3.7: A RHEONIK RMH 06 mass flow meter installed in the heat pump loop

# 4 Expander testing

The first aim for the test work at the Roma test facility was to research the expander behaviour and applicability for different conditions. The single data together should give results for the most efficient working conditions of the expander. Another aim of these tests were to find out the boundary conditions of all single devices of the test facility when they interacting with each other.

All the results were determined at maiximum available speed of the fan at the air loop and as in section 3.3 described, without HX-4 (dislodged). All the tests were carried out without working fluid flow to the oil separator. The oil separator was used to check the minimal oil flow for the expander start up. When the expander was in stable conditions in the power production mode the direct flow pipe was used for all the tests (oil and $CO_2$ together). The minimum data logging time for a series of data was 10 minutes at stable conditions of the temperatures, the mass flows and the pressures in the Roma test facility. In all tests that are performed with 60 bar condensation pressure, fresh water from the drinking water pipeline was used as heat sink for the ethylene-glycol loop.

## 4.1 Test series I with 1.8 kg/min $CO_2$ mass flow through the expander, 60 bar condensation pressure and different heat source temperatures

### 4.1.1 Basic strategy for test series I

The basic set up for this test series was at fixed condensation conditions at 18 °C and 60 bar after HX-10, and before the plunger pump for all the tests. Furthermore the set-up for the $CO_2$ massflow at the expander loop was at 1.8 $\frac{kg}{min}$. There were three different heat source temperatures used at the air loop. These heat-source temperatures had been 65 °C, 90 °C and 110 °C.

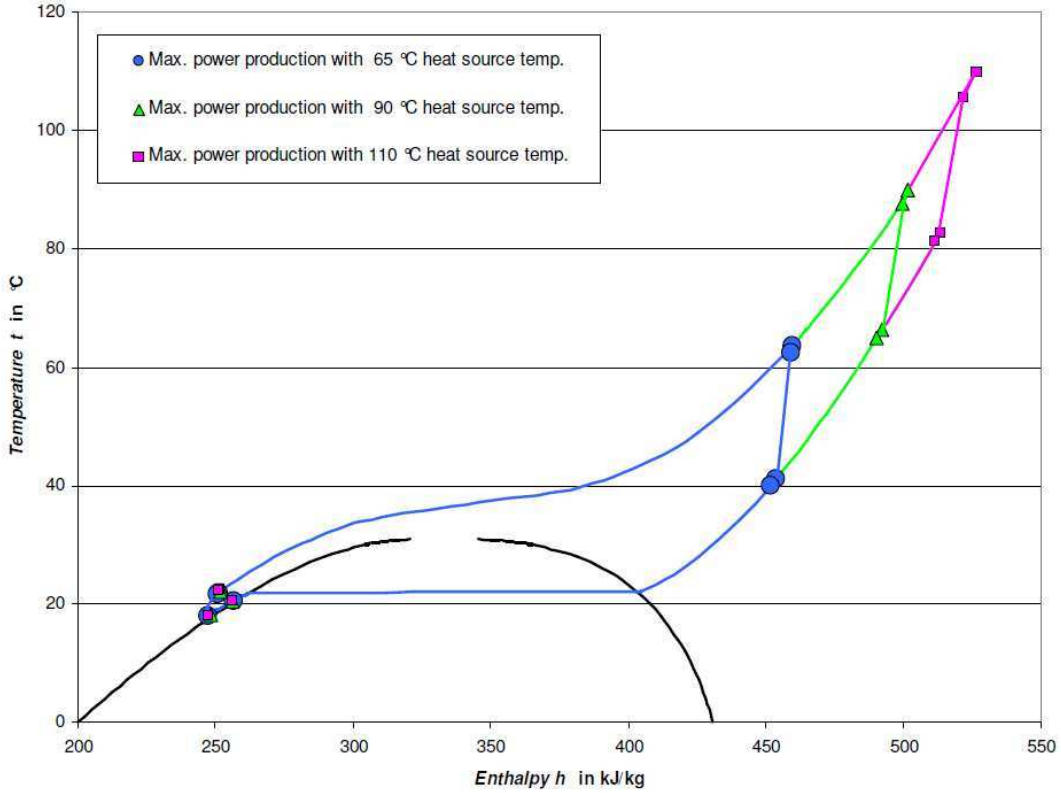


Figure 4.1: The t-h diagram for test series I illustrating the tests with the topmost work production

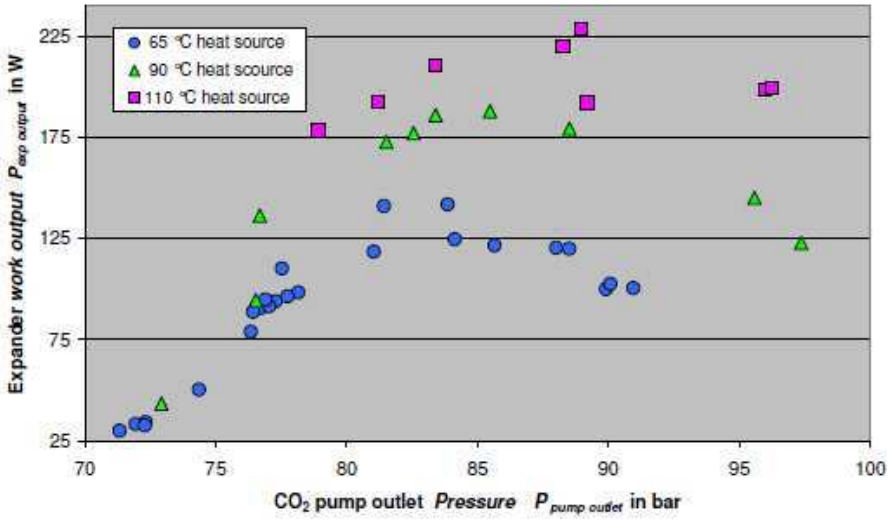


Figure 4.2: Test series I: Expander work output and $CO_2$ pump outlet pressure diagram

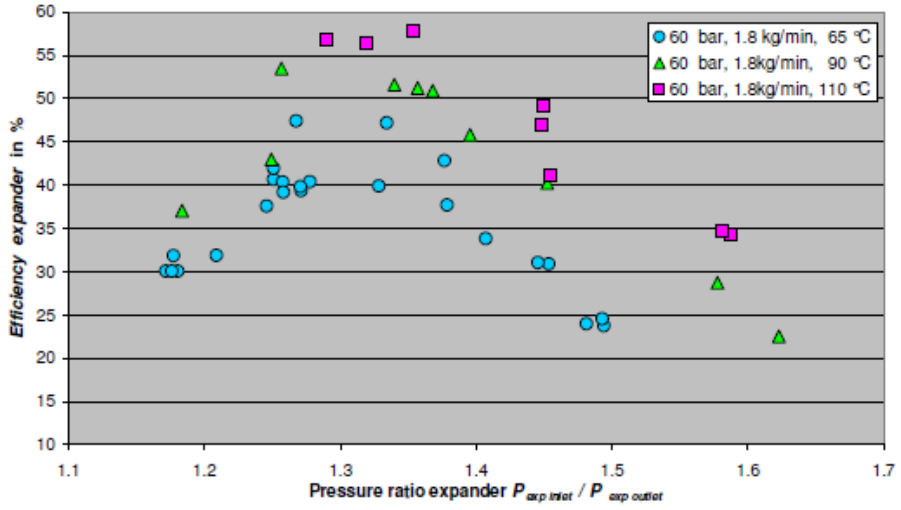


Figure 4.3: Test series I: Expander efficiency and expander pressure ratio diagram

### 4.1.2 Results and discussion for test series I

The t-h diagram in figure 4.1 pesents the results of the three tests at maximal power production of the expander (each at different heat source temperature). It shows the transcritical heat addition in HX-2 as well as the heat rejection to the ethylene-glycol loop, which follow nearly the same pressure conditions to the HX outlet. It can be also seen that the expansion of the $CO_2$ inside the expander is in the supercritical gas region of the t-h diagram. The turbine outlet point, which is in that supercritical gas region, shows that there is a high energy potential that is not used by the expander. One possibility is to utilize this energy potential by installing a recuperator at the expander loop (shown in figure A.1). A second altenative is to reintegrate HX-4 to transfer this energy back to the heat source. A third option, using the existing devices in the test facility, is to increase the $CO_2$ mass flow. More about this third option in section 4.2. Furthermore the diagrams in figures 4.2 and 4.3 show the increased efficiency and work output of the expander with increasing the heat-source temperature of the air loop. In this figures it is obvious that there is a maximum of efficiency and power output of the expander in a range for every temperature set-up. The most efficient working conditions of the plunger pump pressure outlet are at maximum power production of the expander see figure 4.2. The diagram in figure 4.3 shows the expander pressure ratio for the highest efficiency of the expander for the three heat-source temperatures that were choosen. But in the figures 4.2 and 4.3 the effect of different efficiencies and power production were achieved by a similarly range of pressure. This behaviour could be explained by the different amount of oil flowing through the heat exchangers during the single tests. This would be result in a different heat addition from the heat source and heat rejection to the heat sink.

## 4.2 Test series II with 65 °C heat source temperature, 60 bar condensation pressure and different $CO_2$ mass flow through the expander

### 4.2.1 Basic strategy for test series II

With the consideration of the results from test series I (subsection 4.1.2), the goal for this test series was to study the behaviour, and achievable power production with increased $CO_2$ mass flow at the expander loop. So there were three different $CO_2$ massflows of 1.8 $\frac{kg}{min}$, 2.5 $\frac{kg}{min}$ and 3.0 $\frac{kg}{min}$ used for this test series. The basic set up for this test series was to fix the condensation conditions to the range of 18 °C and 60 bar after HX-10, and before the plunger pump for all the tests. Furthermore the set-up for the heat source temperature was fixed to the region of 65 °C at the heater in the air loop .

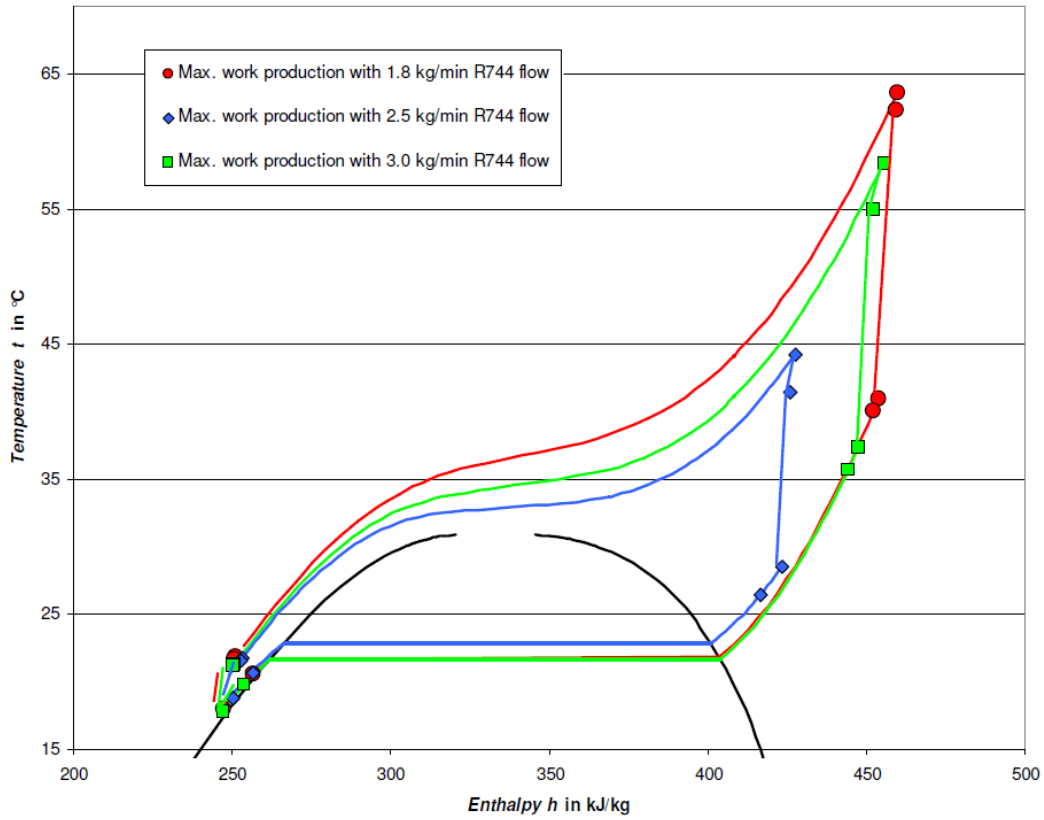


Figure 4.4: The t-h diagram for test serial II illustrating the tests with the maximum work production

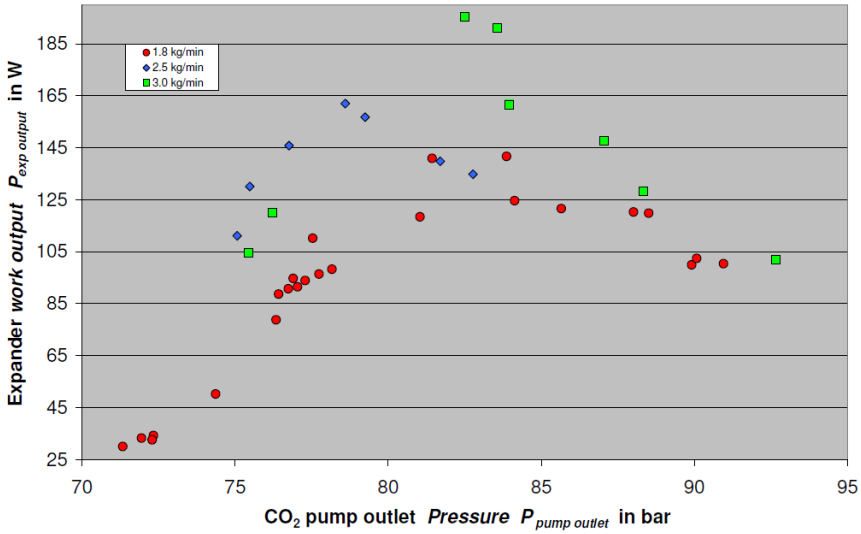


Figure 4.5: Test series II: Expander work output and $CO_2$ pump outlet pressure diagram

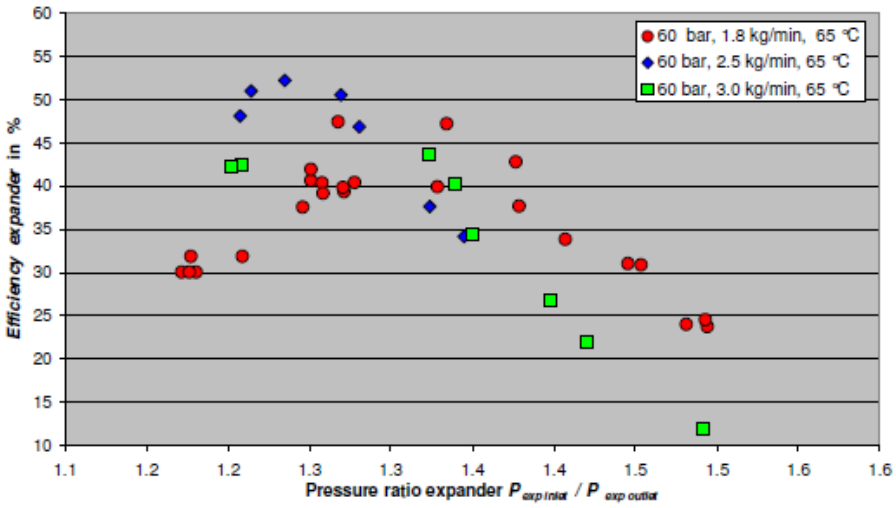


Figure 4.6: Test series II: Expander efficiency and expander pressure ratio diagram

### 4.2.2 Results and discussion for test serial II

The t-h diagram (figure 4.4) presents the results of the three tests (each with a different $CO_2$ mass flow at the expander loop) with the highest work out of the expander. It can be seen that with increasing the mass flow at the expander loop the turbine inlet and outlet temperature is decreasing. For the tests with 1.8 $\frac{kg}{min}$ and 2.5 $\frac{kg}{min}$ $CO_2$ massflow, the expander outlet conditions are in the supercritical gas region in the t-h diagram. The expander outlet conditions of tests with 3.0 $\frac{kg}{min}$ $CO_2$ massflow used at the expander loop, are in the subcritical gas region of the t-h diagram. As a fact of the increased massflow it can be seen in the figures 4.5 and 4.6 that the efficiency and power output of the expander was increasing as well.

For the test series with 110 °C heat source temperature it was difficult to have stable temperature conditions in the air loop, because in some tests the temperature safety device stops the power supply to the heater (these sets of data are not used for the results of this section). So after this test session a velocity measurement was realized at the place were HX-4 was installed . So the velocity profile was measured between heater and fan at the air loop. The result of this velocity measurement was that at one side of the air channel the velocity was at the minimum inlet velocity of the heater. There is a minimum velocity of 0.7 $\frac{m}{s}$ requested by the manufacturer of the heater. So some heating elements had reached dangerous temperature levels at 110 °C heat source temperature. So this is one boundary condition of the air loop. To avoid this effect a fan that provides a higher air velocity at the heater inlet is necessary, because the fan was running for all tests at maximum speed.

But like in the section 4.1.2 in some tests illustrated on figures 4.5 and 4.6 the effect of different efficiencies and power production were achieved in a similar range of pressure. This behaviour could be explained by the different amount of oil flowing through the heat exchangers during the single tests. This would be result in a different heat addition from the heat source and heat rejection to the heat sink.

## 4.3 Test series III with 3.0 kg/min $CO_2$ mass flow through the expander, 60 bar condensation pressure and different heat source temperatures

### 4.3.1 Basic strategy for test series III

After the evaluation of the test results from test series II the next goal was to study the expander behaviour with an increased heat source temperature to 90 °C and a used $CO_2$ mass flow of 3.0 $\frac{kg}{min}$. The results of this test series are compared with the results with

a set-up of 65 °C heat source temperature and 3.0 $\frac{kg}{min}$ mass flow at the expander loop (series II in section 4.2). The set-up for the condensation conditions was like in test serial I and II set to of 18 °C and 60 bar after HX-10, and before the plunger pump for all the tests.

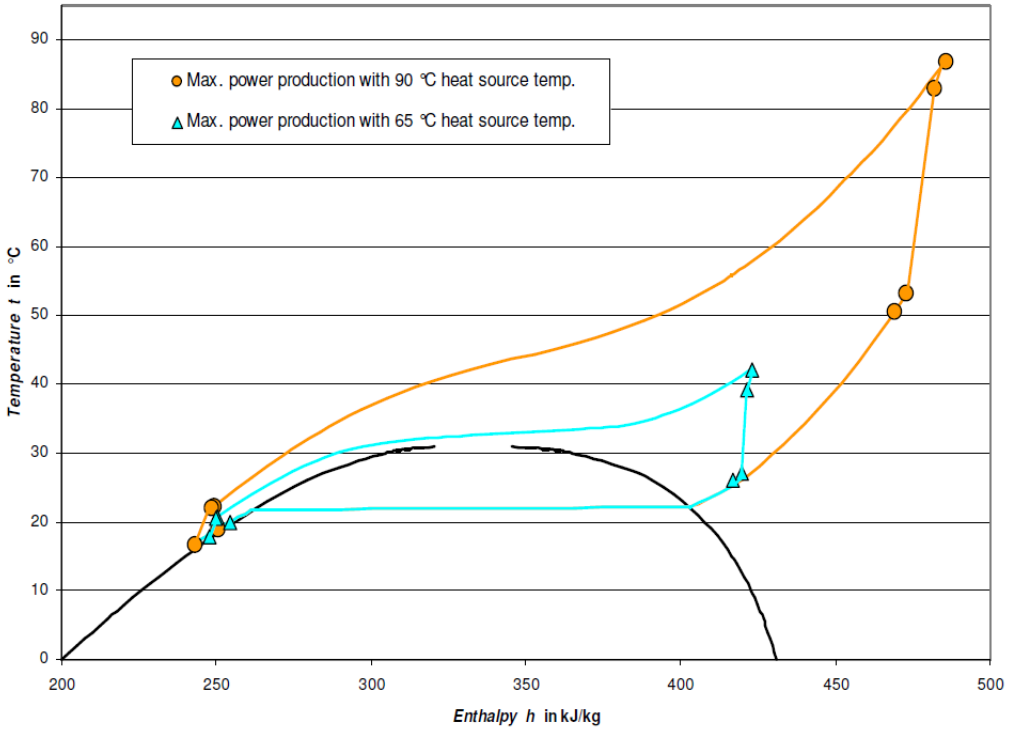


Figure 4.7: The t-h diagram for test series III illustrating the tests with the maximum work production

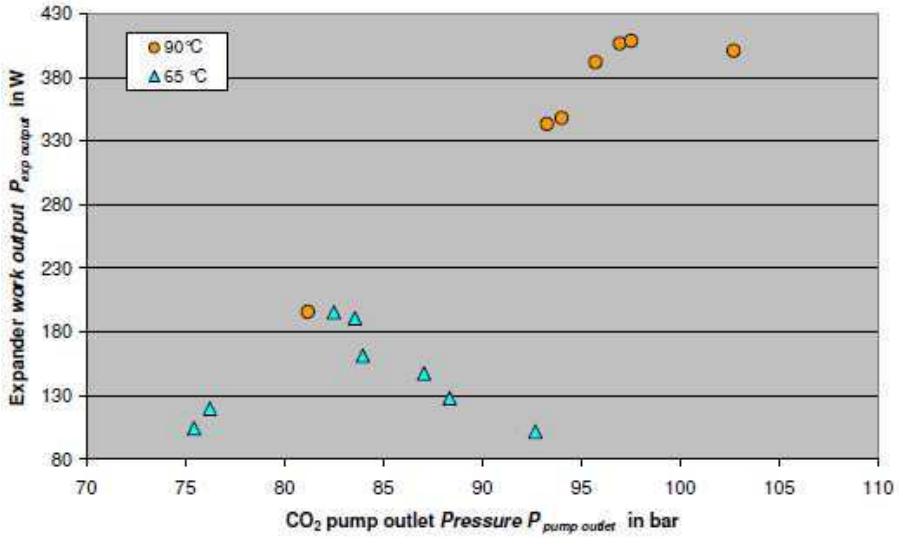


Figure 4.8: Test series III: Expander work output and $CO_2$ pump outlet pressure diagram

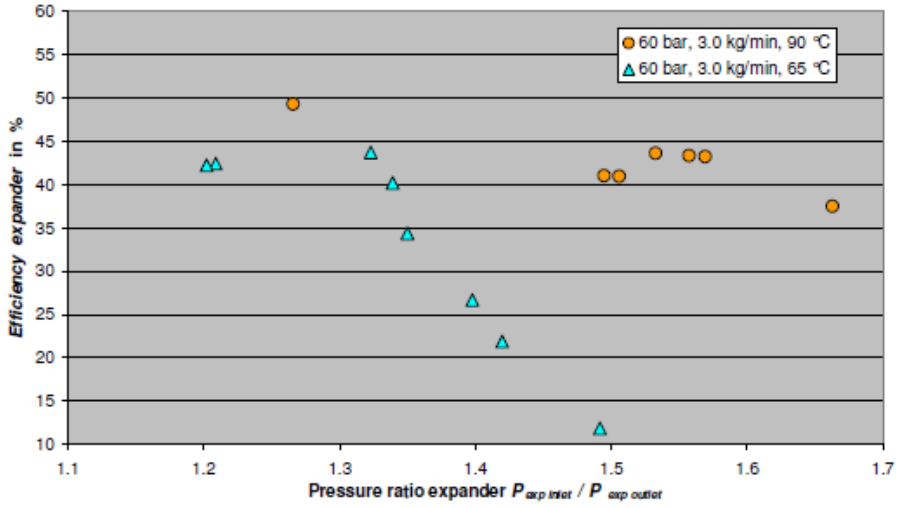


Figure 4.9: Test series III: Expander efficiency and expander pressure ratio diagram

### 4.3.2 Results and discussion for test series III

For these results an effect for the turbine outlet conditions with increasing the heat source temperature at the air loop, like in test series I in section 4.1, can be seen. It shows that the expander outlet point was in supercritical gas region for the test with 90 °C heat source temperature. As described in sub section 4.1.2 exists for this 90 °C temperature set-up at the air loop a possibility to utilize more condensation energy potential with including a recuperator at the expander loop (shown in figure A.1), or to use this amount of energy with a reintegrated HX-4, which is a possible alternative to transfer this energy back to the air loop.

To extract the maximum energy from the heat source the $CO_2$ mass flow is to increase. Because in the test series III with inreasing the $CO_2$ massflow a efficient test set-up was been found, with less heat rejection to the heat sink.

In contrast to efficiency the highest work production for all the tests with a maximum in the range of 400 W was achieved with a heat source temperature of 90 °C. As a result of the increased heat source temperature to 90 °C and a $CO_2$ mass flow of 3.0 $\frac{kg}{min}$ the test rig shows some boundary conditions which are the following. The rotation speed of the expander increased a lot with increase of the heat-source temperature from the maximum rotation speed in the range of 3 800 $\frac{1}{min}$ (at 65 °C) to the range of 5 000 $\frac{1}{min}$ (at 90 °C). At this high range of rotations the bearings of the generator begin to make alarming noises. As another result of overstepped performance characteristics of the generator was an increased housing temperature up to 120 °C and an increase of the output voltage of 32.6 V maximum.

## 4.4 Test series IV with 65 °C heat source temperature, 1.8 kg/min $CO_2$ mass flow through the expander and different condensation pressures

### 4.4.1 Basic strategy for test series IV

For this test series the basic set-up for the heat source (air loop) was in a fixed range of 65 °C. Furthermore the set-up for the $CO_2$ mass flow at the expander loop was fixed in the region of 1.8 $\frac{kg}{min}$.

The gaol was to investigate the behaviour of the test facility on different condensation conditions, which were 60 bar, 55 bar, 50 bar and 42.5 bar condensation pressure. The tests with 60 and 50 bar condensation pressure were performed with fresh water from the drinking-water pipeline used as heat sink for the ethylene-glycol loop. The condensation

conditions of 55 and 42.5 bar the heat pump loop were used to provide the cooling of the ethylene-glycol loop (heat sink).

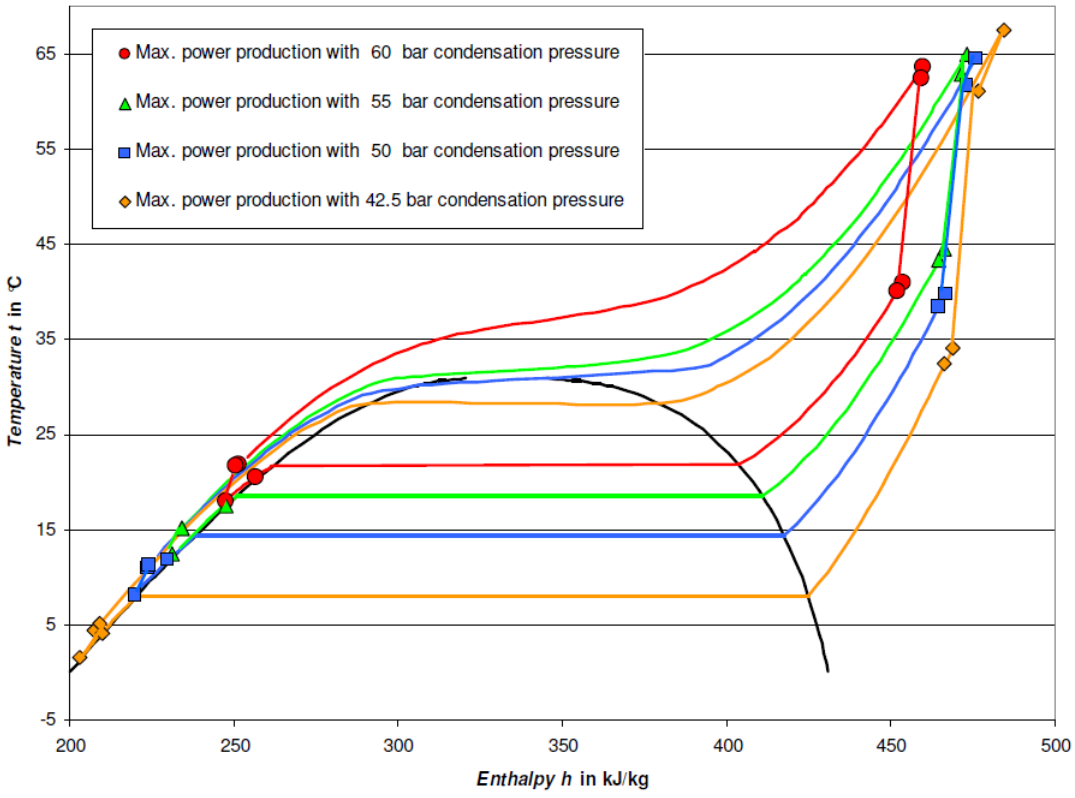


Figure 4.10: The t-h diagram for test series IV illustrating the tests with the maximum work production

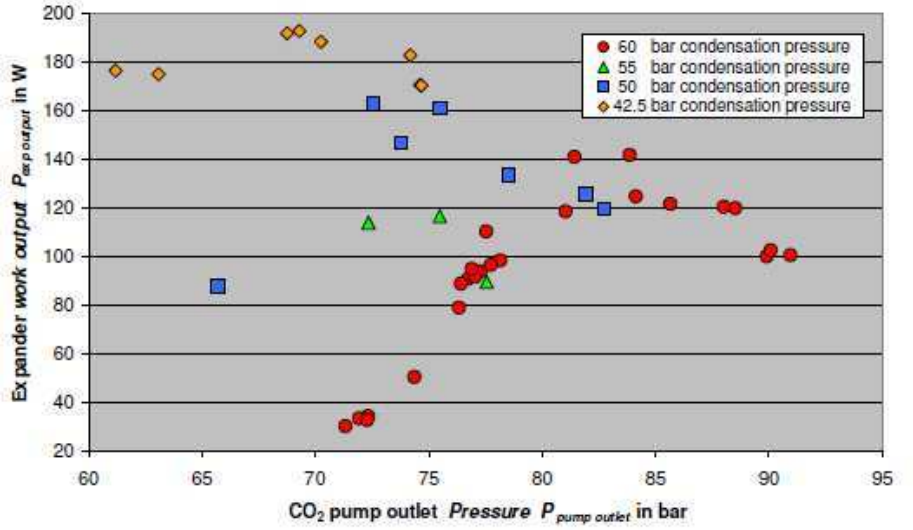


Figure 4.11: Test series IV: Expander work output and $CO_2$ pump outlet pressure diagram

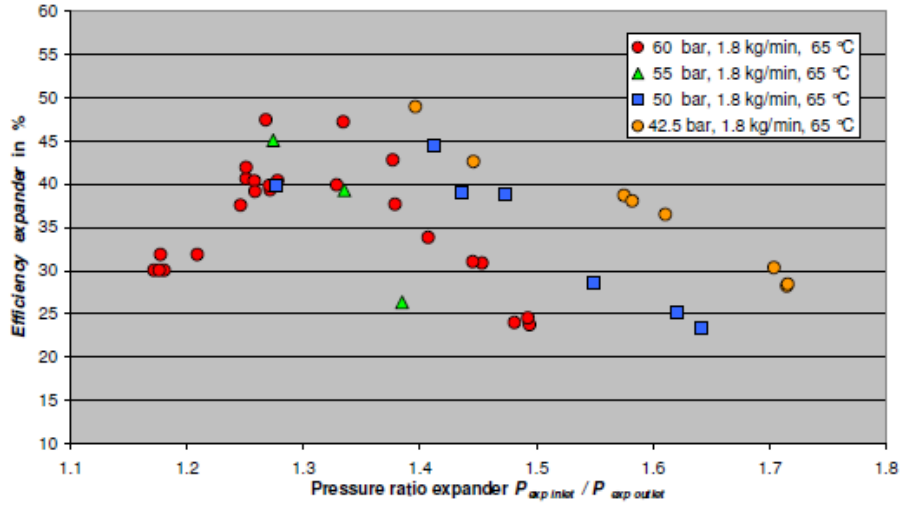


Figure 4.12: Test series IV: expander Efficiency and expander pressure ratio diagram

### 4.4.2 Results and discussion for test series IV

For this test series IV with different condensation conditions it is illustrated in figures 4.11 and 4.12 that with a decreased condensation pressure and temperature the work output and efficiency of the expander was increased. Furthermore there should be noticed that it was a lot of effort to keep the facility in stable conditions for tests with the heat pump providing the cooling for the ethylene-glycol loop. A lot of devices and all four loops have worked and interacted together. In this test series the test facility was working without any problems and without reaching any boundary conditions. The results in test series IV show similar effects as in series I to II. A different work output of the expander appears at a similar region of pump outlet pressure. This is caused by a different heat addition and rejection at the heat exchangers. In the results the effect could be seen, that different efficiencies and power production were achieved in a similarly range of pressure. This effect illustrated on figures 4.11 and 4.12 . This behaviour could be explained by the different amount of oil flowing through the heat exchangers during the single tests. This would be result in a different heat addition from the heat source and heat rejection to the heat sink too.

## 4.5 Error estimation

The error of a measurement is the difference between the measured value and the true value. To express the accuracy of a measured value, the term of uncertainty can help. The uncertainty of each measured variable redounds to the uncertainty of the final result. There was a detailed simulation and error estimation of the test facility in the autumn of 2008, when the work on the Roma project was started. So here is the theroy the methodology of the error estimation explained. For this theory of error estimination it is provided that no gross error happend in the test series. Such a gross error e.g. can happen when the wrong measure range on a flow meter was choosen, or the tests were not performed with the needed carefulness.

For the ratation speed and tourque meter, the thermocouples, the massflow meters and the pressure sensors were the fixed accuracy values given by the manufacturer of the single devices.

To express the accuracy of a measured value, the term of uncertainty can help. It refers to a possible value that an error may have with defined probability. The uncertainty of one measured variable is defined as $\delta X_i$ . The uncertainty of each measured variable redounds to the uncertainty of the final result. The calculated uncertainty for the different variables is represented with a probability of 95 percent. Measurements are distinguished in single measurements, sample measurements or multiple-sample measurements. Multiple-sample means a lot of independent measured values were taken at the same test point, this

leads to a higher quality of the measured values. For single-sample analysis, the value $\delta X_i$ is represented by $2\sigma$ , where $\sigma$ is the standard deviation of the measurements. The single sample $X_i$ was taken from this. The final result R is calculated from a set of measurements by using:

$$R = R_i(X_1, X_2, X_3, ..., X_n), \tag{4.1}$$

Of this final result (R) , $X_1, ..., X_n$ are the independent variables. The sensitivity coefficient for the result R with respect to $X_i$ can be found by partial deviation.

$$\delta R = \frac{\delta R}{\delta X_i}\delta X_i \tag{4.2}$$

All the estimated sensitivity coefficients of the independent variables used in functin R are combined a root-sum-square method.

$$\delta R = \left[\sum_{i=1}^{N}(\frac{\delta R}{\delta X_i}\delta X_i)^2\right]^{\frac{1}{2}} \tag{4.3}$$

The equations are valid if each of the measurements was independent, the uncertainty in each measurement was expressed in the same odds and the measurements would follow the Gaussian distribution. The overall uncertainty consists of fixed errors and random errors. Fixed errors do not change during the tests. They rely on the accuracy of the measurement equipment as sensors and logging system. The residual fixed error and the random error are described by its bias limit and its precision index. Some further information must be given.

- The mean value of a set of N observations of the measurement.
- The precision index of the mean $\delta X$ , an estimate of the standard deviation of the mean of the set of N observations (random error).
- The bias limit of each measurement $\delta X$ (fixed error). The overall uncertainty can then be calculated as a function of the overall fixed error and the overall random error.

$$\delta X = \sqrt{(random\,error)^2 + (fixed\,error)^2} \tag{4.4}$$

# 5 Simulations

## 5.1 The purpose of the simulation

After the data analysis of the results of the tests, the aim was to find solutions and improvements for the existing test facility. Like in chapter 4 described, there are boundary conditions when the single devices has worked together during some tests. The first boundary condition was the low inlet velocity of the heater in the air loop at maximum speed of the fan. As a consequence of this low inlet velocity, the heater has reached the maximum temperature limit at the heating elements. It could be clearly seen that the volume flow of the air loop should be increased for further tests with increased heater temperature in the future. To find out the range of nessesary air volume flow of the new fan the Pro/II simulation program was used. The second limitation of the test facility was the high housing temperature of the DC machine in generator mode for the test series III. Especially with 3.0 $\frac{kg}{min}$ $CO_2$ massflow at the expander loop and 90 °C heat source temperature at the air loop. The housing temperature of 120 °C at the DC machine housing was a result of overloading by work input on the shaft by the expander. A new generator would be necessary to be able to make tests with increased massflow and heat source temperature in the future. This generator has to be designed to convert the increased mechanical work input to electrical power. Like in the case of the fan, the Pro/II simulation program was used to choose a better size of generator.

## 5.2 The used simulation model in Pro/II

To simulate the test facility the program Pro/II version 8.2 was used. Pro/II is a commercial application from Simulation Sciences Incorporated (SimSci) and able to simulate complex technical processes or to calculate different process parameters. The program was used to simulate the expander loop, the heat sink (ethylene-glycol loop) and the heat source (air loop) see figure 5.1. The heat sink in the model consists of only one heat exchanger. The model was build in this lay-out to simplify it. In reality the heat sink consists of the heat exchangers HX-3, HX-8 and HX-10.

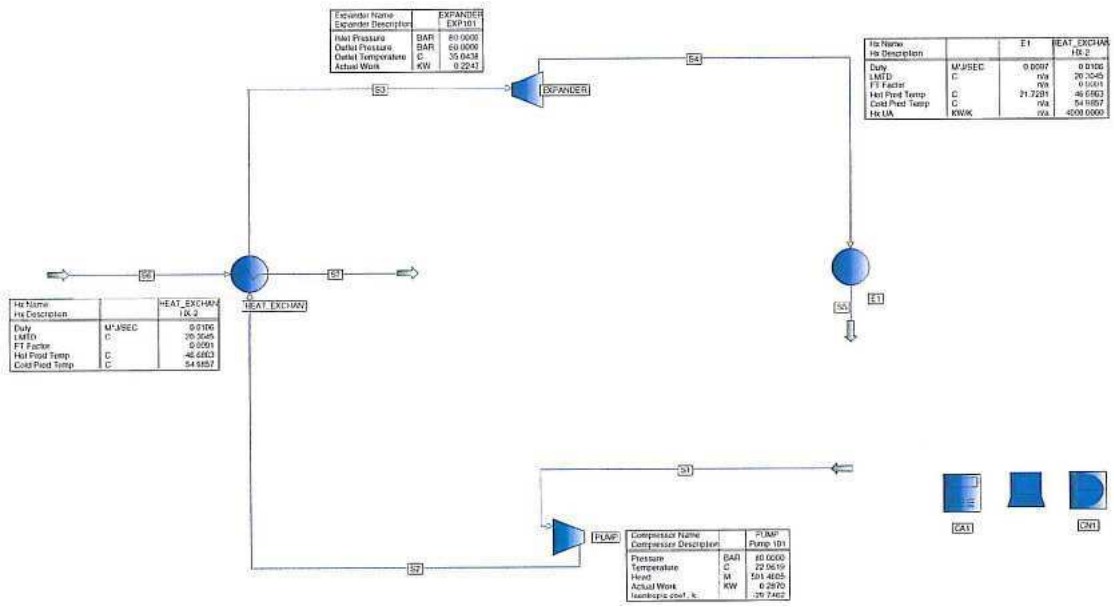


Figure 5.1: The used model in the Pro/II software version 8.2

### 5.2.1 Simulation of the heat transfer coefficient times area of HX-2 with the existing air-volume flow

The first aim was to find out the optimal range of air-volume flow needed in the air loop. To find out this optimum of air-volume flow with the simulation model, the heat transfer coefficient times area (UA value) of HX-2 was needed. This heat exchanger (HX-2) transfers the energy potential of the heat source to the expander loop. For this simulation the model in figure 5.1 was used. The input values for this simulations were based on the results of expander tests. The choosen tests are listed with all the input values in appendix subsection D.1. There were nine simulations made, one for each expander test series. The results of these simulations for the UA-value of HX-2 were not constant. There was a range from 2 288.70 $\frac{kW}{K}$ up to 4 607.95 $\frac{kW}{K}$ for the UA value. This UA value range can be a sign that this heat exchanger design of HX-2 should be improved. But more about this point in subsection 5.2.3.

### 5.2.2 Simulation of the needed air-volume flow in the air loop

To simulate the optimal air-volume flow of the air loop, simulations with two different UA values were performed. The first choosen UA value was 2 000 $\frac{kW}{K}$, and the second one was 4 000 $\frac{kW}{K}$. This two UA values were choosen to get informations on the difference

in the result of the needed air-volume flow at the air loop. For each simulation the UA value was fixed to a constant value. The plunger pump efficiency was set to a constant value of 70 %, and the expander efficiency was set to a constant value of 35 %. The high pressure side of the test facility was increased in steps of 2 bar. The high pressure side is between plunger pump outlet and expander inlet. Starting pressure of the simulations was 70 bar, and the end pressure was 99 bar. At the expander outlet a liquid fraction of the $CO_2$ appears at 97.5 bar or 98.5 bar D.2 pressure at the expander inlet, in the results of the simulations. This pressure at the expander inlet is the starting pressure, were a liquid fraction appears on the expander outlet. The test facility is designed for a maximum pressure of 120 bar in the expander loop. The low pressure side of the simulation modell was fixed to the condenstion conditions like in expander test series I to III. These condensation conditions were 18 °C at the plunger pump inlet and 60 bar pressure at the expander outlet. The inlet and outlet temperatures of the heat exchanger (HX-2) were set to the average temperatures measured on this heat exchanger in the expander test series I to III.

The second result of the simulation was the reacheble increased work output. This increased work output will happen when the air-volume flow at the air loop and of the $CO_2$ massflow at the expander loop will be increased. A new generator will be necessary in the future for tests with incresed energy input on the expander. Like in subsection 4.3.2 describet, the existing generator has reached boundary conditions at test series III, were the energy input to the expander loop was increased. The simulation model was able to calculate the expander work output with an increased air-volume flow at the air loop, and an increased $CO_2$ massflow at the expander loop. With this results a new generator can be choosen, which will be able to convert all the mechanical work input by the expander to electical energy.

The simulation was performed with a $CO_2$ massflow of 3.5 $\frac{kg}{min}$ at the expander loop. The reason for that decision was the positive effect of test series III were, with increasing the $CO_2$ massflow, the highest efficiency at the expander was reachable in combination with less energy losses to the heat sink. With all this given values, the simulation model was able to run the simulation for the necessray volume-flow in the air loop.

The result of this simulation was a maximum of air-volume flow of 1 254.9 $\frac{m^3}{h}$ for a UA value of 2 000 $\frac{kW}{K}$, and for a UA value of 4 000 $\frac{kW}{K}$ a air-volume flow of 1 258.3 $\frac{m^3}{h}$, which would be necessary at the air loop. With the result of this simulation and the results of the expander tests, the new fan can be choosen. The fan should be able to provide the air-volume flow between maximum of 1 258.3 $\frac{m^3}{h}$ and the minimum of 531.7 $\frac{m^3}{h}$. This maximum air-volume flow is a simulation result. The minimum air-volume flow was the minimum of air-volume flow of all expander tests (Test 15) see D.

Another result of the simulation was a maximum work output at the expander of 297 W. This result can be found in appendix D.2.6. The new generator has to be able to convert

this work input by the expander into electrical energy.

### 5.2.3 Simulation of the heat transfer coefficient times area of HX-2 for the new air-volume flow

The aim for this simulations was to find out more about the behavior of HX-2 working on the conditions of the increased air-volume flow at the air loop. Based on results of subsection 5.2.1 nine different UA values of this exchanger between air loop and expander loop (HX-2) were found. This values were in a range from 2 288.70 $\frac{kW}{K}$ up to 4 607.95 $\frac{kW}{K}$. So the goal was to make the simulations for the two different UA values of 2 000 $\frac{kW}{K}$, and for 4 000 $\frac{kW}{K}$, by using the increased air-volume flow of 1 260 $\frac{m^3}{h}$. This air-volume flow was the result of the simulations of subsection 5.2.2. The simulation model in Pro/II has the possibility to plot a zone analysis of the temperature profile of the working fluids, which exchanges heat inside the heat exchanger. The simulations were performed with a constant air-volume flow and inlet tempereature of the heat exchanger. The $CO_2$ on the inlet and outlet temperatures and pressures were given as well, based on the results of expander test series I to III. The heat exchanger outlet temperature on the air side was simulated. This was important to be able to make some simulations with increased air-volume flow for the behavior of the heat sink and the heater of the air loop.

The results of this simulations for the two different UA values were not explainable by comparing the reults. The temperature profiles for the two diffent UA values were not much different in some cases. A disadvantage of this zone analysis modell in Pro/II is that the program is not able to print the single values used for the calculations. There is only a tempereature-profile plot function avilable. But this results of the model were not realistic, so it was necessary to find out the reason for this. After some studys of the PRO/II software a possibility was found the get the used calculation values for this zone analysis out of the programs file report of the simulation model. By using this option, the reason for this not realistic simulation results was found. The simulation model was not able to keep the UA value constant. For a constant setting of the UA value of 2 000 $\frac{kW}{K}$ a maximum difference in the calculations of 1 314.58 $\frac{kW}{K}$ was found in the program file report. This detailed results of the not acceptable simulations can be found in appendix D.3.

To find out more about this behavior of HX-2 and the tempereature profile on the air outlet side, a another simulation program is necessary. More simulations in this point would be necessary to find out how the test facility would be work with the increased air-volume flow at the air loop. Especially it would be impotant to know that the heater at the air loop is able to provide enough heat for the tests with incresed air-volume flow in the future. Another impotant point is that the heat sink has to be able to provide sufficient cooling energy for the increased energy input on the heat source in the future.

So more prelimary simulations would be necessary for further improvements on the Roma test facility.

# 6 Conclusion and future work

This Master Thesis is a work done as part of the Resource Optimization and recovery in the Materials industry project (Roma). This project is involved in the development of a new technology for power production from low temperature heat sources for offgases from aluminum production cells. The technology is based on an trans-critical Rankine cycle with $CO_2$ as a working fluid, as the work recovery circuit.

In the development of this new technology, a laboratory scale test facility was planed and built early in 2009. The center of this test facility is a prototype expander unit. This expander unit is included in a trans-critical Rankine cycle with $CO_2$ as a working fluid. In addition the laboratory test facility constitutes of four different cycles interacting with each other. The air loop delivers heat to the expander cycle and is build to simulate the low-grade heat source, which would be in reality the off gas from the aluminum production cells. Another circuit, the ethylene-glycole loop, provides the cooling for the expander cycle. A heat pump loop working as a supplementary circuit is included. The heat pump loop is build to extract as much as possible of the condensation heat of the expander loop, by using the ethylene-glycole loop as intermediate cycle. This recovered condenstion heat of the expander loop can be transfered back to the heat source (air loop) by using the heat pump loop.

The work on the Roma project and the power production from temperature heat sources started with a detailed simulation and uncertainty analysis of the prototype in the autumn of 2008. This results were used to design the laboratory scaled test faciliy. This work was continued where the main focus was on instrumentation and experimentals and improvements on the laboratory scaled test facily.

The research on the expander loop of the Roma test facility has two main aspects. The first aspect is to take out as much as possible energy from the heat source, which increases the energy input to the prototype expander. The important parameters for that are the expander inlet and outlet temperature and pressure. This expander inlet conditions are provided by the temperature and volume flow in the air loop, and the heat transfer from the heat source to the working fluid in the expander cycle. The expander outlet conditions are important too. There is a clear pressure difference between expander inlet and outlet were the best efficiency of the expander is reachable. The expander outlet pressure and temperature should be close to the two phase area in the t-h diagram, to have to transfer less condensation heat to the heat sink as possible. The other aspect

is to transfer as much as possible of this energy potential to mechanical work in the expander. The isentropic efficiency of the expander is an indicator to estimate this work transerd from the energy potential out of the waste heat to mechanical work. The isentropic efficiency of the expander describes how much of the theoretical expansion work is extracted in reality inside the expander.

The first aim of this Master Thesis was to research the behavoir of the expander. There were 81 tests of the expander unit perfomed during the process time of this thesis. The tests were performed with a set of different working conditions for the expander loop. It was found out that there exists for the expander in every tested set-up a clear maximium of efficiency and work output. The expander outlet point went up in the t-h diagram to the superheated region with increasing the heat source temperature by constant $CO_2$ massflow in the expander loop. In this cases there was an increased energy potential that was not used by the expander. This energy was transferred to the heat sink. One possibility to utilize this energy potential is to instal a recuperator at the expander loop. The second option to use this energy, is to convert it back to the heat sourc by using the heat pump loop. The third option is to increase the $CO_2$ massflow at the expander loop. This third option had the effect in the test serial III that the turbine inlet temperature were decreased and the energy losses to the heat sink were decreased as well. This will be the prefered way to achieve a good cycle efficiency with the existing test facility.

The second aim of this work was to find the boundary conditions when all four different cycles of the test facility interacting with each other. It was found out that there are exist limitations on the generator and the air-volume flow in the air loop. At test series III the generator has reached a housing temperature of 120 °C and an increased output voltage of 32.6 V maximum. This was a consequence of overstepped performance characteristics of the generator. Another boundary condition appears during the tests of series II at the heat-source temperature set-point of 110 °C. The temperature safety device stops the power supply to the heater. This was a result of low inlet velocity of air to the heater by maximal air-volume flow in the air loop. In the future are tests with inceased energy input to the expander loop planed, based on the results of the expander test series of this thesis. To be able to increase this energy input in the air loop, an increased air-volume flow in the air loop is necessary. The existing fan can not provide this increased air-volume flow. As a fact of this, a new fan is needed, which is able to provide an increased air-volume flow.

With the knowledge of this boundary conditions of the existing test facility a simulation model was constructed by using the program Pro/II. The needed air-volume flow and necessary size of the generator was simulated by using the results of the expander test series. The simulation was performed for a massflow of 3.5 $\frac{kg}{min}$ $CO_2$ in the expander loop. This will be the aim of expander tests in the future, based on the positive results of expander test series III. The result of the simulation was the needed range of air-volume flow, and achievable expander power output in the future. The new fan should be able

to provide an air-volume flow between the maximum of 1 258.3 $\frac{m^3}{h}$ and the minimum of 531.7 $\frac{m^3}{h}$. The new generator should be designed for a maximum work input by the expander of 297 W.

Furthermore there were simulations about the air outlet temperarure of the exchanger between air loop and expander loop (HX-2) with increased air-volume flow performed. This results are necessary to perform more simulations to find out how the test facility would work with the increased air-volume flow at the air loop. Especially it would be important to know how the behavoir of the heat source and heat sink will be. By using the zone analysis function in Pro/II, the simulation for the air outlet temperature of heat exchanger (HX-2) was performed. The results of this simulation were not realistic. The heat exchanger zone analysis simulation model was not able to keep the heat transfer coefficient times area value constant. So the resuts of the simulations of the zone analysis model are not acceptable for further calculations. More preliminary studys by using a suitable simulation program for the heat sink and heat source would be necessary, for further improvements at the Roma test facility.

# A Detailed positioning and identify diagrams of the Roma test facility

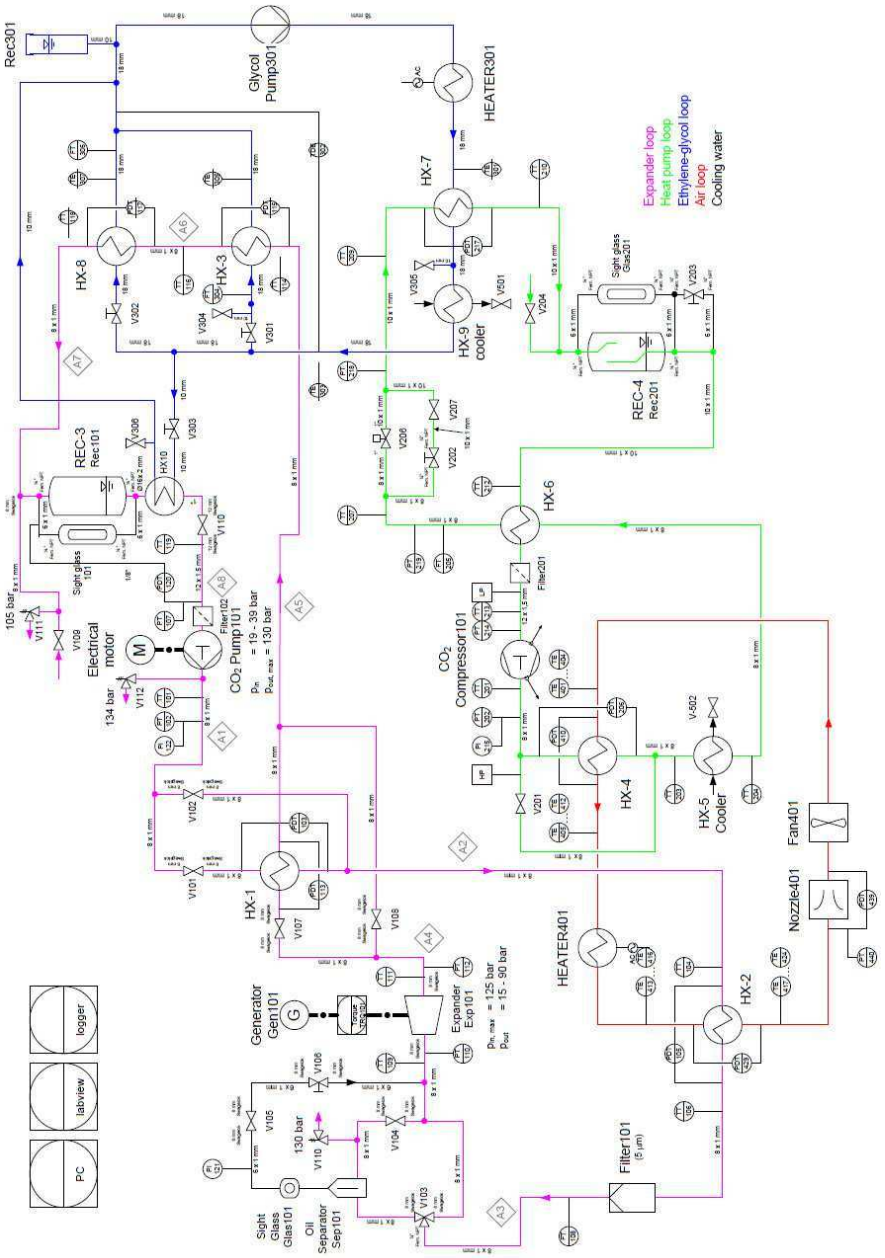




Figure A.1: Positioning and identify diagram of the Roma test facility with recuperator

# B Detailed figure of the existnig generator

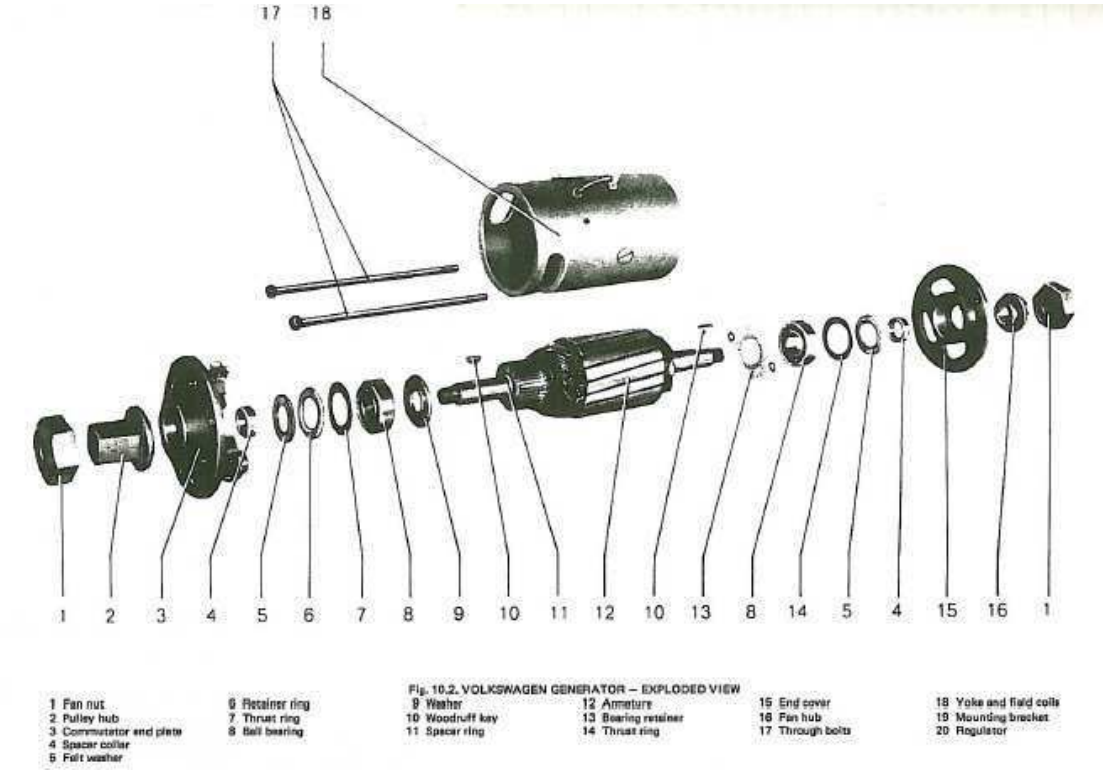


Figure B.1: The existing DC generator at the Roma test facility [26]

# C Test results and diagrams

## C.1 Test results and diagrams with 65 °C heat source temperature, 1.8 kg/min $CO_2$ mass flow at the expander loop and 60 bar condensation pressure

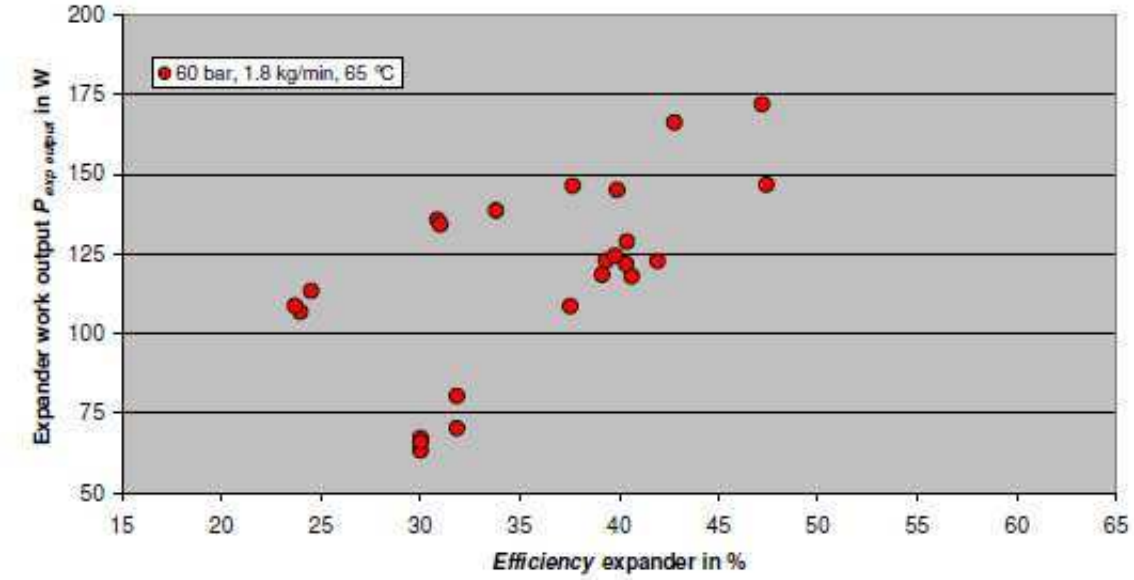


Figure C.1: Expander power output and efficiency, for tests with condensation conditions of 60 bar, 18 °C, with heat source temperature 65 °C and 1.8 $\frac{kg}{min}$ $CO_2$ mass flow at the expander loop

| Test number | Test 1 | Test 2 | Test 3 | Test 4 | Test 5 |
|---|---|---|---|---|---|
| $P_{exp\ output}$ in W | 98.26 | 93.89 | 90.71 | 91.49 | 94.72 |
| $M_{exp\ torque}$ in Nm | 0.39 | 0.37 | 0.36 | 0.36 | 0.37 |
| $rpm_{exp}$ in $min^{-1}$ | 2 400.72 | 2 429.28 | 2 428.27 | 2 448.31 | 2 477.36 |
| $\dot{m}_{CO2}$ in kg/min | 1.82 | 1.81 | 1.80 | 1.81 | 1.81 |
| $P_{pump\ inlet}$ in Pa | 5 858 919.60 | 5 817 805.11 | 5 871 542.36 | 5 898 629.01 | 5 847 951.09 |
| $P_{pump\ inlet}$ in bar | 58.59 | 58.18 | 58.72 | 58.99 | 58.48 |
| $t_{pump\ inlet}$ in °C | 17.86 | 18.02 | 17.72 | 18.31 | 18.22 |
| $s_{pump\ inlet}$ in J/kg*K | 1 156.74 | 1 159.43 | 1 154.83 | 1 161.50 | 1 161.31 |
| $h_{pump\ inlet}$ in J/kg | 246 978.74 | 247 711.98 | 246 441.28 | 248 417.24 | 248 296.95 |
| $h_{S\ pump\ outlet}$ in J/kg*K | 249 387.62 | 250 072.78 | 248 655.93 | 250 651.99 | 250 577.38 |
| $P_{pump\ outlet}$ in Pa | 7 816 051.80 | 7 728 922.65 | 7 673 952.61 | 7 703 730.43 | 7 689 892.34 |
| $P_{pump\ outlet}$ in bar | 78.16 | 77.29 | 76.74 | 77.04 | 76.90 |
| $t_{pump\ outlet}$ in °C | 20.93 | 21.08 | 20.55 | 21.21 | 21.18 |
| $s_{pump\ outlet}$ in J/kg*K | 1 159.72 | 1 162.61 | 1 157.75 | 1 164.40 | 1 164.26 |
| $h_{pump\ outlet}$ in J/kg | 250 263.72 | 251 009.44 | 249 510.80 | 251 503.46 | 251 446.16 |
| $\pi_{press\ ratio\ pump}$ | 1.33 | 1.33 | 1.31 | 1.31 | 1.31 |
| $P_{pump}$ in W | 99.80 | 99.55 | 92.14 | 92.98 | 95.15 |
| $\eta_{pump}$ in % | 73.33 | 71.59 | 72.15 | 72.41 | 72.41 |
| $P_{exp\ outlet}$ in Pa | 5 988 248.92 | 5 949 411.40 | 6 003 125.18 | 6 026 364.89 | 5 981 167.80 |
| $P_{exp\ outlet}$ in bar | 59.88 | 59.49 | 60.03 | 60.26 | 59.81 |
| $t_{exp\ outlet}$ in °C | 46.75 | 47.11 | 47.71 | 48.37 | 48.48 |
| $s_{exp\ outlet}$ in J/kg*K | 1 883.88 | 1 888.31 | 1 887.69 | 1 889.50 | 1 893.01 |
| $h_{exp\ outlet}$ in J/kg*K | 463 565.24 | 464 702.69 | 464 896.07 | 465 643.45 | 466 444.03 |
| $h_{S\ exp\ outlet}$ in J/kg | 457 310.04 | 458 430.53 | 459 157.66 | 460 002.45 | 460 486.53 |
| $P_{exp\ inlet}$ in Pa | 7 651 946.02 | 7 563 924.31 | 7 510 039.00 | 7 539 181.11 | 7 523 906.39 |
| $P_{exp\ inlet}$ in bar | 76.52 | 75.64 | 75.10 | 75.39 | 75.24 |
| $t_{exp\ inlet}$ in °C | 62.71 | 62.61 | 62.24 | 62.99 | 63.32 |
| $s_{exp\ inlet}$ in J/kg*K | 1 864.21 | 1 868.61 | 1 869.71 | 1 871.86 | 1 874.38 |
| $h_{exp\ inlet}$ in J/kg | 467 804.34 | 468 770.68 | 468 824.42 | 469 717.17 | 470 475.34 |
| $\pi_{press\ ratio\ exp}$ | 1.28 | 1.27 | 1.25 | 1.25 | 1.26 |
| $P_{exp}$ in W | 128.78 | 122.81 | 117.92 | 122.73 | 121.80 |
| $\eta_{exp}$ in % | 40.39 | 39.34 | 40.64 | 41.93 | 40.36 |
| $\overline{x}\ t_{HX\text{-}2\ inlet}$ in °C | 71.55 | 71.34 | 70.96 | 72.06 | 72.22 |
| $t_{HX\text{-}2\ inlet\text{-}1}$ in °C | 65.96 | 65.97 | 65.46 | 66.45 | 66.69 |
| $t_{HX\text{-}2\ inlet\text{-}2}$ in °C | 71.63 | 71.46 | 71.17 | 72.12 | 72.15 |
| $t_{HX\text{-}2\ inlet\text{-}3}$ in °C | 76.63 | 76.26 | 76.06 | 77.25 | 77.24 |
| $t_{HX\text{-}2\ inlet\text{-}4}$ in °C | 71.97 | 71.65 | 71.14 | 72.44 | 72.79 |
| $\overline{x}\ t_{HX\text{-}2\ outlet}$ in °C | 35.12 | 35.11 | 34.72 | 35.28 | 35.54 |
| $t_{HX\text{-}2\ outlet\text{-}1}$ in °C | 34.81 | 34.80 | 34.41 | 34.93 | 35.23 |
| $t_{HX\text{-}2\ outlet\text{-}2}$ in °C | 34.79 | 34.77 | 34.41 | 34.94 | 35.18 |
| $t_{HX\text{-}2\ outlet\text{-}3}$ in °C | 36.60 | 36.60 | 36.22 | 36.83 | 37.10 |
| $t_{HX\text{-}2\ outlet\text{-}4}$ in °C | 37.01 | 37.01 | 36.64 | 37.27 | 37.55 |
| $t_{HX\text{-}2\ outlet\text{-}5}$ in °C | 33.64 | 33.63 | 33.22 | 33.74 | 33.95 |
| $t_{HX\text{-}2\ outlet\text{-}6}$ in °C | 34.30 | 34.32 | 33.94 | 34.45 | 34.70 |
| $t_{HX\text{-}2\ outlet\text{-}7}$ in °C | 35.43 | 35.41 | 35.00 | 35.58 | 35.83 |
| $t_{HX\text{-}2\ outlet\text{-}8}$ in °C | 34.36 | 34.34 | 33.95 | 34.51 | 34.79 |
| $P_{HX\text{-}2\ inlet}$ in Pa | 100 706.09 | 100 637.70 | 100 592.48 | 100 530.16 | 100 526.96 |
| $P_{HX\text{-}2\ inlet}$ in bar | 1.01 | 1.01 | 1.01 | 1.01 | 1.01 |
| $P_{HX\text{-}2\ outlet}$ in Pa | 99 653.36 | 99 585.20 | 99 539.39 | 99 478.12 | 99 476.55 |
| $P_{HX\text{-}2\ outlet}$ in bar | 1.00 | 1.00 | 1.00 | 0.99 | 0.99 |
| $\eta_{cycle}$ in % | 129.05 | 123.37 | 127.98 | 132.00 | 128.01 |

Table C.1: Tests 1-5

| Test number | Test 6 | Test 7 | Test 8 | Test 9 | Test 10 |
|---|---|---|---|---|---|
| $P_{exp\ output}$ in W | 30.06 | 34.26 | 96.37 | 88.70 | 33.30 |
| $M_{exp\ torque}$ in Nm | 0.17 | 0.19 | 0.41 | 0.37 | 0.19 |
| $rpm_{exp}$ in $min^{-1}$ | 1 663.01 | 1 702.26 | 2 224.63 | 2 288.80 | 1 713.56 |
| $\dot{m}_{CO2}$ in kg/min | 1.75 | 1.79 | 1.82 | 1.81 | 1.78 |
| $P_{pump\ inlet}$ in Pa | 5 814 433.06 | 5 845 968.30 | 5 857 782.64 | 5 808 639.94 | 5 829 574.91 |
| $P_{pump\ inlet}$ in bar | 58.14 | 58.46 | 58.58 | 58.09 | 58.30 |
| $t_{pump\ inlet}$ in °C | 17.76 | 17.93 | 18.06 | 17.63 | 17.77 |
| $s_{pump\ inlet}$ in J/kg*K | 1 156.35 | 1 157.79 | 1 159.24 | 1 154.82 | 1 156.16 |
| $h_{pump\ inlet}$ in J/kg | 246 811.54 | 247 270.85 | 247 705.26 | 246 360.35 | 246 775.04 |
| $h_{S\ pump\ outlet}$ in J/kg*K | 248 438.44 | 248 984.10 | 250 070.95 | 248 614.15 | 248 457.57 |
| $P_{pump\ outlet}$ in Pa | 7 133 144.92 | 7 233 040.83 | 7 773 935.66 | 7 642 260.07 | 7 194 094.29 |
| $P_{pump\ outlet}$ in bar | 71.33 | 72.33 | 77.74 | 76.42 | 71.94 |
| $t_{pump\ outlet}$ in °C | 19.99 | 20.24 | 21.11 | 20.55 | 20.04 |
| $s_{pump\ outlet}$ in J/kg*K | 1 159.89 | 1 161.06 | 1 162.29 | 1 158.19 | 1 159.51 |
| $h_{pump\ outlet}$ in J/kg | 249 474.60 | 249 942.80 | 250 969.60 | 249 602.73 | 249 437.84 |
| $\pi_{press\ ratio\ pump}$ | 1.23 | 1.24 | 1.33 | 1.32 | 1.23 |
| $P_{pump}$ in W | 77.62 | 79.86 | 98.85 | 97.67 | 78.97 |
| $\eta_{pump}$ in % | 61.09 | 64.12 | 72.47 | 69.51 | 63.19 |
| $P_{exp\ outlet}$ in Pa | 5 939 421.88 | 5 978 025.77 | 5 988 682.15 | 5 940 566.97 | 5 960 425.13 |
| $P_{exp\ outlet}$ in bar | 59.39 | 59.78 | 59.89 | 59.41 | 59.60 |
| $t_{exp\ outlet}$ in °C | 54.00 | 52.86 | 47.34 | 48.53 | 53.75 |
| $s_{exp\ outlet}$ in J/kg*K | 1 921.81 | 1 914.17 | 1 886.82 | 1 895.93 | 1 919.38 |
| $h_{exp\ outlet}$ in J/kg*K | 475 469.22 | 473 272.78 | 464 510.33 | 467 082.82 | 474 837.04 |
| $h_{S\ exp\ outlet}$ in J/kg | 470 401.91 | 468 033.25 | 458 303.29 | 460 976.37 | 469 768.58 |
| $P_{exp\ inlet}$ in Pa | 6 960 149.81 | 7 057 636.67 | 7 610 502.05 | 7 475 881.18 | 7 018 137.82 |
| $P_{exp\ inlet}$ in bar | 69.60 | 70.58 | 76.11 | 74.76 | 70.18 |
| $t_{exp\ inlet}$ in °C | 63.53 | 62.91 | 62.87 | 63.28 | 63.68 |
| $s_{exp\ inlet}$ in J/kg*K | 1 906.24 | 1 898.02 | 1 867.34 | 1 876.83 | 1 903.79 |
| $h_{exp\ inlet}$ in J/kg | 477 643.00 | 475 520.73 | 468 615.56 | 471 012.69 | 477 205.10 |
| $\pi_{press\ ratio\ exp}$ | 1.17 | 1.18 | 1.27 | 1.26 | 1.18 |
| $P_{exp}$ in W | 63.36 | 67.19 | 124.31 | 118.38 | 70.23 |
| $\eta_{exp}$ in % | 30.02 | 30.02 | 39.81 | 39.16 | 31.84 |
| $\overline{x}\ t_{HX\text{-}2\ inlet}$ in °C | 72.75 | 72.00 | 71.81 | 72.32 | 73.16 |
| $t_{HX\text{-}2\ inlet\text{-}1}$ in °C | 66.94 | 66.20 | 66.34 | 66.74 | 67.31 |
| $t_{HX\text{-}2\ inlet\text{-}2}$ in °C | 72.50 | 71.75 | 71.74 | 72.09 | 72.76 |
| $t_{HX\text{-}2\ inlet\text{-}3}$ in °C | 78.05 | 77.26 | 76.97 | 77.49 | 78.53 |
| $t_{HX\text{-}2\ inlet\text{-}4}$ in °C | 73.50 | 72.80 | 72.21 | 72.96 | 74.06 |
| $\overline{x}\ t_{HX\text{-}2\ outlet}$ in °C | 35.11 | 34.16 | 35.39 | 35.34 | 34.71 |
| $t_{HX\text{-}2\ outlet\text{-}1}$ in °C | 34.59 | 33.82 | 35.08 | 35.01 | 34.29 |
| $t_{HX\text{-}2\ outlet\text{-}2}$ in °C | 35.34 | 34.03 | 35.08 | 34.97 | 34.68 |
| $t_{HX\text{-}2\ outlet\text{-}3}$ in °C | 36.63 | 35.46 | 36.99 | 36.97 | 36.08 |
| $t_{HX\text{-}2\ outlet\text{-}4}$ in °C | 36.96 | 35.74 | 37.45 | 37.45 | 36.48 |
| $t_{HX\text{-}2\ outlet\text{-}5}$ in °C | 33.71 | 32.71 | 33.82 | 33.71 | 33.17 |
| $t_{HX\text{-}2\ outlet\text{-}6}$ in °C | 34.42 | 33.40 | 34.52 | 34.45 | 33.99 |
| $t_{HX\text{-}2\ outlet\text{-}7}$ in °C | 35.18 | 34.56 | 35.61 | 35.56 | 34.98 |
| $t_{HX\text{-}2\ outlet\text{-}8}$ in °C | 34.05 | 33.59 | 34.57 | 34.56 | 34.04 |
| $P_{HX\text{-}2\ inlet}$ in Pa | 100 818.89 | 100 833.68 | 100 866.07 | 100 901.24 | 100 941.64 |
| $P_{HX\text{-}2\ inlet}$ in bar | 1.01 | 1.01 | 1.01 | 1.01 | 1.01 |
| $P_{HX\text{-}2\ outlet}$ in Pa | 99 769.86 | 99 781.57 | 99 813.77 | 99 847.72 | 99 890.57 |
| $P_{HX\text{-}2\ outlet}$ in bar | 1.00 | 1.00 | 1.00 | 1.00 | 1.00 |
| $\eta_{cycle}$ in % | 81.63 | 84.13 | 125.76 | 121.20 | 88.93 |

Table C.2: Tests 6-10

| Test number | Test 11 | Test 12 | Test 13 | Test 14 | Test 15 |
|---|---|---|---|---|---|
| $P_{exp\ output}$ in W | 50.25 | 78.82 | 118.39 | 124.62 | 121.55 |
| $M_{exp\ torque}$ in Nm | 0.27 | 0.35 | 0.54 | 0.68 | 0.73 |
| $rpm_{exp}$ in $min^{-1}$ | 1 792.09 | 2 140.21 | 2 083.30 | 1 759.40 | 1 581.70 |
| $\dot{m}_{CO2}$ in kg/min | 1.79 | 1.81 | 1.82 | 1.79 | 1.80 |
| $P_{pump\ inlet}$ in Pa | 5 880 727.27 | 5 860 681.79 | 5 847 948.91 | 5 872 794.75 | 5 858 036.78 |
| $P_{pump\ inlet}$ in bar | 58.81 | 58.61 | 58.48 | 58.73 | 58.58 |
| $t_{pump\ inlet}$ in °C | 18.29 | 18.09 | 17.97 | 18.26 | 18.11 |
| $s_{pump\ inlet}$ in J/kg*K | 1 161.52 | 1 159.52 | 1 158.23 | 1 161.38 | 1 159.83 |
| $h_{pump\ inlet}$ in J/kg | 248 398.98 | 247 791.53 | 247 400.64 | 248 349.83 | 247 879.38 |
| $h_{S\ pump\ outlet}$ in J/kg*K | 250 327.18 | 249 982.14 | 250 179.14 | 251 486.30 | 251 214.20 |
| $P_{pump\ outlet}$ in Pa | 7 436 443.45 | 7 633 505.31 | 8 103 802.80 | 8 413 197.93 | 8 565 460.87 |
| $P_{pump\ outlet}$ in bar | 74.36 | 76.34 | 81.04 | 84.13 | 85.65 |
| $t_{pump\ outlet}$ in °C | 20.85 | 20.95 | 21.47 | 22.19 | 22.24 |
| $s_{pump\ outlet}$ in J/kg*K | 1 164.59 | 1 162.64 | 1 161.33 | 1 164.41 | 1 162.85 |
| $h_{pump\ outlet}$ in J/kg | 251 228.67 | 250 900.01 | 251 092.43 | 252 380.95 | 252 104.62 |
| $\pi_{press\ ratio\ pump}$ | 1.26 | 1.30 | 1.39 | 1.43 | 1.46 |
| $P_{pump}$ in W | 84.59 | 93.93 | 112.18 | 119.98 | 126.69 |
| $\eta_{pump}$ in % | 68.14 | 70.47 | 75.26 | 77.81 | 78.93 |
| $P_{exp\ outlet}$ in Pa | 6 010 541.94 | 5 992 551.06 | 5 979 376.14 | 5 994 597.55 | 5 982 977.78 |
| $P_{exp\ outlet}$ in bar | 60.11 | 59.93 | 59.79 | 59.95 | 59.83 |
| $t_{exp\ outlet}$ in °C | 51.45 | 48.58 | 45.06 | 41.92 | 40.74 |
| $s_{exp\ outlet}$ in J/kg*K | 1 905.51 | 1 892.75 | 1 875.72 | 1 857.66 | 1 851.79 |
| $h_{exp\ outlet}$ in J/kg*K | 470 698.74 | 466 443.55 | 460 898.78 | 455 287.06 | 453 362.57 |
| $h_{S\ exp\ outlet}$ in J/kg | 464 947.63 | 460 472.11 | 453 709.75 | 447 155.86 | 444 319.95 |
| $P_{exp\ inlet}$ in Pa | 7 267 365.10 | 7 466 866.33 | 7 944 520.27 | 8 265 295.91 | 8 419 158.04 |
| $P_{exp\ inlet}$ in bar | 72.67 | 74.67 | 79.45 | 82.65 | 84.19 |
| $t_{exp\ inlet}$ in °C | 63.16 | 62.63 | 63.65 | 63.01 | 62.97 |
| $s_{exp\ inlet}$ in J/kg*K | 1 887.69 | 1 874.08 | 1 852.97 | 1 831.67 | 1 822.76 |
| $h_{exp\ inlet}$ in J/kg | 473 387.06 | 470 034.91 | 465 671.33 | 460 201.25 | 457 981.59 |
| $\pi_{press\ ratio\ exp}$ | 1.21 | 1.25 | 1.33 | 1.38 | 1.41 |
| $P_{exp}$ in W | 80.36 | 108.52 | 145.02 | 146.26 | 138.50 |
| $\eta_{exp}$ in % | 31.85 | 37.56 | 39.90 | 37.67 | 33.81 |
| $\overline{x}\ t_{HX\text{-}2\ inlet}$ in °C | 72.03 | 71.59 | 72.79 | 71.67 | 71.60 |
| $t_{HX\text{-}2\ inlet\text{-}1}$ in °C | 66.54 | 65.92 | 67.06 | 66.36 | 66.38 |
| $t_{HX\text{-}2\ inlet\text{-}2}$ in °C | 72.01 | 71.59 | 72.71 | 71.61 | 71.65 |
| $t_{HX\text{-}2\ inlet\text{-}3}$ in °C | 77.09 | 76.79 | 78.03 | 76.60 | 76.56 |
| $t_{HX\text{-}2\ inlet\text{-}4}$ in °C | 72.46 | 72.05 | 73.34 | 72.13 | 71.83 |
| $\overline{x}\ t_{HX\text{-}2\ outlet}$ in °C | 35.37 | 34.95 | 36.55 | 37.30 | 37.17 |
| $t_{HX\text{-}2\ outlet\text{-}1}$ in °C | 35.34 | 34.65 | 36.16 | 36.86 | 36.68 |
| $t_{HX\text{-}2\ outlet\text{-}2}$ in °C | 35.04 | 34.61 | 36.25 | 37.07 | 36.86 |
| $t_{HX\text{-}2\ outlet\text{-}3}$ in °C | 36.84 | 36.54 | 38.20 | 39.03 | 38.96 |
| $t_{HX\text{-}2\ outlet\text{-}4}$ in °C | 37.28 | 37.00 | 38.62 | 39.35 | 39.30 |
| $t_{HX\text{-}2\ outlet\text{-}5}$ in °C | 33.84 | 33.40 | 34.93 | 35.44 | 35.46 |
| $t_{HX\text{-}2\ outlet\text{-}6}$ in °C | 34.51 | 34.10 | 35.70 | 36.47 | 36.21 |
| $t_{HX\text{-}2\ outlet\text{-}7}$ in °C | 35.57 | 35.17 | 36.81 | 37.70 | 37.54 |
| $t_{HX\text{-}2\ outlet\text{-}8}$ in °C | 34.51 | 34.15 | 35.72 | 36.51 | 36.36 |
| $P_{HX\text{-}2\ inlet}$ in Pa | 100 973.82 | 101 015.86 | 101 058.71 | 101 090.95 | 101 103.27 |
| $P_{HX\text{-}2\ inlet}$ in bar | 1.01 | 1.01 | 1.01 | 1.01 | 1.01 |
| $P_{HX\text{-}2\ outlet}$ in Pa | 99 921.14 | 99 959.71 | 100 007.16 | 100 039.39 | 100 050.98 |
| $P_{HX\text{-}2\ outlet}$ in bar | 1.00 | 1.00 | 1.00 | 1.00 | 1.00 |
| $\eta_{cycle}$ in % | 95.00 | 115.53 | 129.28 | 121.91 | 109.32 |

Table C.3: Tests 11-15

| Test number | Test 16 | Test 17 | Test 18 | Test 19 | Test 20 |
|---|---|---|---|---|---|
| $P_{exp\ output}$ in W | 119.83 | 120.29 | 99.94 | 100.40 | 102.45 |
| $M_{exp\ torque}$ in Nm | 0.85 | 0.83 | 0.94 | 0.97 | 0.95 |
| $rpm_{exp}$ in $min^{-1}$ | 1 342.20 | 1 386.44 | 1 018.07 | 989.54 | 1 029.19 |
| $\dot{m}_{CO2}$ in kg/min | 1.81 | 1.81 | 1.79 | 1.82 | 1.81 |
| $P_{pump\ inlet}$ in Pa | 5 867 556.65 | 5 865 737.05 | 5 855 262.56 | 5 866 716.79 | 5 819 593.10 |
| $P_{pump\ inlet}$ in bar | 58.68 | 58.66 | 58.55 | 58.67 | 58.20 |
| $t_{pump\ inlet}$ in °C | 18.17 | 18.17 | 18.05 | 18.13 | 17.89 |
| $s_{pump\ inlet}$ in J/kg*K | 1 160.29 | 1 160.33 | 1 159.08 | 1 159.87 | 1 157.80 |
| $h_{pump\ inlet}$ in J/kg | 248 024.08 | 248 033.88 | 247 656.46 | 247 900.95 | 247 239.86 |
| $h_{S\ pump\ outlet}$ in J/kg*K | 251 697.32 | 251 648.67 | 251 510.26 | 251 870.17 | 251 152.18 |
| $P_{pump\ outlet}$ in Pa | 8 851 235.85 | 8 801 264.24 | 8 991 308.78 | 9 095 113.32 | 9 007 616.71 |
| $P_{pump\ outlet}$ in bar | 88.51 | 88.01 | 89.91 | 90.95 | 90.08 |
| $t_{pump\ outlet}$ in °C | 22.66 | 22.60 | 22.74 | 22.95 | 22.55 |
| $s_{pump\ outlet}$ in J/kg*K | 1 163.22 | 1 163.27 | 1 162.17 | 1 162.89 | 1 160.11 |
| $h_{pump\ outlet}$ in J/kg | 252 563.31 | 252 518.28 | 252 423.85 | 252 765.11 | 251 834.37 |
| $\pi_{press\ ratio\ pump}$ | 1.51 | 1.50 | 1.54 | 1.55 | 1.55 |
| $P_{pump}$ in W | 136.83 | 134.94 | 142.00 | 147.45 | 138.95 |
| $\eta_{pump}$ in % | 80.92 | 80.61 | 80.84 | 81.60 | 85.15 |
| $P_{exp\ outlet}$ in Pa | 5 991 848.55 | 5 989 850.19 | 5 975 995.91 | 5 992 362.48 | 5 940 296.10 |
| $P_{exp\ outlet}$ in bar | 59.92 | 59.90 | 59.76 | 59.92 | 59.40 |
| $t_{exp\ outlet}$ in °C | 38.87 | 38.86 | 37.31 | 36.61 | 37.13 |
| $s_{exp\ outlet}$ in J/kg*K | 1 840.16 | 1 840.27 | 1 831.89 | 1 826.13 | 1 833.63 |
| $h_{exp\ outlet}$ in J/kg*K | 449 783.44 | 449 803.06 | 447 104.23 | 445 423.53 | 447 410.72 |
| $h_{S\ exp\ outlet}$ in J/kg | 439 706.77 | 439 890.58 | 435 732.16 | 433 892.07 | 435 875.43 |
| $P_{exp\ inlet}$ in Pa | 8 709 068.42 | 8 658 609.44 | 8 852 585.37 | 8 953 791.99 | 8 868 274.07 |
| $P_{exp\ inlet}$ in bar | 87.09 | 86.59 | 88.53 | 89.54 | 88.68 |
| $t_{exp\ inlet}$ in °C | 63.18 | 62.81 | 62.48 | 62.41 | 62.80 |
| $s_{exp\ inlet}$ in J/kg*K | 1 807.60 | 1 808.24 | 1 794.93 | 1 788.57 | 1 796.11 |
| $h_{exp\ inlet}$ in J/kg | 454 284.62 | 454 261.80 | 450 689.24 | 449 007.56 | 451 157.36 |
| $\pi_{press\ ratio\ exp}$ | 1.45 | 1.45 | 1.48 | 1.49 | 1.49 |
| $P_{exp}$ in W | 135.68 | 134.17 | 106.78 | 108.65 | 113.31 |
| $\eta_{exp}$ in % | 30.88 | 31.03 | 23.97 | 23.71 | 24.52 |
| $\overline{x}\ t_{HX\text{-}2\ inlet}$ in °C | 71.72 | 71.10 | 70.62 | 70.84 | 71.09 |
| $t_{HX\text{-}2\ inlet\text{-}1}$ in °C | 66.64 | 66.12 | 65.67 | 65.65 | 66.04 |
| $t_{HX\text{-}2\ inlet\text{-}2}$ in °C | 71.83 | 71.30 | 70.81 | 71.09 | 71.28 |
| $t_{HX\text{-}2\ inlet\text{-}3}$ in °C | 76.49 | 75.79 | 75.31 | 75.69 | 75.85 |
| $t_{HX\text{-}2\ inlet\text{-}4}$ in °C | 71.92 | 71.17 | 70.68 | 70.95 | 71.19 |
| $\overline{x}\ t_{HX\text{-}2\ outlet}$ in °C | 37.70 | 37.43 | 37.87 | 37.67 | 37.73 |
| $t_{HX\text{-}2\ outlet\text{-}1}$ in °C | 37.37 | 37.18 | 37.71 | 37.56 | 37.59 |
| $t_{HX\text{-}2\ outlet\text{-}2}$ in °C | 37.34 | 37.13 | 37.62 | 37.47 | 37.48 |
| $t_{HX\text{-}2\ outlet\text{-}3}$ in °C | 39.39 | 39.04 | 39.37 | 39.04 | 39.12 |
| $t_{HX\text{-}2\ outlet\text{-}4}$ in °C | 39.68 | 39.34 | 39.59 | 39.31 | 39.39 |
| $t_{HX\text{-}2\ outlet\text{-}5}$ in °C | 36.26 | 36.04 | 36.57 | 36.44 | 36.48 |
| $t_{HX\text{-}2\ outlet\text{-}6}$ in °C | 36.82 | 36.59 | 37.08 | 36.93 | 36.94 |
| $t_{HX\text{-}2\ outlet\text{-}7}$ in °C | 37.87 | 37.59 | 38.03 | 37.85 | 37.93 |
| $t_{HX\text{-}2\ outlet\text{-}8}$ in °C | 36.84 | 36.56 | 36.97 | 36.79 | 36.92 |
| $P_{HX\text{-}2\ inlet}$ in Pa | 101 111.10 | 101 127.93 | 101 161.61 | 101 188.46 | 101 545.35 |
| $P_{HX\text{-}2\ inlet}$ in bar | 1.01 | 1.01 | 1.01 | 1.01 | 1.02 |
| $P_{HX\text{-}2\ outlet}$ in Pa | 100 059.47 | 100 076.14 | 100 111.57 | 100 138.27 | 100 491.33 |
| $P_{HX\text{-}2\ outlet}$ in bar | 1.00 | 1.00 | 1.00 | 1.00 | 1.00 |
| $\eta_{cycle}$ in % | 99.16 | 99.43 | 75.20 | 73.68 | 81.55 |

Table C.4: Tests 16-20

| Test number | Test 21 | Test 22 | Test 23 | Test 24 |
|---|---|---|---|---|
| $P_{exp\ output}$ in W | 141.70 | 140.91 | 110.19 | 32.59 |
| $M_{exp\ torque}$ in Nm | 0.68 | 0.56 | 0.38 | 0.19 |
| $rpm_{exp}$ in $min^{-1}$ | 2 003.05 | 2 389.16 | 2 734.77 | 1 653.18 |
| $\dot{m}_{CO2}$ in kg/min | 1.80 | 1.81 | 1.82 | 1.79 |
| $P_{pump\ inlet}$ in Pa | 5 861 041.15 | 5 860 760.74 | 5 857 910.56 | 5 867 691.35 |
| $P_{pump\ inlet}$ in bar | 58.61 | 58.61 | 58.58 | 58.68 |
| $t_{pump\ inlet}$ in °C | 17.99 | 17.99 | 17.96 | 18.02 |
| $s_{pump\ inlet}$ in J/kg*K | 1 158.30 | 1 158.31 | 1 157.92 | 1 158.48 |
| $h_{pump\ inlet}$ in J/kg | 247 437.34 | 247 438.25 | 247 321.88 | 247 496.20 |
| $h_{S\ pump\ outlet}$ in J/kg*K | 250 544.83 | 250 249.25 | 249 658.45 | 249 178.69 |
| $P_{pump\ outlet}$ in Pa | 8 386 560.11 | 8 143 252.78 | 7 753 239.10 | 7 228 866.70 |
| $P_{pump\ outlet}$ in bar | 83.87 | 81.43 | 77.53 | 72.29 |
| $t_{pump\ outlet}$ in °C | 21.82 | 21.49 | 20.94 | 20.28 |
| $s_{pump\ outlet}$ in J/kg*K | 1 160.96 | 1 160.98 | 1 160.74 | 1 161.54 |
| $h_{pump\ outlet}$ in J/kg | 251 329.20 | 251 036.24 | 250 489.19 | 250 078.28 |
| $\pi_{press\ ratio\ pump}$ | 1.43 | 1.39 | 1.32 | 1.23 |
| $P_{pump}$ in W | 116.88 | 108.28 | 95.82 | 76.89 |
| $\eta_{pump}$ in % | 79.85 | 78.13 | 73.77 | 65.16 |
| $P_{exp\ outlet}$ in Pa | 5 982 142.95 | 5 985 863.91 | 5 986 244.59 | 5 996 455.11 |
| $P_{exp\ outlet}$ in bar | 59.82 | 59.86 | 59.86 | 59.96 |
| $t_{exp\ outlet}$ in °C | 40.98 | 44.26 | 46.97 | 53.70 |
| $s_{exp\ outlet}$ in J/kg*K | 1 853.24 | 1 871.02 | 1 885.08 | 1 916.91 |
| $h_{exp\ outlet}$ in J/kg*K | 453 812.95 | 459 453.32 | 463 937.17 | 474 305.07 |
| $h_{S\ exp\ outlet}$ in J/kg | 446 420.24 | 453 064.36 | 458 563.27 | 469 150.42 |
| $P_{exp\ inlet}$ in Pa | 8 236 244.67 | 7 986 947.37 | 7 588 850.80 | 7 053 847.20 |
| $P_{exp\ inlet}$ in bar | 82.36 | 79.87 | 75.89 | 70.54 |
| $t_{exp\ inlet}$ in °C | 62.35 | 63.67 | 62.81 | 63.51 |
| $s_{exp\ inlet}$ in J/kg*K | 1 829.56 | 1 850.78 | 1 868.21 | 1 901.05 |
| $h_{exp\ inlet}$ in J/kg | 459 344.61 | 465 163.36 | 468 783.13 | 476 516.96 |
| $\pi_{press\ ratio\ exp}$ | 1.38 | 1.33 | 1.27 | 1.18 |
| $P_{exp}$ in W | 166.12 | 171.84 | 146.60 | 65.86 |
| $\eta_{exp}$ in % | 42.80 | 47.19 | 47.42 | 30.03 |
| $\overline{x}\ t_{HX\text{-}2\ inlet}$ in °C | 70.91 | 72.63 | 71.81 | 72.60 |
| $t_{HX\text{-}2\ inlet\text{-}1}$ in °C | 65.71 | 67.08 | 66.23 | 66.76 |
| $t_{HX\text{-}2\ inlet\text{-}2}$ in °C | 70.96 | 72.61 | 71.73 | 72.65 |
| $t_{HX\text{-}2\ inlet\text{-}3}$ in °C | 75.67 | 77.68 | 76.78 | 77.90 |
| $t_{HX\text{-}2\ inlet\text{-}4}$ in °C | 71.29 | 73.14 | 72.49 | 73.10 |
| $\overline{x}\ t_{HX\text{-}2\ outlet}$ in °C | 36.39 | 36.86 | 35.31 | 34.84 |
| $t_{HX\text{-}2\ outlet\text{-}1}$ in °C | 36.01 | 36.49 | 35.00 | 34.46 |
| $t_{HX\text{-}2\ outlet\text{-}2}$ in °C | 36.03 | 36.55 | 34.99 | 34.81 |
| $t_{HX\text{-}2\ outlet\text{-}3}$ in °C | 38.05 | 38.50 | 36.87 | 36.12 |
| $t_{HX\text{-}2\ outlet\text{-}4}$ in °C | 38.42 | 38.91 | 37.32 | 36.45 |
| $t_{HX\text{-}2\ outlet\text{-}5}$ in °C | 34.77 | 35.12 | 33.76 | 33.41 |
| $t_{HX\text{-}2\ outlet\text{-}6}$ in °C | 35.45 | 35.96 | 34.44 | 34.23 |
| $t_{HX\text{-}2\ outlet\text{-}7}$ in °C | 36.72 | 37.22 | 35.58 | 35.13 |
| $t_{HX\text{-}2\ outlet\text{-}8}$ in °C | 35.69 | 36.16 | 34.55 | 34.10 |
| $P_{HX\text{-}2\ inlet}$ in Pa | 101 565.68 | 101 580.04 | 101 580.29 | 101 586.56 |
| $P_{HX\text{-}2\ inlet}$ in bar | 1.02 | 1.02 | 1.02 | 1.02 |
| $P_{HX\text{-}2\ outlet}$ in Pa | 100 508.90 | 100 523.47 | 100 519.08 | 100 529.30 |
| $P_{HX\text{-}2\ outlet}$ in bar | 1.01 | 1.01 | 1.01 | 1.01 |
| $\eta_{cycle}$ in % | 142.13 | 158.70 | 153.00 | 85.66 |

Table C.5: Tests 21-24

## C.2 Test results and diagrams with 90 °C heat source temperature, 1.8 kg/min $CO_2$ mass flow at the expander loop and 60 bar condensation pressure

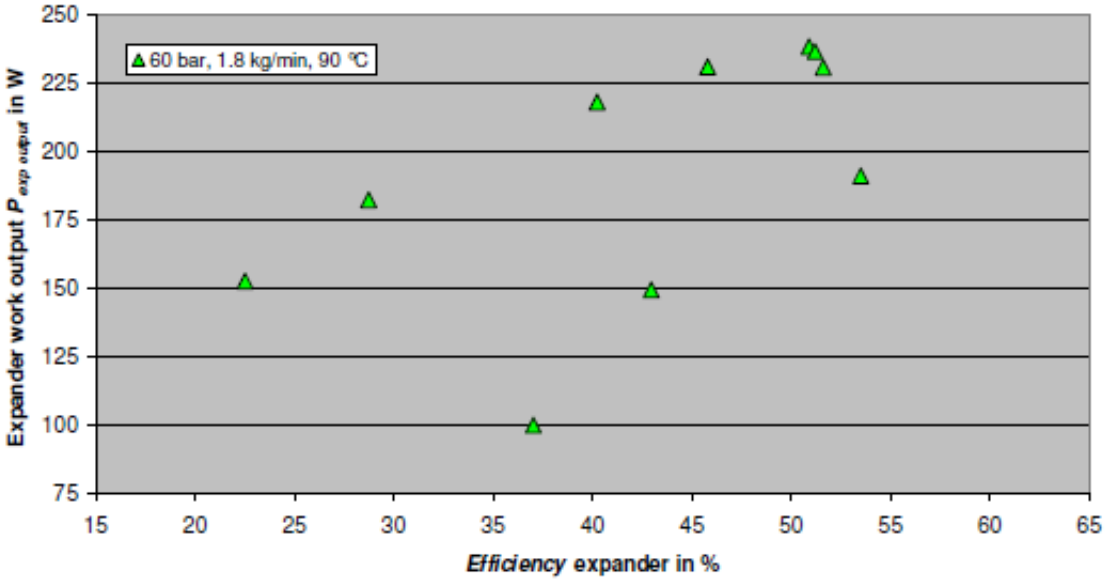


Figure C.2: Expander power output and efficiency, for tests with condensation conditions of 60 bar, 18 °C, with heat source temperature 65 °C and 1.8 $\frac{kg}{min}$ $CO_2$ mass flow at the expander loop

| Test number | Test 25 | Test 26 | Test 27 | Test 28 | Test 29 |
|---|---|---|---|---|---|
| $P_{exp\ output}$ in W | 122.75 | 185.91 | 136.21 | 94.63 | 43.55 |
| $M_{exp\ torque}$ in Nm | 1.20 | 0.60 | 0.38 | 0.33 | 0.18 |
| $rpm_{exp}$ in $min^{-1}$ | 974.05 | 2 980.71 | 3 462.47 | 2 724.24 | 2 311.23 |
| $\dot{m}_{CO2}$ in kg/min | 1.82 | 1.79 | 1.79 | 1.79 | 1.80 |
| $P_{pump\ inlet}$ in Pa | 5 750 367.81 | 5 824 218.18 | 5 801 222.82 | 5 825 336.28 | 5 838 959.58 |
| $P_{pump\ inlet}$ in bar | 57.50 | 58.24 | 58.01 | 58.25 | 58.39 |
| $t_{pump\ inlet}$ in °C | 17.53 | 18.16 | 17.92 | 18.17 | 18.08 |
| $s_{pump\ inlet}$ in J/kg*K | 1 154.64 | 1 160.99 | 1 158.48 | 1 161.20 | 1 159.78 |
| $h_{pump\ inlet}$ in J/kg | 246 235.20 | 248 174.12 | 247 415.14 | 248 236.41 | 247 839.24 |
| $h_{S\ pump\ outlet}$ in J/kg*K | 251 099.15 | 251 279.61 | 249 719.71 | 250 499.63 | 249 638.14 |
| $P_{pump\ outlet}$ in Pa | 9 736 966.28 | 8 339 482.23 | 7 668 332.49 | 7 653 181.60 | 7 292 265.21 |
| $P_{pump\ outlet}$ in bar | 97.37 | 83.39 | 76.68 | 76.53 | 72.92 |
| $t_{pump\ outlet}$ in °C | 23.29 | 22.07 | 20.93 | 21.12 | 20.48 |
| $s_{pump\ outlet}$ in J/kg*K | 1 158.24 | 1 164.19 | 1 161.88 | 1 164.23 | 1 162.79 |
| $h_{pump\ outlet}$ in J/kg | 252 164.09 | 252 225.24 | 250 718.04 | 251 390.79 | 250 523.67 |
| $\pi_{press\ ratio\ pump}$ | 1.69 | 1.43 | 1.32 | 1.31 | 1.25 |
| $P_{pump}$ in W | 179.60 | 120.54 | 98.49 | 94.19 | 80.59 |
| $\eta_{pump}$ in % | 82.04 | 76.66 | 69.77 | 71.75 | 67.01 |
| $P_{exp\ outlet}$ in Pa | 5 901 609.06 | 5 966 573.57 | 5 949 288.45 | 5 973 334.15 | 5 992 119.67 |
| $P_{exp\ outlet}$ in bar | 59.02 | 59.67 | 59.49 | 59.73 | 59.92 |
| $t_{exp\ outlet}$ in °C | 58.83 | 66.48 | 72.85 | 73.74 | 77.20 |
| $s_{exp\ outlet}$ in J/kg*K | 1 945.29 | 1 973.11 | 1 998.67 | 2 000.73 | 2 012.56 |
| $h_{exp\ outlet}$ in J/kg*K | 482 908.67 | 492 784.22 | 501 399.56 | 502 324.68 | 506 614.58 |
| $h_{S\ exp\ outlet}$ in J/kg | 465 557.77 | 485 058.47 | 495 829.11 | 495 677.84 | 500 954.37 |
| $P_{exp\ inlet}$ in Pa | 9 577 279.70 | 8 162 852.96 | 7 477 966.05 | 7 463 714.81 | 7 093 287.16 |
| $P_{exp\ inlet}$ in bar | 95.77 | 81.63 | 74.78 | 74.64 | 70.93 |
| $t_{exp\ inlet}$ in °C | 87.35 | 87.20 | 87.93 | 87.49 | 87.08 |
| $s_{exp\ inlet}$ in J/kg*K | 1 892.08 | 1 950.17 | 1 982.47 | 1 981.43 | 1 996.30 |
| $h_{exp\ inlet}$ in J/kg | 487 952.08 | 500 796.31 | 507 810.38 | 507 330.88 | 509 943.22 |
| $\pi_{press\ ratio\ exp}$ | 1.62 | 1.37 | 1.26 | 1.25 | 1.18 |
| $P_{exp}$ in W | 152.77 | 238.40 | 191.17 | 149.48 | 99.93 |
| $\eta_{exp}$ in % | 22.52 | 50.91 | 53.51 | 42.96 | 37.03 |
| $\overline{x}\ t_{HX\text{-}2\ inlet}$ in °C | 99.56 | 100.15 | 101.40 | 100.83 | 100.41 |
| $t_{HX\text{-}2\ inlet\text{-}1}$ in °C | 91.69 | 92.08 | 92.96 | 92.38 | 92.16 |
| $t_{HX\text{-}2\ inlet\text{-}2}$ in °C | 98.44 | 98.83 | 100.02 | 99.35 | 98.90 |
| $t_{HX\text{-}2\ inlet\text{-}3}$ in °C | 105.82 | 106.51 | 107.92 | 107.41 | 106.66 |
| $t_{HX\text{-}2\ inlet\text{-}4}$ in °C | 102.30 | 103.20 | 104.70 | 104.18 | 103.94 |
| $\overline{x}\ t_{HX\text{-}2\ outlet}$ in °C | 54.28 | 53.22 | 52.89 | 52.65 | 51.67 |
| $t_{HX\text{-}2\ outlet\text{-}1}$ in °C | 53.71 | 51.90 | 51.98 | 51.90 | 49.94 |
| $t_{HX\text{-}2\ outlet\text{-}2}$ in °C | 54.35 | 53.10 | 52.85 | 52.63 | 51.63 |
| $t_{HX\text{-}2\ outlet\text{-}3}$ in °C | 56.75 | 56.40 | 56.43 | 56.10 | 55.31 |
| $t_{HX\text{-}2\ outlet\text{-}4}$ in °C | 57.98 | 58.03 | 57.33 | 57.05 | 56.72 |
| $t_{HX\text{-}2\ outlet\text{-}5}$ in °C | 51.61 | 49.77 | 49.17 | 48.94 | 46.86 |
| $t_{HX\text{-}2\ outlet\text{-}6}$ in °C | 52.70 | 51.05 | 50.56 | 50.28 | 49.31 |
| $t_{HX\text{-}2\ outlet\text{-}7}$ in °C | 54.23 | 53.14 | 53.07 | 52.86 | 52.29 |
| $t_{HX\text{-}2\ outlet\text{-}8}$ in °C | 52.93 | 52.33 | 51.69 | 51.42 | 51.29 |
| $P_{HX\text{-}2\ inlet}$ in Pa | 100 031.66 | 100 036.43 | 100 061.85 | 100 062.63 | 100 049.40 |
| $P_{HX\text{-}2\ inlet}$ in bar | 1.00 | 1.00 | 1.00 | 1.00 | 1.00 |
| $P_{HX\text{-}2\ outlet}$ in Pa | 99 050.65 | 99 053.94 | 99 079.31 | 99 077.88 | 99 063.04 |
| $P_{HX\text{-}2\ outlet}$ in bar | 0.99 | 0.99 | 0.99 | 0.99 | 0.99 |
| $\eta_{cycle}$ in % | 85.07 | 197.78 | 194.10 | 158.71 | 124.00 |

Table C.6: Tests 25-29

| Test number | Test 30 | Test 31 | Test 32 | Test 33 | Test 34 |
|---|---|---|---|---|---|
| $P_{exp\ output}$ in W | 187.72 | 179.26 | 176.92 | 172.69 | 144.92 |
| $M_{exp\ torque}$ in Nm | 0.68 | 0.84 | 0.58 | 0.54 | 1.12 |
| $rpm_{exp}$ in $min^{-1}$ | 2 650.98 | 2 039.23 | 2 902.30 | 3 063.82 | 1 232.50 |
| $\dot{m}_{CO2}$ in kg/min | 1.82 | 1.79 | 1.80 | 1.81 | 1.78 |
| $P_{pump\ inlet}$ in Pa | 5 845 614.57 | 5 841 800.13 | 5 813 580.86 | 5 807 402.79 | 5 829 965.75 |
| $P_{pump\ inlet}$ in bar | 58.46 | 58.42 | 58.14 | 58.07 | 58.30 |
| $t_{pump\ inlet}$ in °C | 18.17 | 17.88 | 18.00 | 17.96 | 18.11 |
| $s_{pump\ inlet}$ in J/kg*K | 1 160.72 | 1 157.25 | 1 159.26 | 1 158.88 | 1 160.33 |
| $h_{pump\ inlet}$ in J/kg | 248 122.60 | 247 106.29 | 247 657.32 | 247 538.79 | 247 988.55 |
| $h_{S\ pump\ outlet}$ in J/kg*K | 251 453.94 | 250 797.93 | 250 667.75 | 250 427.79 | 252 566.46 |
| $P_{pump\ outlet}$ in Pa | 8 547 145.56 | 8 850 504.44 | 8 255 884.12 | 8 151 246.94 | 9 557 126.99 |
| $P_{pump\ outlet}$ in bar | 85.47 | 88.51 | 82.56 | 81.51 | 95.57 |
| $t_{pump\ outlet}$ in °C | 22.28 | 22.35 | 21.70 | 21.56 | 23.53 |
| $s_{pump\ outlet}$ in J/kg*K | 1 163.46 | 1 160.14 | 1 161.59 | 1 161.55 | 1 162.79 |
| $h_{pump\ outlet}$ in J/kg | 252 261.44 | 251 651.82 | 251 353.91 | 251 213.25 | 253 296.27 |
| $\pi_{press\ ratio\ pump}$ | 1.46 | 1.52 | 1.42 | 1.40 | 1.64 |
| $P_{pump}$ in W | 125.69 | 135.72 | 111.00 | 110.90 | 157.03 |
| $\eta_{pump}$ in % | 80.49 | 81.21 | 81.44 | 78.62 | 86.25 |
| $P_{exp\ outlet}$ in Pa | 5 996 857.00 | 5 981 567.91 | 5 953 225.51 | 5 949 450.41 | 5 963 836.50 |
| $P_{exp\ outlet}$ in bar | 59.97 | 59.82 | 59.53 | 59.49 | 59.64 |
| $t_{exp\ outlet}$ in °C | 66.21 | 63.41 | 66.96 | 67.66 | 60.68 |
| $s_{exp\ outlet}$ in J/kg*K | 1 970.37 | 1 959.86 | 1 975.74 | 1 978.72 | 1 949.51 |
| $h_{exp\ outlet}$ in J/kg*K | 492 109.70 | 488 431.47 | 493 567.67 | 494 549.20 | 484 816.77 |
| $h_{S\ exp\ outlet}$ in J/kg | 483 105.36 | 477 575.03 | 486 056.53 | 487 374.66 | 469 509.71 |
| $P_{exp\ inlet}$ in Pa | 8 369 688.16 | 8 687 129.64 | 8 079 171.26 | 7 971 392.16 | 9 408 671.73 |
| $P_{exp\ inlet}$ in bar | 83.70 | 86.87 | 80.79 | 79.71 | 94.09 |
| $t_{exp\ inlet}$ in °C | 87.73 | 86.99 | 87.14 | 86.99 | 88.24 |
| $s_{exp\ inlet}$ in J/kg*K | 1 943.58 | 1 927.23 | 1 953.48 | 1 957.50 | 1 902.91 |
| $h_{exp\ inlet}$ in J/kg | 499 720.40 | 495 738.69 | 501 451.66 | 502 199.11 | 490 985.60 |
| $\pi_{press\ ratio\ exp}$ | 1.40 | 1.45 | 1.36 | 1.34 | 1.58 |
| $P_{exp}$ in W | 231.13 | 218.18 | 236.75 | 230.88 | 182.51 |
| $\eta_{exp}$ in % | 45.81 | 40.23 | 51.21 | 51.60 | 28.72 |
| $\overline{x}\ t_{HX\text{-}2\ inlet}$ in °C | 100.56 | 99.16 | 100.37 | 100.32 | 101.42 |
| $t_{HX\text{-}2\ inlet\text{-}1}$ in °C | 92.52 | 91.54 | 91.98 | 92.05 | 93.29 |
| $t_{HX\text{-}2\ inlet\text{-}2}$ in °C | 99.13 | 98.15 | 99.17 | 99.22 | 100.40 |
| $t_{HX\text{-}2\ inlet\text{-}3}$ in °C | 107.05 | 105.25 | 106.71 | 106.93 | 107.65 |
| $t_{HX\text{-}2\ inlet\text{-}4}$ in °C | 103.53 | 101.71 | 103.63 | 103.08 | 104.32 |
| $\overline{x}\ t_{HX\text{-}2\ outlet}$ in °C | 53.16 | 54.05 | 53.50 | 53.16 | 56.56 |
| $t_{HX\text{-}2\ outlet\text{-}1}$ in °C | 52.15 | 53.22 | 52.21 | 51.79 | 55.79 |
| $t_{HX\text{-}2\ outlet\text{-}2}$ in °C | 53.13 | 54.14 | 53.64 | 53.20 | 56.74 |
| $t_{HX\text{-}2\ outlet\text{-}3}$ in °C | 56.11 | 56.78 | 56.83 | 56.52 | 59.38 |
| $t_{HX\text{-}2\ outlet\text{-}4}$ in °C | 57.81 | 58.24 | 58.05 | 57.75 | 60.36 |
| $t_{HX\text{-}2\ outlet\text{-}5}$ in °C | 49.94 | 51.04 | 49.83 | 49.46 | 53.70 |
| $t_{HX\text{-}2\ outlet\text{-}6}$ in °C | 51.06 | 52.10 | 51.17 | 50.80 | 54.81 |
| $t_{HX\text{-}2\ outlet\text{-}7}$ in °C | 52.95 | 53.85 | 53.49 | 53.27 | 56.55 |
| $t_{HX\text{-}2\ outlet\text{-}8}$ in °C | 52.09 | 53.01 | 52.75 | 52.50 | 55.15 |
| $P_{HX\text{-}2\ inlet}$ in Pa | 100 057.77 | 100 346.53 | 101 017.52 | 100 992.40 | 100 988.32 |
| $P_{HX\text{-}2\ inlet}$ in bar | 1.00 | 1.00 | 1.01 | 1.01 | 1.01 |
| $P_{HX\text{-}2\ outlet}$ in Pa | 99 074.42 | 99 364.23 | 100 027.92 | 100 003.23 | 100 006.60 |
| $P_{HX\text{-}2\ outlet}$ in bar | 0.99 | 0.99 | 1.00 | 1.00 | 1.00 |
| $\eta_{cycle}$ in % | 183.88 | 160.76 | 213.28 | 208.19 | 116.22 |

Table C.7: Tests 30-34

## C.3 Test results and diagrams with 110 °C heat source temperature, 1.8 kg/min $CO_2$ mass flow at the expander loop and 60 bar condensation pressure

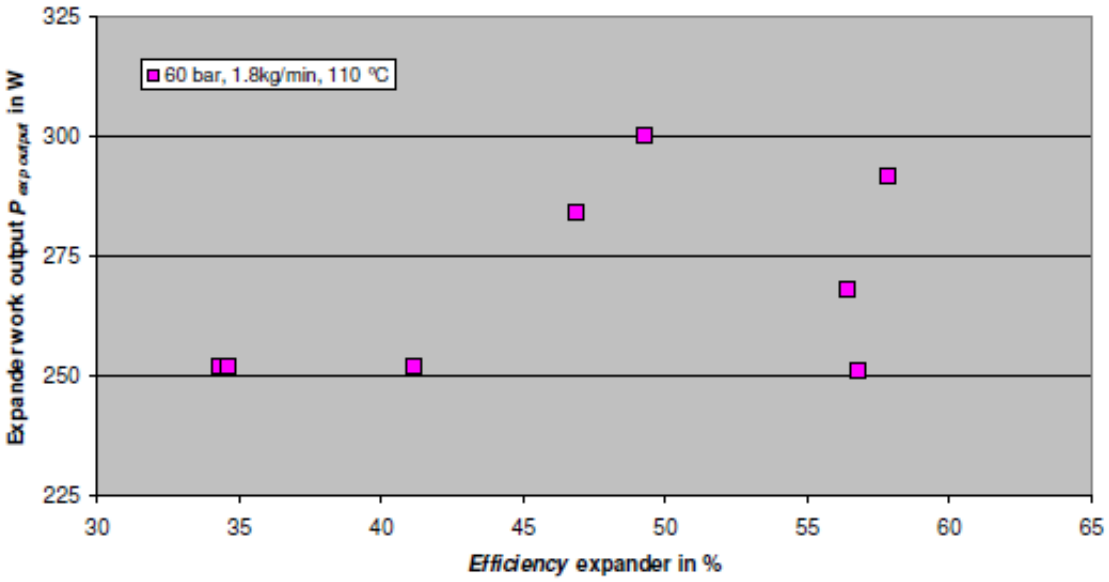


Figure C.3: Expander power output and efficiency, for tests with condensation conditions of 60 bar, 18 °C, with heat source temperature 110 °C and 1.8 $\frac{kg}{min}$ $CO_2$ mass flow at the expander loop

| Test number | Test 35 | Test 36 | Test 37 | Test 38 | Test 39 |
|---|---|---|---|---|---|
| $P_{exp\ output}$ in W | 228.46 | 192.06 | 178.10 | 219.50 | 198.20 |
| $M_{exp\ torque}$ in Nm | 0.84 | 0.85 | 0.49 | 0.82 | 1.12 |
| $rpm_{exp}$ in $min^{-1}$ | 2 609.83 | 2 163.60 | 3 478.53 | 2 565.43 | 1 687.93 |
| $\dot{m}_{CO2}$ in kg/min | 1.79 | 1.79 | 1.81 | 1.81 | 1.80 |
| $P_{pump\ inlet}$ in Pa | 5 857 029.73 | 5 855 344.10 | 5 804 954.48 | 5 820 213.55 | 5 788 887.98 |
| $P_{pump\ inlet}$ in bar | 58.57 | 58.55 | 58.05 | 58.20 | 57.89 |
| $t_{pump\ inlet}$ in °C | 17.90 | 17.90 | 18.04 | 18.10 | 17.79 |
| $s_{pump\ inlet}$ in J/kg*K | 1 157.28 | 1 157.25 | 1 159.97 | 1 160.33 | 1 157.10 |
| $h_{pump\ inlet}$ in J/kg | 247 135.96 | 247 122.99 | 247 854.60 | 247 978.61 | 246 999.42 |
| $h_{S\ pump\ outlet}$ in J/kg*K | 250 862.00 | 250 880.11 | 250 433.39 | 251 681.51 | 251 663.18 |
| $P_{pump\ outlet}$ in Pa | 8 894 276.35 | 8 918 296.89 | 7 892 407.40 | 8 827 002.31 | 9 599 701.96 |
| $P_{pump\ outlet}$ in bar | 88.94 | 89.18 | 78.92 | 88.27 | 96.00 |
| $t_{pump\ outlet}$ in °C | 22.45 | 22.48 | 21.35 | 22.62 | 23.33 |
| $s_{pump\ outlet}$ in J/kg*K | 1 160.55 | 1 160.57 | 1 163.07 | 1 163.12 | 1 160.32 |
| $h_{pump\ outlet}$ in J/kg | 251 828.08 | 251 861.38 | 251 344.54 | 252 505.19 | 252 615.22 |
| $\pi_{press\ ratio\ pump}$ | 1.52 | 1.52 | 1.36 | 1.52 | 1.66 |
| $P_{pump}$ in W | 140.14 | 141.44 | 105.52 | 136.39 | 168.12 |
| $\eta_{pump}$ in % | 79.41 | 79.29 | 73.89 | 81.80 | 83.05 |
| $P_{exp\ outlet}$ in Pa | 6 011 143.15 | 6 007 227.26 | 5 960 413.69 | 5 970 186.76 | 5 939 074.18 |
| $P_{exp\ outlet}$ in bar | 60.11 | 60.07 | 59.60 | 59.70 | 59.39 |
| $t_{exp\ outlet}$ in °C | 82.12 | 82.71 | 89.21 | 80.44 | 78.48 |
| $s_{exp\ outlet}$ in J/kg*K | 2 029.28 | 2 031.58 | 2 056.23 | 2 025.39 | 2 019.93 |
| $h_{exp\ outlet}$ in J/kg*K | 512 684.72 | 513 469.20 | 521 880.21 | 510 931.12 | 508 723.20 |
| $h_{S\ exp\ outlet}$ in J/kg | 502 329.84 | 501 386.55 | 515 559.98 | 500 241.73 | 492 608.81 |
| $P_{exp\ inlet}$ in Pa | 8 716 621.54 | 8 742 480.79 | 7 689 847.24 | 8 644 542.98 | 9 429 768.68 |
| $P_{exp\ inlet}$ in bar | 87.17 | 87.42 | 76.90 | 86.45 | 94.30 |
| $t_{exp\ inlet}$ in °C | 106.08 | 105.61 | 106.13 | 103.95 | 105.84 |
| $s_{exp\ inlet}$ in J/kg*K | 1 999.79 | 1 997.17 | 2 038.67 | 1 994.79 | 1 973.27 |
| $h_{exp\ inlet}$ in J/kg | 522 728.60 | 521 904.55 | 530 178.90 | 520 365.29 | 517 132.89 |
| $\pi_{press\ ratio\ exp}$ | 1.45 | 1.46 | 1.29 | 1.45 | 1.59 |
| $P_{exp}$ in W | 299.98 | 251.79 | 250.91 | 284.26 | 251.76 |
| $\eta_{exp}$ in % | 49.24 | 41.11 | 56.77 | 46.88 | 34.29 |
| $\overline{x}\ t_{HX\text{-}2\ inlet}$ in °C | 123.51 | 122.20 | 123.03 | 120.52 | 122.23 |
| $t_{HX\text{-}2\ inlet\text{-}1}$ in °C | 113.12 | 112.07 | 112.84 | 110.35 | 112.38 |
| $t_{HX\text{-}2\ inlet\text{-}2}$ in °C | 121.43 | 120.38 | 120.65 | 118.55 | 120.56 |
| $t_{HX\text{-}2\ inlet\text{-}3}$ in °C | 130.37 | 129.22 | 129.98 | 127.59 | 129.06 |
| $t_{HX\text{-}2\ inlet\text{-}4}$ in °C | 129.13 | 127.14 | 128.65 | 125.61 | 126.93 |
| $\overline{x}\ t_{HX\text{-}2\ outlet}$ in °C | 68.38 | 68.09 | 66.89 | 66.36 | 68.32 |
| $t_{HX\text{-}2\ outlet\text{-}1}$ in °C | 67.90 | 67.49 | 66.42 | 65.48 | 67.69 |
| $t_{HX\text{-}2\ outlet\text{-}2}$ in °C | 68.44 | 68.12 | 67.17 | 66.46 | 68.63 |
| $t_{HX\text{-}2\ outlet\text{-}3}$ in °C | 72.65 | 72.33 | 71.59 | 70.74 | 72.20 |
| $t_{HX\text{-}2\ outlet\text{-}4}$ in °C | 72.53 | 72.20 | 70.24 | 70.67 | 72.82 |
| $t_{HX\text{-}2\ outlet\text{-}5}$ in °C | 64.14 | 63.91 | 62.75 | 61.96 | 64.12 |
| $t_{HX\text{-}2\ outlet\text{-}6}$ in °C | 65.81 | 65.54 | 64.58 | 63.84 | 65.73 |
| $t_{HX\text{-}2\ outlet\text{-}7}$ in °C | 69.08 | 68.87 | 67.94 | 67.11 | 68.52 |
| $t_{HX\text{-}2\ outlet\text{-}8}$ in °C | 66.48 | 66.30 | 64.47 | 64.64 | 66.81 |
| $P_{HX\text{-}2\ inlet}$ in Pa | 100 328.33 | 100 334.62 | 100 056.17 | 100 064.43 | 100 066.86 |
| $P_{HX\text{-}2\ inlet}$ in bar | 1.00 | 1.00 | 1.00 | 1.00 | 1.00 |
| $P_{HX\text{-}2\ outlet}$ in Pa | 99 387.72 | 99 394.61 | 99 118.25 | 99 121.63 | 99 131.03 |
| $P_{HX\text{-}2\ outlet}$ in bar | 0.99 | 0.99 | 0.99 | 0.99 | 0.99 |
| $\eta_{cycle}$ in % | 214.06 | 178.02 | 237.79 | 208.42 | 149.75 |

Table C.8: Tests 35-39

| Test number | Test 40 | Test 41 | Test 42 |
|---|---|---|---|
| $P_{exp\ output}$ in W | 199.05 | 210.28 | 192.36 |
| $M_{exp\ torque}$ in Nm | 1.12 | 0.58 | 0.50 |
| $rpm_{exp}$ in $min^{-1}$ | 1 697.15 | 3 486.19 | 3 676.77 |
| $\dot{m}_{CO2}$ in kg/min | 1.79 | 1.78 | 1.81 |
| $P_{pump\ inlet}$ in Pa | 5 831 987.18 | 5 876 842.29 | 5 853 948.59 |
| $P_{pump\ inlet}$ in bar | 58.32 | 58.77 | 58.54 |
| $t_{pump\ inlet}$ in °C | 18.02 | 18.24 | 18.05 |
| $s_{pump\ inlet}$ in J/kg*K | 1 159.14 | 1 161.05 | 1 159.16 |
| $h_{pump\ inlet}$ in J/kg | 247 644.26 | 248 258.46 | 247 677.24 |
| $h_{S\ pump\ outlet}$ in J/kg*K | 252 295.41 | 251 299.49 | 250 471.92 |
| $P_{pump\ outlet}$ in Pa | 9 624 818.20 | 8 340 252.73 | 8 120 717.43 |
| $P_{pump\ outlet}$ in bar | 96.25 | 83.40 | 81.21 |
| $t_{pump\ outlet}$ in °C | 23.57 | 22.07 | 21.58 |
| $s_{pump\ outlet}$ in J/kg*K | 1 162.30 | 1 164.14 | 1 162.24 |
| $h_{pump\ outlet}$ in J/kg | 253 232.55 | 252 209.78 | 251 381.64 |
| $\pi_{press\ ratio\ pump}$ | 1.65 | 1.42 | 1.39 |
| $P_{pump}$ in W | 166.97 | 117.21 | 111.59 |
| $\eta_{pump}$ in % | 83.23 | 76.96 | 75.44 |
| $P_{exp\ outlet}$ in Pa | 5 980 891.25 | 6 018 972.94 | 6 003 665.18 |
| $P_{exp\ outlet}$ in bar | 59.81 | 60.19 | 60.04 |
| $t_{exp\ outlet}$ in °C | 78.93 | 84.87 | 87.64 |
| $s_{exp\ outlet}$ in J/kg*K | 2 019.43 | 2 038.55 | 2 048.81 |
| $h_{exp\ outlet}$ in J/kg*K | 508 927.28 | 516 065.14 | 519 608.21 |
| $h_{S\ exp\ outlet}$ in J/kg | 493 022.99 | 508 888.79 | 512 728.32 |
| $P_{exp\ inlet}$ in Pa | 9 455 429.99 | 8 152 690.19 | 7 923 877.60 |
| $P_{exp\ inlet}$ in bar | 94.55 | 81.53 | 79.24 |
| $t_{exp\ inlet}$ in °C | 106.13 | 105.39 | 106.12 |
| $s_{exp\ inlet}$ in J/kg*K | 1 973.45 | 2 018.35 | 2 029.59 |
| $h_{exp\ inlet}$ in J/kg | 517 353.46 | 525 901.47 | 528 501.70 |
| $\pi_{press\ ratio\ exp}$ | 1.58 | 1.35 | 1.32 |
| $P_{exp}$ in W | 251.76 | 291.78 | 267.90 |
| $\eta_{exp}$ in % | 34.63 | 57.82 | 56.38 |
| $\overline{x}\ t_{HX\text{-}2\ inlet}$ in °C | 122.49 | 122.67 | 123.54 |
| $t_{HX\text{-}2\ inlet\text{-}1}$ in °C | 112.57 | 112.57 | 113.25 |
| $t_{HX\text{-}2\ inlet\text{-}2}$ in °C | 120.28 | 120.56 | 121.49 |
| $t_{HX\text{-}2\ inlet\text{-}3}$ in °C | 129.56 | 129.41 | 130.35 |
| $t_{HX\text{-}2\ inlet\text{-}4}$ in °C | 127.56 | 128.13 | 129.09 |
| $\overline{x}\ t_{HX\text{-}2\ outlet}$ in °C | 68.68 | 67.48 | 67.05 |
| $t_{HX\text{-}2\ outlet\text{-}1}$ in °C | 68.11 | 67.11 | 66.56 |
| $t_{HX\text{-}2\ outlet\text{-}2}$ in °C | 69.02 | 67.88 | 67.45 |
| $t_{HX\text{-}2\ outlet\text{-}3}$ in °C | 72.52 | 71.95 | 71.76 |
| $t_{HX\text{-}2\ outlet\text{-}4}$ in °C | 73.13 | 70.83 | 70.37 |
| $t_{HX\text{-}2\ outlet\text{-}5}$ in °C | 64.54 | 63.38 | 62.85 |
| $t_{HX\text{-}2\ outlet\text{-}6}$ in °C | 66.11 | 65.19 | 64.77 |
| $t_{HX\text{-}2\ outlet\text{-}7}$ in °C | 68.87 | 68.41 | 68.12 |
| $t_{HX\text{-}2\ outlet\text{-}8}$ in °C | 67.15 | 65.07 | 64.55 |
| $P_{HX\text{-}2\ inlet}$ in Pa | 100 073.33 | 100 072.80 | 100 072.13 |
| $P_{HX\text{-}2\ inlet}$ in bar | 1.00 | 1.00 | 1.00 |
| $P_{HX\text{-}2\ outlet}$ in Pa | 99 138.23 | 99 133.38 | 99 133.31 |
| $P_{HX\text{-}2\ outlet}$ in bar | 0.99 | 0.99 | 0.99 |
| $\eta_{cycle}$ in % | 150.78 | 248.94 | 240.08 |

Table C.9: Tests 40-42

## C.4 Test results and diagrams with 65 °C heat source temperature, 2.5 kg/min $CO_2$ mass flow at the expander loop and 60 bar condensation pressure

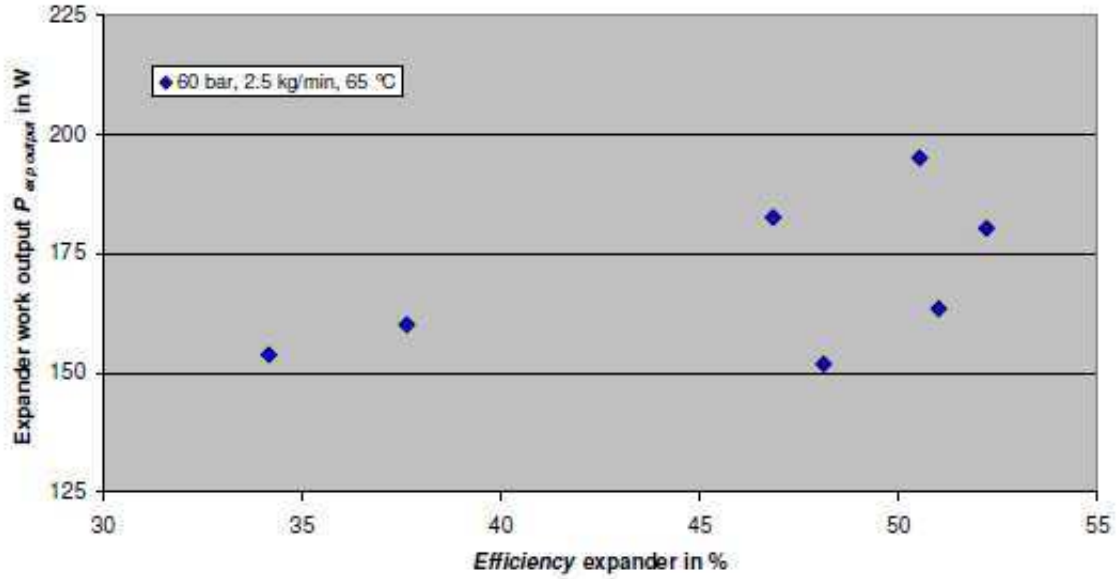


Figure C.4: Expander power output and efficiency, for tests with condensation conditions of 60 bar, 18 °C, with heat source temperature 65 °C and 2.5 $\frac{kg}{min}$ $CO_2$ mass flow at the expander loop

| Test number | Test 43 | Test 44 | Test 45 | Test 46 | Test 47 |
|---|---|---|---|---|---|
| $P_{exp\ output}$ in W | 139.82 | 134.85 | 156.76 | 161.98 | 130.11 |
| $M_{exp\ torque}$ in Nm | 0.56 | 0.63 | 0.49 | 0.46 | 0.32 |
| $rpm_{exp}$ in $min^{-1}$ | 2 372.74 | 2 049.44 | 3 080.86 | 3 369.47 | 3 827.39 |
| $\dot{m}_{CO2}$ in kg/min | 2.40 | 2.52 | 2.50 | 2.50 | 2.51 |
| $P_{pump\ inlet}$ in Pa | 5 762 393.38 | 5 756 805.30 | 5 774 105.86 | 5 765 355.28 | 5 769 675.33 |
| $P_{pump\ inlet}$ in bar | 57.62 | 57.57 | 57.74 | 57.65 | 57.70 |
| $t_{pump\ inlet}$ in °C | 17.93 | 17.87 | 18.04 | 17.96 | 18.30 |
| $s_{pump\ inlet}$ in J/kg*K | 1 159.32 | 1 158.74 | 1 160.52 | 1 159.71 | 1 163.81 |
| $h_{pump\ inlet}$ in J/kg | 247 611.77 | 247 436.08 | 247 975.21 | 247 727.58 | 248 928.92 |
| $h_{S\ pump\ outlet}$ in J/kg*K | 250 580.76 | 250 541.08 | 250 633.21 | 250 314.45 | 251 138.71 |
| $P_{pump\ outlet}$ in Pa | 8 169 626.25 | 8 276 948.73 | 7 924 296.26 | 7 859 396.70 | 7 547 676.82 |
| $P_{pump\ outlet}$ in bar | 81.70 | 82.77 | 79.24 | 78.59 | 75.48 |
| $t_{pump\ outlet}$ in °C | 21.64 | 21.71 | 21.41 | 21.24 | 21.21 |
| $s_{pump\ outlet}$ in J/kg*K | 1 162.15 | 1 161.33 | 1 163.22 | 1 162.37 | 1 166.74 |
| $h_{pump\ outlet}$ in J/kg | 251 412.62 | 251 304.44 | 251 428.77 | 251 096.88 | 252 001.10 |
| $\pi_{press\ ratio\ pump}$ | 1.42 | 1.44 | 1.37 | 1.36 | 1.31 |
| $P_{pump}$ in W | 151.91 | 162.32 | 144.09 | 140.67 | 128.77 |
| $\eta_{pump}$ in % | 78.11 | 80.27 | 76.96 | 76.78 | 71.93 |
| $P_{exp\ outlet}$ in Pa | 5 994 726.25 | 5 985 485.04 | 6 003 981.84 | 6 000 821.92 | 6 009 937.80 |
| $P_{exp\ outlet}$ in bar | 59.95 | 59.85 | 60.04 | 60.01 | 60.10 |
| $t_{exp\ outlet}$ in °C | 35.95 | 32.71 | 35.20 | 36.99 | 38.37 |
| $s_{exp\ outlet}$ in J/kg*K | 1 821.70 | 1 800.20 | 1 815.92 | 1 827.84 | 1 835.69 |
| $h_{exp\ outlet}$ in J/kg*K | 444 067.64 | 437 399.70 | 442 342.33 | 446 007.76 | 448 507.93 |
| $h_{S\ exp\ outlet}$ in J/kg | 437 431.39 | 430 333.93 | 437 377.37 | 441 435.75 | 444 762.07 |
| $P_{exp\ inlet}$ in Pa | 7 935 795.70 | 8 049 781.35 | 7 688 773.97 | 7 617 174.00 | 7 297 991.12 |
| $P_{exp\ inlet}$ in bar | 79.36 | 80.50 | 76.89 | 76.17 | 72.98 |
| $t_{exp\ inlet}$ in °C | 54.56 | 52.32 | 52.00 | 53.32 | 51.63 |
| $s_{exp\ inlet}$ in J/kg*K | 1 800.12 | 1 776.98 | 1 799.76 | 1 813.04 | 1 823.63 |
| $h_{exp\ inlet}$ in J/kg | 448 072.13 | 441 065.19 | 446 716.79 | 450 676.64 | 452 407.23 |
| $\pi_{press\ ratio\ exp}$ | 1.32 | 1.34 | 1.28 | 1.27 | 1.21 |
| $P_{exp}$ in W | 160.05 | 153.80 | 182.52 | 194.93 | 163.44 |
| $\eta_{exp}$ in % | 37.63 | 34.16 | 46.84 | 50.52 | 51.00 |
| $\overline{x}\ t_{HX\text{-}2\ inlet}$ in °C | 74.58 | 72.92 | 72.87 | 73.97 | 73.26 |
| $t_{HX\text{-}2\ inlet\text{-}1}$ in °C | 67.70 | 66.38 | 66.21 | 67.09 | 66.44 |
| $t_{HX\text{-}2\ inlet\text{-}2}$ in °C | 73.71 | 72.35 | 72.18 | 73.43 | 72.62 |
| $t_{HX\text{-}2\ inlet\text{-}3}$ in °C | 80.37 | 78.36 | 78.57 | 79.93 | 79.04 |
| $t_{HX\text{-}2\ inlet\text{-}4}$ in °C | 76.52 | 74.60 | 74.52 | 75.42 | 74.95 |
| $\overline{x}\ t_{HX\text{-}2\ outlet}$ in °C | 30.10 | 29.96 | 29.22 | 29.17 | 28.23 |
| $t_{HX\text{-}2\ outlet\text{-}1}$ in °C | 30.11 | 29.98 | 29.27 | 29.19 | 28.37 |
| $t_{HX\text{-}2\ outlet\text{-}2}$ in °C | 30.26 | 30.12 | 29.41 | 29.34 | 28.46 |
| $t_{HX\text{-}2\ outlet\text{-}3}$ in °C | 31.44 | 31.21 | 30.50 | 30.48 | 29.45 |
| $t_{HX\text{-}2\ outlet\text{-}4}$ in °C | 32.03 | 31.69 | 30.98 | 30.97 | 29.96 |
| $t_{HX\text{-}2\ outlet\text{-}5}$ in °C | 28.89 | 28.84 | 28.07 | 28.00 | 27.12 |
| $t_{HX\text{-}2\ outlet\text{-}6}$ in °C | 29.32 | 29.24 | 28.47 | 28.42 | 27.50 |
| $t_{HX\text{-}2\ outlet\text{-}7}$ in °C | 29.87 | 29.77 | 28.99 | 28.96 | 27.95 |
| $t_{HX\text{-}2\ outlet\text{-}8}$ in °C | 28.91 | 28.82 | 28.07 | 28.01 | 27.05 |
| $P_{HX\text{-}2\ inlet}$ in Pa | 100 289.45 | 100 292.57 | 100 277.98 | 100 257.71 | 100 237.93 |
| $P_{HX\text{-}2\ inlet}$ in bar | 1.00 | 1.00 | 1.00 | 1.00 | 1.00 |
| $P_{HX\text{-}2\ outlet}$ in Pa | 99 230.61 | 99 232.05 | 99 213.80 | 99 193.99 | 99 170.28 |
| $P_{HX\text{-}2\ outlet}$ in bar | 0.99 | 0.99 | 0.99 | 0.99 | 0.99 |
| $\eta_{cycle}$ in % | 105.36 | 94.76 | 126.67 | 138.57 | 126.92 |

Table C.10: Tests 43-47

| Test number | Test 48 | Test 49 |
|---|---|---|
| $P_{exp\ output}$ in W | 111.16 | 145.86 |
| $M_{exp\ torque}$ in Nm | 0.27 | 0.38 |
| $rpm_{exp}$ in $min^{-1}$ | 3 883.82 | 3 708.45 |
| $\dot{m}_{CO2}$ in kg/min | 2.47 | 2.52 |
| $P_{pump\ inlet}$ in Pa | 5 773 050.83 | 5 777 863.51 |
| $P_{pump\ inlet}$ in bar | 57.73 | 57.78 |
| $t_{pump\ inlet}$ in °C | 18.31 | 18.37 |
| $s_{pump\ inlet}$ in J/kg*K | 1 163.90 | 1 164.54 |
| $h_{pump\ inlet}$ in J/kg | 248 959.30 | 249 150.89 |
| $h_{S\ pump\ outlet}$ in J/kg*K | 251 114.08 | 251 510.70 |
| $P_{pump\ outlet}$ in Pa | 7 506 341.15 | 7 675 963.64 |
| $P_{pump\ outlet}$ in bar | 75.06 | 76.76 |
| $t_{pump\ outlet}$ in °C | 21.16 | 21.44 |
| $s_{pump\ outlet}$ in J/kg*K | 1 166.90 | 1 167.32 |
| $h_{pump\ outlet}$ in J/kg | 251 995.16 | 252 329.03 |
| $\pi_{press\ ratio\ pump}$ | 1.30 | 1.33 |
| $P_{pump}$ in W | 124.89 | 133.61 |
| $\eta_{pump}$ in % | 70.98 | 74.25 |
| $P_{exp\ outlet}$ in Pa | 6 009 441.32 | 6 017 082.33 |
| $P_{exp\ outlet}$ in bar | 60.09 | 60.17 |
| $t_{exp\ outlet}$ in °C | 41.34 | 37.46 |
| $s_{exp\ outlet}$ in J/kg*K | 1 853.26 | 1 829.47 |
| $h_{exp\ outlet}$ in J/kg*K | 454 003.62 | 446 618.83 |
| $h_{S\ exp\ outlet}$ in J/kg | 450 022.14 | 442 692.39 |
| $P_{exp\ inlet}$ in Pa | 7 257 018.99 | 7 430 633.34 |
| $P_{exp\ inlet}$ in bar | 72.57 | 74.31 |
| $t_{exp\ inlet}$ in °C | 54.05 | 51.95 |
| $s_{exp\ inlet}$ in J/kg*K | 1 840.55 | 1 816.79 |
| $h_{exp\ inlet}$ in J/kg | 457 694.05 | 450 906.70 |
| $\pi_{press\ ratio\ exp}$ | 1.21 | 1.23 |
| $P_{exp}$ in W | 151.82 | 180.26 |
| $\eta_{exp}$ in % | 48.10 | 52.20 |
| $\overline{x}\ t_{HX\text{-}2\ inlet}$ in °C | 74.00 | 73.47 |
| $t_{HX\text{-}2\ inlet\text{-}1}$ in °C | 67.05 | 66.82 |
| $t_{HX\text{-}2\ inlet\text{-}2}$ in °C | 73.24 | 72.78 |
| $t_{HX\text{-}2\ inlet\text{-}3}$ in °C | 79.85 | 79.22 |
| $t_{HX\text{-}2\ inlet\text{-}4}$ in °C | 75.84 | 75.07 |
| $\overline{x}\ t_{HX\text{-}2\ outlet}$ in °C | 28.46 | 28.62 |
| $t_{HX\text{-}2\ outlet\text{-}1}$ in °C | 28.56 | 28.70 |
| $t_{HX\text{-}2\ outlet\text{-}2}$ in °C | 28.67 | 28.81 |
| $t_{HX\text{-}2\ outlet\text{-}3}$ in °C | 29.71 | 29.82 |
| $t_{HX\text{-}2\ outlet\text{-}4}$ in °C | 30.31 | 30.33 |
| $t_{HX\text{-}2\ outlet\text{-}5}$ in °C | 27.32 | 27.53 |
| $t_{HX\text{-}2\ outlet\text{-}6}$ in °C | 27.70 | 27.92 |
| $t_{HX\text{-}2\ outlet\text{-}7}$ in °C | 28.17 | 28.38 |
| $t_{HX\text{-}2\ outlet\text{-}8}$ in °C | 27.26 | 27.47 |
| $P_{HX\text{-}2\ inlet}$ in Pa | 100 241.53 | 100 219.02 |
| $P_{HX\text{-}2\ inlet}$ in bar | 1.00 | 1.00 |
| $P_{HX\text{-}2\ outlet}$ in Pa | 99 175.52 | 99 153.09 |
| $P_{HX\text{-}2\ outlet}$ in bar | 0.99 | 0.99 |
| $\eta_{cycle}$ in % | 121.56 | 134.92 |

Table C.11: Tests 48-49

## C.5 Test results and diagrams with 65 °C heat source temperature, 3.0 kg/min $CO_2$ mass flow at the expander loop and 60 bar condensation pressure

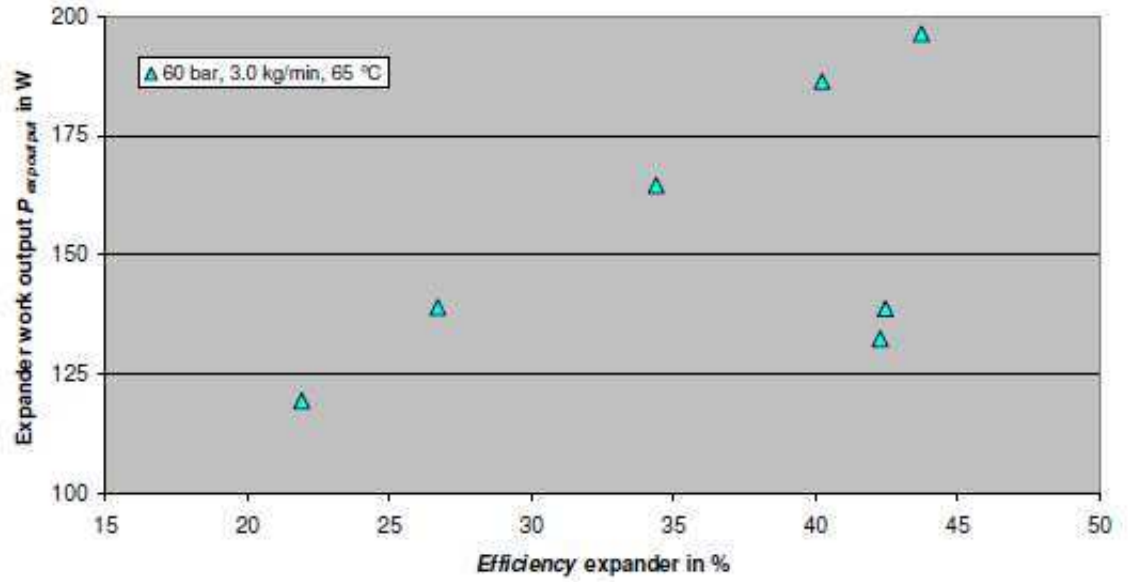


Figure C.5: Expander power output and efficiency, for tests with condensation conditions of 60 bar, 18 °C, with heat source temperature 65 °C and 3.0 $\frac{kg}{min}$ $CO_2$ mass flow at the expander loop

| Test number | Test 50 | Test 51 | Test 52 | Test 53 | Test 54 |
|---|---|---|---|---|---|
| $P_{exp\ output}$ in W | 101.83 | 161.62 | 147.58 | 128.30 | 191.03 |
| $M_{exp\ torque}$ in Nm | 0.92 | 0.61 | 0.73 | 0.78 | 0.59 |
| $rpm_{exp}$ in $min^{-1}$ | 1 059.89 | 2 526.34 | 1 928.62 | 1 578.36 | 3 073.85 |
| $\dot{m}_{CO2}$ in kg/min | 3.00 | 3.02 | 2.99 | 2.97 | 3.06 |
| $P_{pump\ inlet}$ in Pa | 5 759 244.70 | 5 712 107.25 | 5 744 600.68 | 5 746 053.44 | 5 726 800.16 |
| $P_{pump\ inlet}$ in bar | 57.59 | 57.12 | 57.45 | 57.46 | 57.27 |
| $t_{pump\ inlet}$ in °C | 17.98 | 17.75 | 18.03 | 18.03 | 17.89 |
| $s_{pump\ inlet}$ in J/kg*K | 1 160.07 | 1 158.14 | 1 161.00 | 1 160.89 | 1 159.61 |
| $h_{pump\ inlet}$ in J/kg | 247 826.32 | 247 204.27 | 248 078.55 | 248 047.87 | 247 650.34 |
| $h_{S\ pump\ outlet}$ in J/kg*K | 252 139.15 | 250 508.34 | 251 730.97 | 251 855.25 | 250 891.91 |
| $P_{pump\ outlet}$ in Pa | 9 266 954.67 | 8 396 395.95 | 8 705 958.36 | 8 834 870.21 | 8 355 610.41 |
| $P_{pump\ outlet}$ in bar | 92.67 | 83.96 | 87.06 | 88.35 | 83.56 |
| $t_{pump\ outlet}$ in °C | 22.91 | 21.58 | 22.29 | 22.48 | 21.72 |
| $s_{pump\ outlet}$ in J/kg*K | 1 160.34 | 1 158.42 | 1 161.39 | 1 161.64 | 1 160.42 |
| $h_{pump\ outlet}$ in J/kg | 252 217.00 | 250 592.29 | 251 846.07 | 252 076.48 | 251 131.94 |
| $\pi_{press\ ratio\ pump}$ | 1.61 | 1.47 | 1.52 | 1.54 | 1.46 |
| $P_{pump}$ in W | 219.28 | 170.43 | 187.62 | 199.14 | 177.36 |
| $\eta_{pump}$ in % | 98.23 | 97.52 | 96.95 | 94.51 | 93.11 |
| $P_{exp\ outlet}$ in Pa | 6 053 154.63 | 6 024 002.04 | 6 047 684.21 | 6 047 580.43 | 6 040 571.97 |
| $P_{exp\ outlet}$ in bar | 60.53 | 60.24 | 60.48 | 60.48 | 60.41 |
| $t_{exp\ outlet}$ in °C | 24.33 | 25.87 | 25.75 | 26.25 | 25.17 |
| $s_{exp\ outlet}$ in J/kg*K | 1 713.55 | 1 736.34 | 1 731.90 | 1 737.38 | 1 726.04 |
| $h_{exp\ outlet}$ in J/kg*K | 411 677.91 | 418 323.37 | 417 120.18 | 418 760.04 | 415 333.20 |
| $h_{S\ exp\ outlet}$ in J/kg | 401 249.26 | 412 079.65 | 409 452.79 | 410 145.24 | 409 896.45 |
| $P_{exp\ inlet}$ in Pa | 9 030 163.64 | 8 132 157.23 | 8 453 355.85 | 8 586 452.68 | 8 088 756.09 |
| $P_{exp\ inlet}$ in bar | 90.30 | 81.32 | 84.53 | 85.86 | 80.89 |
| $t_{exp\ inlet}$ in °C | 50.01 | 45.81 | 47.76 | 49.14 | 44.69 |
| $s_{exp\ inlet}$ in J/kg*K | 1 678.36 | 1 715.40 | 1 706.16 | 1 708.49 | 1 707.77 |
| $h_{exp\ inlet}$ in J/kg | 413 079.17 | 421 594.59 | 419 912.27 | 421 177.25 | 418 990.61 |
| $\pi_{press\ ratio\ exp}$ | 1.49 | 1.35 | 1.40 | 1.42 | 1.34 |
| $P_{exp}$ in W | 69.98 | 164.56 | 139.04 | 119.49 | 186.32 |
| $\eta_{exp}$ in % | 11.85 | 34.38 | 26.69 | 21.91 | 40.22 |
| $\overline{x}\ t_{HX\text{-}2\ inlet}$ in °C | 73.26 | 73.90 | 74.06 | 74.29 | 73.23 |
| $t_{HX\text{-}2\ inlet\text{-}1}$ in °C | 66.68 | 66.98 | 66.97 | 67.32 | 66.22 |
| $t_{HX\text{-}2\ inlet\text{-}2}$ in °C | 72.90 | 72.93 | 73.29 | 73.68 | 72.67 |
| $t_{HX\text{-}2\ inlet\text{-}3}$ in °C | 78.77 | 79.50 | 79.92 | 80.05 | 78.94 |
| $t_{HX\text{-}2\ inlet\text{-}4}$ in °C | 74.68 | 76.18 | 76.04 | 76.13 | 75.10 |
| $\overline{x}\ t_{HX\text{-}2\ outlet}$ in °C | 28.55 | 29.50 | 29.95 | 28.40 | 28.29 |
| $t_{HX\text{-}2\ outlet\text{-}1}$ in °C | 28.74 | 29.63 | 30.05 | 28.56 | 28.49 |
| $t_{HX\text{-}2\ outlet\text{-}2}$ in °C | 28.79 | 29.69 | 30.12 | 28.62 | 28.54 |
| $t_{HX\text{-}2\ outlet\text{-}3}$ in °C | 29.72 | 30.63 | 31.07 | 29.51 | 29.45 |
| $t_{HX\text{-}2\ outlet\text{-}4}$ in °C | 30.19 | 31.06 | 31.46 | 29.93 | 29.91 |
| $t_{HX\text{-}2\ outlet\text{-}5}$ in °C | 27.48 | 28.48 | 28.95 | 27.39 | 27.24 |
| $t_{HX\text{-}2\ outlet\text{-}6}$ in °C | 27.82 | 28.82 | 29.30 | 27.72 | 27.57 |
| $t_{HX\text{-}2\ outlet\text{-}7}$ in °C | 28.27 | 29.29 | 29.79 | 28.16 | 28.01 |
| $t_{HX\text{-}2\ outlet\text{-}8}$ in °C | 27.37 | 28.39 | 28.87 | 27.27 | 27.11 |
| $P_{HX\text{-}2\ inlet}$ in Pa | 100 682.50 | 100 674.44 | 100 663.29 | 100 670.12 | 100 668.28 |
| $P_{HX\text{-}2\ inlet}$ in bar | 1.01 | 1.01 | 1.01 | 1.01 | 1.01 |
| $P_{HX\text{-}2\ outlet}$ in Pa | 99 617.72 | 99 601.41 | 99 592.60 | 99 600.69 | 99 593.66 |
| $P_{HX\text{-}2\ outlet}$ in bar | 1.00 | 1.00 | 1.00 | 1.00 | 1.00 |
| $\eta_{cycle}$ in % | 31.91 | 96.55 | 74.11 | 60.00 | 105.05 |

Table C.12: Tests 50-54

| Test number | Test 55 | Test 56 |
|---|---|---|
| $P_{exp\ output}$ in W | 195.47 | 120.09 |
| $M_{exp\ torque}$ in Nm | 0.56 | 0.30 |
| $rpm_{exp}$ in $min^{-1}$ | 3 359.24 | 3 831.03 |
| $\dot{m}_{CO2}$ in kg/min | 3.01 | 2.99 |
| $P_{pump\ inlet}$ in Pa | 5 723 932.01 | 5 733 074.43 |
| $P_{pump\ inlet}$ in bar | 57.24 | 57.33 |
| $t_{pump\ inlet}$ in °C | 17.86 | 17.90 |
| $s_{pump\ inlet}$ in J/kg*K | 1 159.20 | 1 159.60 |
| $h_{pump\ inlet}$ in J/kg | 247 529.67 | 247 657.29 |
| $h_{S\ pump\ outlet}$ in J/kg*K | 250 645.10 | 249 993.96 |
| $P_{pump\ outlet}$ in Pa | 8 250 609.47 | 7 622 841.20 |
| $P_{pump\ outlet}$ in bar | 82.51 | 76.23 |
| $t_{pump\ outlet}$ in °C | 21.52 | 20.71 |
| $s_{pump\ outlet}$ in J/kg*K | 1 159.72 | 1 160.19 |
| $h_{pump\ outlet}$ in J/kg | 250 796.02 | 250 165.23 |
| $\pi_{press\ ratio\ pump}$ | 1.44 | 1.33 |
| $P_{pump}$ in W | 163.98 | 125.04 |
| $\eta_{pump}$ in % | 95.38 | 93.17 |
| $P_{exp\ outlet}$ in Pa | 6 034 348.73 | 6 058 719.88 |
| $P_{exp\ outlet}$ in bar | 60.34 | 60.59 |
| $t_{exp\ outlet}$ in °C | 26.01 | 30.05 |
| $s_{exp\ outlet}$ in J/kg*K | 1 736.57 | 1 772.29 |
| $h_{exp\ outlet}$ in J/kg*K | 418 447.16 | 429 336.61 |
| $h_{S\ exp\ outlet}$ in J/kg | 413 414.05 | 425 564.02 |
| $P_{exp\ inlet}$ in Pa | 7 983 780.42 | 7 325 340.11 |
| $P_{exp\ inlet}$ in bar | 79.84 | 73.25 |
| $t_{exp\ inlet}$ in °C | 44.88 | 42.83 |
| $s_{exp\ inlet}$ in J/kg*K | 1 719.71 | 1 759.82 |
| $h_{exp\ inlet}$ in J/kg | 422 357.16 | 432 120.49 |
| $\pi_{press\ ratio\ exp}$ | 1.32 | 1.21 |
| $P_{exp}$ in W | 196.29 | 138.80 |
| $\eta_{exp}$ in % | 43.72 | 42.46 |
| $\overline{x}\ t_{HX\text{-}2\ inlet}$ in °C | 73.30 | 74.30 |
| $t_{HX\text{-}2\ inlet\text{-}1}$ in °C | 66.40 | 66.91 |
| $t_{HX\text{-}2\ inlet\text{-}2}$ in °C | 72.58 | 73.20 |
| $t_{HX\text{-}2\ inlet\text{-}3}$ in °C | 79.06 | 80.29 |
| $t_{HX\text{-}2\ inlet\text{-}4}$ in °C | 75.16 | 76.78 |
| $\overline{x}\ t_{HX\text{-}2\ outlet}$ in °C | 26.90 | 26.38 |
| $t_{HX\text{-}2\ outlet\text{-}1}$ in °C | 27.26 | 26.78 |
| $t_{HX\text{-}2\ outlet\text{-}2}$ in °C | 27.31 | 26.82 |
| $t_{HX\text{-}2\ outlet\text{-}3}$ in °C | 28.19 | 27.64 |
| $t_{HX\text{-}2\ outlet\text{-}4}$ in °C | 28.79 | 28.23 |
| $t_{HX\text{-}2\ outlet\text{-}5}$ in °C | 25.70 | 25.20 |
| $t_{HX\text{-}2\ outlet\text{-}6}$ in °C | 26.01 | 25.52 |
| $t_{HX\text{-}2\ outlet\text{-}7}$ in °C | 26.39 | 25.85 |
| $t_{HX\text{-}2\ outlet\text{-}8}$ in °C | 25.54 | 24.97 |
| $P_{HX\text{-}2\ inlet}$ in Pa | 100 672.44 | 100 659.39 |
| $P_{HX\text{-}2\ inlet}$ in bar | 1.01 | 1.01 |
| $P_{HX\text{-}2\ outlet}$ in Pa | 99 597.44 | 99 580.24 |
| $P_{HX\text{-}2\ outlet}$ in bar | 1.00 | 1.00 |
| $\eta_{cycle}$ in % | 119.71 | 111.00 |

Table C.13: Tests 55-56

## C.6 Test results and diagrams with 90 °C heat source temperature, 3.0 kg/min $CO_2$ mass flow at the expander loop and 60 bar condensation pressure

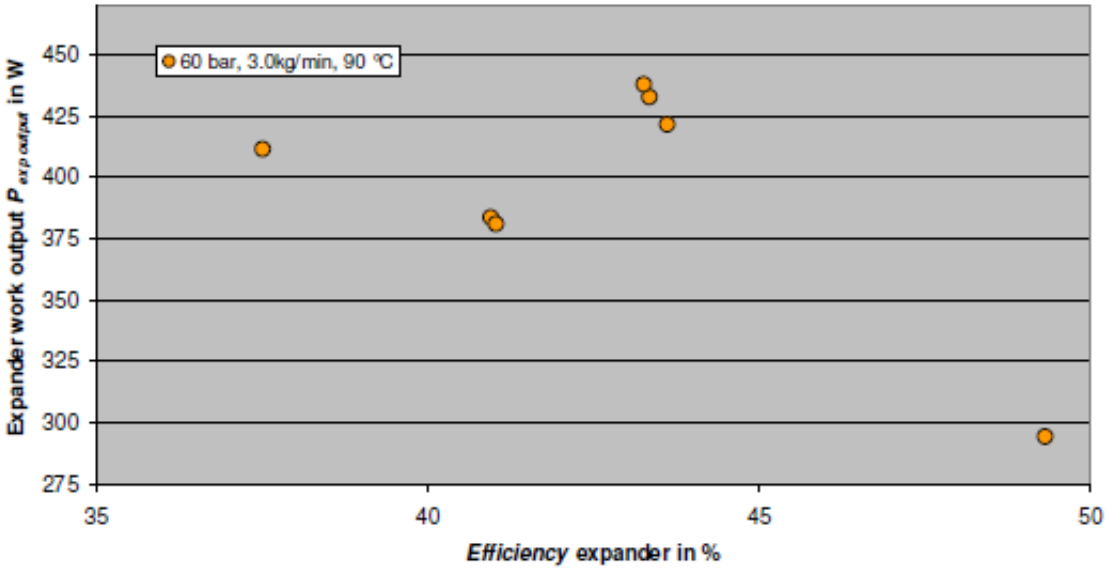


Figure C.6: Expander power output and efficiency, for tests with condensation conditions of 60 bar, 18 °C, with heat source temperature 90 °C and 3.0 $\frac{kg}{min}$ $CO_2$ mass flow at the expander loop

| Test number | Test 57 | Test 58 | Test 59 | Test 60 | Test 61 |
|---|---|---|---|---|---|
| $P_{exp\ output}$ in W | 400.98 | 406.58 | 348.04 | 408.54 | 391.93 |
| $M_{exp\ torque}$ in Nm | 1.19 | 0.95 | 0.78 | 0.97 | 0.89 |
| $rpm_{exp}$ in $min^{-1}$ | 3 207.59 | 4 100.85 | 4 259.83 | 4 015.65 | 4 216.16 |
| $\dot{m}_{CO2}$ in kg/min | 2.98 | 3.03 | 3.01 | 2.99 | 2.99 |
| $P_{pump\ inlet}$ in Pa | 5 590 634.51 | 5 595 338.20 | 5 594 900.61 | 5 593 732.93 | 5 616 152.25 |
| $P_{pump\ inlet}$ in bar | 55.91 | 55.95 | 55.95 | 55.94 | 56.16 |
| $t_{pump\ inlet}$ in °C | 16.45 | 16.53 | 16.52 | 16.53 | 16.70 |
| $s_{pump\ inlet}$ in J/kg*K | 1 144.60 | 1 145.45 | 1 145.38 | 1 145.48 | 1 147.09 |
| $h_{pump\ inlet}$ in J/kg | 243 126.45 | 243 378.14 | 243 355.08 | 243 383.42 | 243 876.80 |
| $h_{S\ pump\ outlet}$ in J/kg*K | 248 767.75 | 248 333.26 | 247 960.97 | 248 409.86 | 248 669.23 |
| $P_{pump\ outlet}$ in Pa | 10 270 176.92 | 9 694 721.20 | 9 402 080.09 | 9 752 747.96 | 9 572 691.01 |
| $P_{pump\ outlet}$ in bar | 102.70 | 96.95 | 94.02 | 97.53 | 95.73 |
| $t_{pump\ outlet}$ in °C | 22.77 | 22.17 | 21.81 | 22.26 | 22.20 |
| $s_{pump\ outlet}$ in J/kg*K | 1 147.44 | 1 148.22 | 1 148.11 | 1 148.34 | 1 149.88 |
| $h_{pump\ outlet}$ in J/kg | 249 605.89 | 249 151.15 | 248 765.91 | 249 254.65 | 249 493.05 |
| $\pi_{press\ ratio\ pump}$ | 1.84 | 1.73 | 1.68 | 1.74 | 1.70 |
| $P_{pump}$ in W | 321.59 | 291.19 | 271.51 | 292.80 | 279.95 |
| $\eta_{pump}$ in % | 87.06 | 85.83 | 85.12 | 85.61 | 85.33 |
| $P_{exp\ outlet}$ in Pa | 5 995 655.60 | 6 017 453.78 | 6 021 916.83 | 6 011 984.66 | 6 033 767.06 |
| $P_{exp\ outlet}$ in bar | 59.96 | 60.17 | 60.22 | 60.12 | 60.34 |
| $t_{exp\ outlet}$ in °C | 49.62 | 52.13 | 54.86 | 53.08 | 54.12 |
| $s_{exp\ outlet}$ in J/kg*K | 1 897.65 | 1 908.30 | 1 920.66 | 1 913.08 | 1 916.54 |
| $h_{exp\ outlet}$ in J/kg*K | 468 045.14 | 471 659.55 | 475 730.36 | 473 174.30 | 474 470.16 |
| $h_{S\ exp\ outlet}$ in J/kg | 454 231.64 | 460 443.49 | 464 707.82 | 461 656.80 | 463 536.12 |
| $P_{exp\ inlet}$ in Pa | 9 970 325.68 | 9 370 940.62 | 9 068 505.16 | 9 434 010.29 | 9 248 640.16 |
| $P_{exp\ inlet}$ in bar | 99.70 | 93.71 | 90.69 | 94.34 | 92.49 |
| $t_{exp\ inlet}$ in °C | 82.84 | 81.48 | 81.50 | 82.88 | 82.33 |
| $s_{exp\ inlet}$ in J/kg*K | 1 854.28 | 1 873.44 | 1 886.68 | 1 877.37 | 1 882.76 |
| $h_{exp\ inlet}$ in J/kg | 476 336.64 | 480 239.95 | 483 375.06 | 481 954.54 | 482 925.67 |
| $\pi_{press\ ratio\ exp}$ | 1.66 | 1.56 | 1.51 | 1.57 | 1.53 |
| $P_{exp}$ in W | 411.53 | 432.79 | 383.60 | 437.88 | 421.47 |
| $\eta_{exp}$ in % | 37.51 | 43.34 | 40.95 | 43.26 | 43.61 |
| $\overline{x}\ t_{HX\text{-}2\ inlet}$ in °C | 104.33 | 104.25 | 104.46 | 105.14 | 104.59 |
| $t_{HX\text{-}2\ inlet\text{-}1}$ in °C | 93.08 | 92.92 | 92.93 | 93.55 | 93.06 |
| $t_{HX\text{-}2\ inlet\text{-}2}$ in °C | 101.82 | 101.44 | 101.78 | 102.43 | 101.83 |
| $t_{HX\text{-}2\ inlet\text{-}3}$ in °C | 111.50 | 111.44 | 111.83 | 112.47 | 111.85 |
| $t_{HX\text{-}2\ inlet\text{-}4}$ in °C | 110.92 | 111.22 | 111.31 | 112.12 | 111.61 |
| $\overline{x}\ t_{HX\text{-}2\ outlet}$ in °C | 37.87 | 36.10 | 35.65 | 36.72 | 36.31 |
| $t_{HX\text{-}2\ outlet\text{-}1}$ in °C | 37.86 | 36.04 | 35.48 | 36.58 | 36.09 |
| $t_{HX\text{-}2\ outlet\text{-}2}$ in °C | 38.17 | 36.36 | 35.83 | 36.89 | 36.42 |
| $t_{HX\text{-}2\ outlet\text{-}3}$ in °C | 39.99 | 38.28 | 37.90 | 38.93 | 38.52 |
| $t_{HX\text{-}2\ outlet\text{-}4}$ in °C | 41.81 | 40.29 | 40.00 | 41.05 | 40.65 |
| $t_{HX\text{-}2\ outlet\text{-}5}$ in °C | 35.64 | 33.77 | 33.26 | 34.34 | 33.96 |
| $t_{HX\text{-}2\ outlet\text{-}6}$ in °C | 36.18 | 34.35 | 33.87 | 34.94 | 34.56 |
| $t_{HX\text{-}2\ outlet\text{-}7}$ in °C | 37.13 | 35.28 | 34.85 | 35.92 | 35.58 |
| $t_{HX\text{-}2\ outlet\text{-}8}$ in °C | 36.15 | 34.39 | 33.99 | 35.08 | 34.68 |
| $P_{HX\text{-}2\ inlet}$ in Pa | 100 896.49 | 100 860.20 | 100 851.96 | 100 834.17 | 100 797.01 |
| $P_{HX\text{-}2\ inlet}$ in bar | 1.01 | 1.01 | 1.01 | 1.01 | 1.01 |
| $P_{HX\text{-}2\ outlet}$ in Pa | 99 858.57 | 99 816.83 | 99 806.38 | 99 791.96 | 99 753.83 |
| $P_{HX\text{-}2\ outlet}$ in bar | 1.00 | 1.00 | 1.00 | 1.00 | 1.00 |
| $\eta_{cycle}$ in % | 127.97 | 148.63 | 141.29 | 149.55 | 150.55 |

Table C.14: Tests 57-61

| Test number | Test 62 | Test 63 |
|---|---|---|
| $P_{exp\ output}$ in W | 343.31 | 195.69 |
| $M_{exp\ torque}$ in Nm | 0.74 | 0.37 |
| $rpm_{exp}$ in $min^{-1}$ | 4 456.67 | 5 001.05 |
| $\dot{m}_{CO2}$ in kg/min | 3.01 | 3.06 |
| $P_{pump\ inlet}$ in Pa | 5 581 847.72 | 5 611 946.69 |
| $P_{pump\ inlet}$ in bar | 55.82 | 56.12 |
| $t_{pump\ inlet}$ in °C | 16.44 | 16.66 |
| $s_{pump\ inlet}$ in J/kg*K | 1 144.54 | 1 146.65 |
| $h_{pump\ inlet}$ in J/kg | 243 097.17 | 243 745.47 |
| $h_{S\ pump\ outlet}$ in J/kg*K | 247 626.22 | 246 795.72 |
| $P_{pump\ outlet}$ in Pa | 9 327 807.12 | 8 119 035.51 |
| $P_{pump\ outlet}$ in bar | 93.28 | 81.19 |
| $t_{pump\ outlet}$ in °C | 21.63 | 20.31 |
| $s_{pump\ outlet}$ in J/kg*K | 1 147.25 | 1 149.17 |
| $h_{pump\ outlet}$ in J/kg | 248 425.38 | 247 533.98 |
| $\pi_{press\ ratio\ pump}$ | 1.67 | 1.45 |
| $P_{pump}$ in W | 267.71 | 193.52 |
| $\eta_{pump}$ in % | 85.00 | 80.51 |
| $P_{exp\ outlet}$ in Pa | 6 015 337.95 | 6 085 207.30 |
| $P_{exp\ outlet}$ in bar | 60.15 | 60.85 |
| $t_{exp\ outlet}$ in °C | 55.85 | 65.37 |
| $s_{exp\ outlet}$ in J/kg*K | 1 925.51 | 1 962.11 |
| $h_{exp\ outlet}$ in J/kg*K | 477 271.78 | 490 038.95 |
| $h_{S\ exp\ outlet}$ in J/kg | 466 372.54 | 484 117.90 |
| $P_{exp\ inlet}$ in Pa | 8 991 415.23 | 7 704 521.56 |
| $P_{exp\ inlet}$ in bar | 89.91 | 77.05 |
| $t_{exp\ inlet}$ in °C | 81.92 | 80.85 |
| $s_{exp\ inlet}$ in J/kg*K | 1 892.01 | 1 944.51 |
| $h_{exp\ inlet}$ in J/kg | 484 854.86 | 495 799.37 |
| $\pi_{press\ ratio\ exp}$ | 1.49 | 1.27 |
| $P_{exp}$ in W | 381.00 | 294.24 |
| $\eta_{exp}$ in % | 41.03 | 49.31 |
| $\overline{x}\ t_{HX\text{-}2\ inlet}$ in °C | 105.13 | 106.79 |
| $t_{HX\text{-}2\ inlet\text{-}1}$ in °C | 93.47 | 94.45 |
| $t_{HX\text{-}2\ inlet\text{-}2}$ in °C | 102.47 | 103.66 |
| $t_{HX\text{-}2\ inlet\text{-}3}$ in °C | 112.39 | 114.22 |
| $t_{HX\text{-}2\ inlet\text{-}4}$ in °C | 112.19 | 114.84 |
| $\overline{x}\ t_{HX\text{-}2\ outlet}$ in °C | 35.62 | 32.51 |
| $t_{HX\text{-}2\ outlet\text{-}1}$ in °C | 35.34 | 32.42 |
| $t_{HX\text{-}2\ outlet\text{-}2}$ in °C | 35.74 | 32.94 |
| $t_{HX\text{-}2\ outlet\text{-}3}$ in °C | 37.90 | 34.97 |
| $t_{HX\text{-}2\ outlet\text{-}4}$ in °C | 40.08 | 37.30 |
| $t_{HX\text{-}2\ outlet\text{-}5}$ in °C | 33.21 | 29.90 |
| $t_{HX\text{-}2\ outlet\text{-}6}$ in °C | 33.87 | 30.57 |
| $t_{HX\text{-}2\ outlet\text{-}7}$ in °C | 34.87 | 31.48 |
| $t_{HX\text{-}2\ outlet\text{-}8}$ in °C | 33.93 | 30.47 |
| $P_{HX\text{-}2\ inlet}$ in Pa | 100 778.62 | 100 759.79 |
| $P_{HX\text{-}2\ inlet}$ in bar | 1.01 | 1.01 |
| $P_{HX\text{-}2\ outlet}$ in Pa | 99 734.75 | 99 707.67 |
| $P_{HX\text{-}2\ outlet}$ in bar | 1.00 | 1.00 |
| $\eta_{cycle}$ in % | 142.32 | 152.05 |

Table C.15: Tests 62-63

## C.7 Test results and diagrams with 65 °C heat source temperature, 1.8 kg/min $CO_2$ mass flow at the expander loop and 55 bar condensation pressure

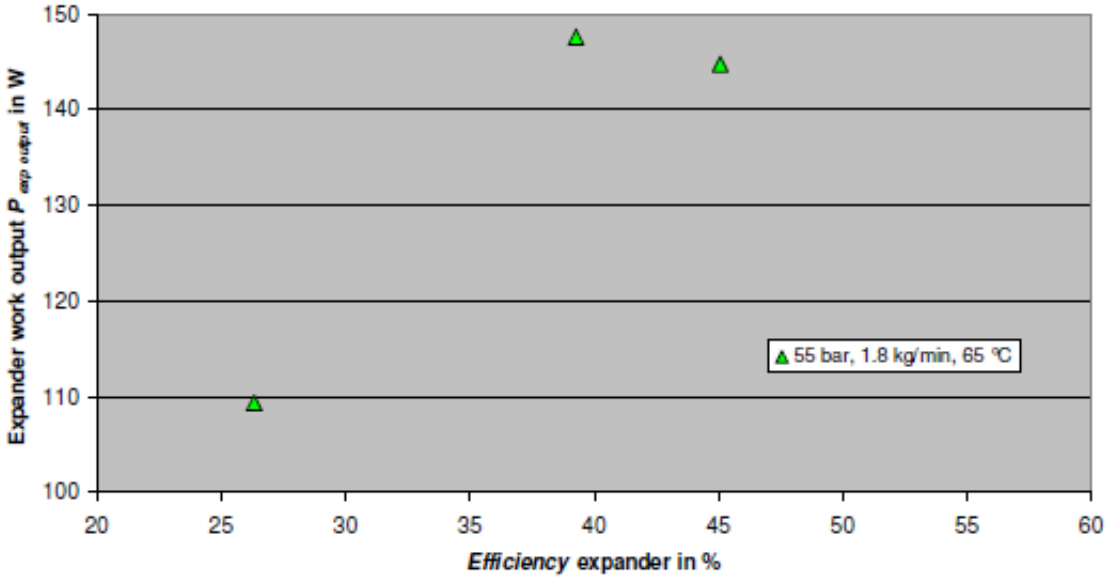


Figure C.7: Expander power output and efficiency, for tests with condensation conditions of 55 bar, 18 °C, with heat source temperature 65 °C and 1.8 $\frac{kg}{min}$ $CO_2$ mass flow at the expander loop

| Test number | Test 64 | Test 65 | Test 66 |
|---|---|---|---|
| $P_{exp\ output}$ in W | 116.59 | 89.47 | 113.81 |
| $M_{exp\ torque}$ in Nm | 0.56 | 0.67 | 0.41 |
| $rpm_{exp}$ in $min^{-1}$ | 1 970.82 | 1 275.00 | 2 662.44 |
| $\dot{m}_{CO2}$ in kg/min | 1.80 | 1.79 | 1.77 |
| $P_{pump\ inlet}$ in Pa | 5 415 833.26 | 5 357 565.19 | 5 419 226.51 |
| $P_{pump\ inlet}$ in bar | 54.16 | 53.58 | 54.19 |
| $t_{pump\ inlet}$ in °C | 12.49 | 13.70 | 14.31 |
| $s_{pump\ inlet}$ in J/kg*K | 1 103.21 | 1 116.97 | 1 122.74 |
| $h_{pump\ inlet}$ in J/kg | 231 009.98 | 234 880.22 | 236 611.11 |
| $h_{S\ pump\ outlet}$ in J/kg*K | 233 494.97 | 237 711.42 | 238 771.33 |
| $P_{pump\ outlet}$ in Pa | 7 548 478.22 | 7 754 727.56 | 7 234 847.02 |
| $P_{pump\ outlet}$ in bar | 75.48 | 77.55 | 72.35 |
| $t_{pump\ outlet}$ in °C | 15.12 | 16.86 | 16.81 |
| $s_{pump\ outlet}$ in J/kg*K | 1 105.05 | 1 119.46 | 1 125.07 |
| $h_{pump\ outlet}$ in J/kg | 234 024.28 | 238 431.63 | 239 445.10 |
| $\pi_{press\ ratio\ pump}$ | 1.39 | 1.45 | 1.34 |
| $P_{pump}$ in W | 90.19 | 105.96 | 83.57 |
| $\eta_{pump}$ in % | 82.44 | 79.72 | 76.23 |
| $P_{exp\ outlet}$ in Pa | 5 528 840.78 | 5 484 517.88 | 5 543 569.90 |
| $P_{exp\ outlet}$ in bar | 55.29 | 54.85 | 55.44 |
| $t_{exp\ outlet}$ in °C | 44.46 | 43.54 | 48.04 |
| $s_{exp\ outlet}$ in J/kg*K | 1 903.81 | 1 902.41 | 1 919.77 |
| $h_{exp\ outlet}$ in J/kg*K | 466 445.43 | 465 647.76 | 471 660.76 |
| $h_{S\ exp\ outlet}$ in J/kg | 458 819.93 | 455 391.30 | 465 680.57 |
| $P_{exp\ inlet}$ in Pa | 7 381 235.81 | 7 594 523.18 | 7 062 671.81 |
| $P_{exp\ inlet}$ in bar | 73.81 | 75.95 | 70.63 |
| $t_{exp\ inlet}$ in °C | 62.80 | 63.16 | 63.61 |
| $s_{exp\ inlet}$ in J/kg*K | 1 879.62 | 1 869.69 | 1 901.04 |
| $h_{exp\ inlet}$ in J/kg | 471 378.11 | 469 314.04 | 476 569.89 |
| $\pi_{press\ ratio\ exp}$ | 1.34 | 1.38 | 1.27 |
| $P_{exp}$ in W | 147.59 | 109.38 | 144.76 |
| $\eta_{exp}$ in % | 39.28 | 26.33 | 45.08 |
| $\overline{x}\ t_{HX\text{-}2\ inlet}$ in °C | 72.52 | 71.88 | 72.58 |
| $t_{HX\text{-}2\ inlet\text{-}1}$ in °C | 66.42 | 66.22 | 66.52 |
| $t_{HX\text{-}2\ inlet\text{-}2}$ in °C | 72.39 | 71.78 | 72.54 |
| $t_{HX\text{-}2\ inlet\text{-}3}$ in °C | 78.01 | 77.04 | 77.92 |
| $t_{HX\text{-}2\ inlet\text{-}4}$ in °C | 73.25 | 72.49 | 73.33 |
| $\overline{x}\ t_{HX\text{-}2\ outlet}$ in °C | 33.59 | 34.72 | 34.02 |
| $t_{HX\text{-}2\ outlet\text{-}1}$ in °C | 33.57 | 34.66 | 33.91 |
| $t_{HX\text{-}2\ outlet\text{-}2}$ in °C | 33.83 | 34.90 | 34.22 |
| $t_{HX\text{-}2\ outlet\text{-}3}$ in °C | 35.42 | 36.48 | 35.52 |
| $t_{HX\text{-}2\ outlet\text{-}4}$ in °C | 35.79 | 36.88 | 36.04 |
| $t_{HX\text{-}2\ outlet\text{-}5}$ in °C | 31.70 | 32.88 | 32.26 |
| $t_{HX\text{-}2\ outlet\text{-}6}$ in °C | 32.44 | 33.66 | 32.84 |
| $t_{HX\text{-}2\ outlet\text{-}7}$ in °C | 33.56 | 34.70 | 34.11 |
| $t_{HX\text{-}2\ outlet\text{-}8}$ in °C | 32.41 | 33.60 | 33.31 |
| $P_{HX\text{-}2\ inlet}$ in Pa | 101 028.31 | 100 939.06 | 100 923.33 |
| $P_{HX\text{-}2\ inlet}$ in bar | 1.01 | 1.01 | 1.01 |
| $P_{HX\text{-}2\ outlet}$ in Pa | 99 985.58 | 99 899.58 | 99 885.91 |
| $P_{HX\text{-}2\ outlet}$ in bar | 1.00 | 1.00 | 1.00 |
| $\eta_{cycle}$ in % | 163.64 | 103.23 | 173.22 |

Table C.16: Tests 64-66

## C.8 Test results and diagrams with 65 °C heat source temperature, 1.8 kg/min $CO_2$ mass flow at the expander loop and 50 bar condensation pressure

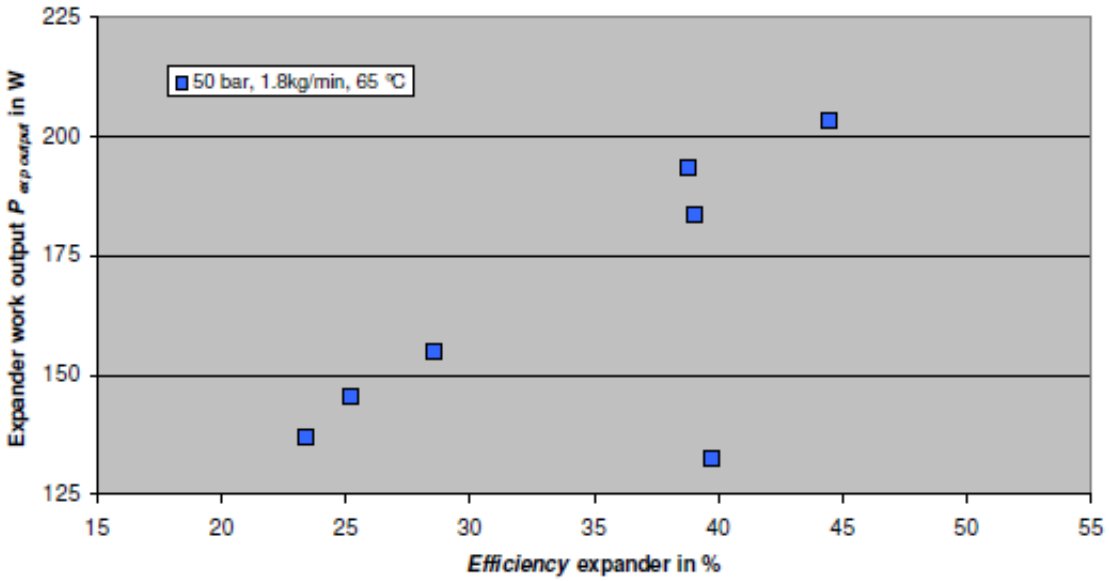


Figure C.8: Expander power output and efficiency, for tests with condensation conditions of 50 bar, 18 °C, with heat source temperature 65 °C and 1.8 $\frac{kg}{min}$ $CO_2$ mass flow at the expander loop

| Test number | Test 67 | Test 68 | Test 69 | Test 70 | Test 71 |
|---|---|---|---|---|---|
| $P_{exp\ output}$ in W | 146.84 | 160.72 | 133.44 | 125.52 | 119.62 |
| $M_{exp\ torque}$ in Nm | 0.60 | 0.70 | 0.86 | 1.00 | 1.04 |
| $rpm_{exp}$ in $min^{-1}$ | 2 326.97 | 2 205.91 | 1 488.84 | 1 197.70 | 1 097.84 |
| $\dot{m}_{CO2}$ in kg/min | 1.81 | 1.83 | 1.81 | 1.79 | 1.78 |
| $P_{pump\ inlet}$ in Pa | 4 873 528.37 | 4 861 664.04 | 4 821 571.22 | 4 824 989.28 | 4 807 008.86 |
| $P_{pump\ inlet}$ in bar | 48.74 | 48.62 | 48.22 | 48.25 | 48.07 |
| $t_{pump\ inlet}$ in °C | 8.70 | 8.53 | 8.09 | 7.85 | 7.59 |
| $s_{pump\ inlet}$ in J/kg*K | 1 070.83 | 1 069.30 | 1 065.30 | 1 062.88 | 1 060.58 |
| $h_{pump\ inlet}$ in J/kg | 221 195.83 | 220 749.87 | 219 580.01 | 218 903.16 | 218 234.80 |
| $h_{S\ pump\ outlet}$ in J/kg*K | 224 033.60 | 223 788.61 | 222 992.57 | 222 684.19 | 222 115.14 |
| $P_{pump\ outlet}$ in Pa | 7 379 340.93 | 7 549 622.38 | 7 852 741.71 | 8 193 158.91 | 8 271 041.98 |
| $P_{pump\ outlet}$ in bar | 73.79 | 75.50 | 78.53 | 81.93 | 82.71 |
| $t_{pump\ outlet}$ in °C | 11.57 | 11.62 | 11.54 | 11.59 | 11.44 |
| $s_{pump\ outlet}$ in J/kg*K | 1 073.64 | 1 072.52 | 1 069.13 | 1 066.72 | 1 064.77 |
| $h_{pump\ outlet}$ in J/kg | 224 832.46 | 224 704.36 | 224 079.77 | 223 774.73 | 223 306.94 |
| $\pi_{press\ ratio\ pump}$ | 1.51 | 1.55 | 1.63 | 1.70 | 1.72 |
| $P_{pump}$ in W | 109.52 | 120.54 | 135.63 | 145.14 | 150.66 |
| $\eta_{pump}$ in % | 78.03 | 76.84 | 75.84 | 77.61 | 76.50 |
| $P_{exp\ outlet}$ in Pa | 5 018 388.53 | 5 008 661.10 | 4 965 614.58 | 4 962 597.86 | 4 944 445.54 |
| $P_{exp\ outlet}$ in bar | 50.18 | 50.09 | 49.66 | 49.63 | 49.44 |
| $t_{exp\ outlet}$ in °C | 39.10 | 36.70 | 34.68 | 32.78 | 32.01 |
| $s_{exp\ outlet}$ in J/kg*K | 1 914.46 | 1 903.57 | 1 896.79 | 1 887.25 | 1 884.65 |
| $h_{exp\ outlet}$ in J/kg*K | 465 548.66 | 462 075.98 | 459 614.75 | 456 659.97 | 455 714.42 |
| $h_{S\ exp\ outlet}$ in J/kg | 456 023.98 | 452 048.14 | 446 744.46 | 442 160.47 | 440 590.03 |
| $P_{exp\ inlet}$ in Pa | 7 204 857.18 | 7 377 219.83 | 7 690 596.24 | 8 039 185.11 | 8 116 200.81 |
| $P_{exp\ inlet}$ in bar | 72.05 | 73.77 | 76.91 | 80.39 | 81.16 |
| $t_{exp\ inlet}$ in °C | 61.63 | 61.01 | 61.26 | 62.08 | 62.00 |
| $s_{exp\ inlet}$ in J/kg*K | 1 883.65 | 1 870.87 | 1 854.44 | 1 839.17 | 1 834.35 |
| $h_{exp\ inlet}$ in J/kg | 471 642.21 | 468 422.26 | 464 750.23 | 461 544.13 | 460 332.78 |
| $\pi_{press\ ratio\ exp}$ | 1.44 | 1.47 | 1.55 | 1.62 | 1.64 |
| $P_{exp}$ in W | 183.51 | 193.44 | 154.80 | 145.52 | 137.18 |
| $\eta_{exp}$ in % | 39.02 | 38.76 | 28.52 | 25.20 | 23.39 |
| $\overline{x}\ t_{HX\text{-}2\ inlet}$ in °C | 72.83 | 72.16 | 72.25 | 72.94 | 72.81 |
| $t_{HX\text{-}2\ inlet\text{-}1}$ in °C | 66.36 | 65.75 | 66.03 | 66.77 | 66.80 |
| $t_{HX\text{-}2\ inlet\text{-}2}$ in °C | 72.57 | 71.83 | 72.01 | 72.72 | 72.60 |
| $t_{HX\text{-}2\ inlet\text{-}3}$ in °C | 78.24 | 77.84 | 77.65 | 78.35 | 78.04 |
| $t_{HX\text{-}2\ inlet\text{-}4}$ in °C | 74.14 | 73.22 | 73.33 | 73.92 | 73.82 |
| $\overline{x}\ t_{HX\text{-}2\ outlet}$ in °C | 31.93 | 31.79 | 32.79 | 34.10 | 34.30 |
| $t_{HX\text{-}2\ outlet\text{-}1}$ in °C | 32.13 | 31.87 | 32.89 | 34.15 | 34.29 |
| $t_{HX\text{-}2\ outlet\text{-}2}$ in °C | 32.24 | 32.09 | 33.16 | 34.49 | 34.68 |
| $t_{HX\text{-}2\ outlet\text{-}3}$ in °C | 33.80 | 33.60 | 34.65 | 36.08 | 36.28 |
| $t_{HX\text{-}2\ outlet\text{-}4}$ in °C | 34.03 | 34.12 | 35.14 | 36.50 | 36.73 |
| $t_{HX\text{-}2\ outlet\text{-}5}$ in °C | 30.03 | 29.93 | 30.86 | 32.05 | 32.24 |
| $t_{HX\text{-}2\ outlet\text{-}6}$ in °C | 30.64 | 30.59 | 31.65 | 32.91 | 33.19 |
| $t_{HX\text{-}2\ outlet\text{-}7}$ in °C | 31.84 | 31.66 | 32.63 | 34.01 | 34.21 |
| $t_{HX\text{-}2\ outlet\text{-}8}$ in °C | 30.70 | 30.45 | 31.34 | 32.65 | 32.79 |
| $P_{HX\text{-}2\ inlet}$ in Pa | 100 910.12 | 100 917.99 | 100 929.08 | 100 922.38 | 100 934.48 |
| $P_{HX\text{-}2\ inlet}$ in bar | 1.01 | 1.01 | 1.01 | 1.01 | 1.01 |
| $P_{HX\text{-}2\ outlet}$ in Pa | 99 851.18 | 99 856.67 | 99 869.33 | 99 865.83 | 99 880.11 |
| $P_{HX\text{-}2\ outlet}$ in bar | 1.00 | 1.00 | 1.00 | 1.00 | 1.00 |
| $\eta_{cycle}$ in % | 167.56 | 160.48 | 114.13 | 100.26 | 91.05 |

Table C.17: Tests 67-71

| Test number | Test 72 | Test 73 |
|---|---|---|
| $P_{exp\ output}$ in W | 162.83 | 87.62 |
| $M_{exp\ torque}$ in Nm | 0.52 | 0.25 |
| $rpm_{exp}$ in $min^{-1}$ | 2 962.63 | 3 352.43 |
| $\dot{m}_{CO2}$ in kg/min | 1.82 | 1.78 |
| $P_{pump\ inlet}$ in Pa | 4 860 747.05 | 4 847 472.19 |
| $P_{pump\ inlet}$ in bar | 48.61 | 48.47 |
| $t_{pump\ inlet}$ in °C | 8.19 | 8.29 |
| $s_{pump\ inlet}$ in J/kg*K | 1 065.84 | 1 066.99 |
| $h_{pump\ inlet}$ in J/kg | 219 776.50 | 220 084.38 |
| $h_{S\ pump\ outlet}$ in J/kg*K | 222 476.00 | 222 033.28 |
| $P_{pump\ outlet}$ in Pa | 7 254 428.22 | 6 570 989.32 |
| $P_{pump\ outlet}$ in bar | 72.54 | 65.71 |
| $t_{pump\ outlet}$ in °C | 11.03 | 10.49 |
| $s_{pump\ outlet}$ in J/kg*K | 1 069.77 | 1 071.07 |
| $h_{pump\ outlet}$ in J/kg | 223 591.02 | 223 190.20 |
| $\pi_{press\ ratio\ pump}$ | 1.49 | 1.36 |
| $P_{pump}$ in W | 115.59 | 92.11 |
| $\eta_{pump}$ in % | 70.77 | 62.75 |
| $P_{exp\ outlet}$ in Pa | 5 010 119.71 | 4 995 839.07 |
| $P_{exp\ outlet}$ in bar | 50.10 | 49.96 |
| $t_{exp\ outlet}$ in °C | 39.76 | 46.55 |
| $s_{exp\ outlet}$ in J/kg*K | 1 918.19 | 1 949.80 |
| $h_{exp\ outlet}$ in J/kg*K | 466 641.96 | 476 508.13 |
| $h_{S\ exp\ outlet}$ in J/kg | 458 280.14 | 469 737.93 |
| $P_{exp\ inlet}$ in Pa | 7 073 693.62 | 6 375 246.46 |
| $P_{exp\ inlet}$ in bar | 70.74 | 63.75 |
| $t_{exp\ inlet}$ in °C | 61.68 | 61.24 |
| $s_{exp\ inlet}$ in J/kg*K | 1 891.23 | 1 928.46 |
| $h_{exp\ inlet}$ in J/kg | 473 348.60 | 480 978.81 |
| $\pi_{press\ ratio\ exp}$ | 1.41 | 1.28 |
| $P_{exp}$ in W | 203.23 | 132.58 |
| $\eta_{exp}$ in % | 44.51 | 39.77 |
| $\overline{x}\ t_{HX\text{-}2\ inlet}$ in °C | 72.79 | 72.70 |
| $t_{HX\text{-}2\ inlet\text{-}1}$ in °C | 66.44 | 66.20 |
| $t_{HX\text{-}2\ inlet\text{-}2}$ in °C | 72.54 | 72.29 |
| $t_{HX\text{-}2\ inlet\text{-}3}$ in °C | 78.32 | 78.14 |
| $t_{HX\text{-}2\ inlet\text{-}4}$ in °C | 73.85 | 74.15 |
| $\overline{x}\ t_{HX\text{-}2\ outlet}$ in °C | 31.17 | 30.55 |
| $t_{HX\text{-}2\ outlet\text{-}1}$ in °C | 31.41 | 30.19 |
| $t_{HX\text{-}2\ outlet\text{-}2}$ in °C | 31.49 | 30.69 |
| $t_{HX\text{-}2\ outlet\text{-}3}$ in °C | 32.82 | 32.41 |
| $t_{HX\text{-}2\ outlet\text{-}4}$ in °C | 33.37 | 33.25 |
| $t_{HX\text{-}2\ outlet\text{-}5}$ in °C | 29.67 | 28.61 |
| $t_{HX\text{-}2\ outlet\text{-}6}$ in °C | 29.93 | 28.96 |
| $t_{HX\text{-}2\ outlet\text{-}7}$ in °C | 30.94 | 30.46 |
| $t_{HX\text{-}2\ outlet\text{-}8}$ in °C | 29.75 | 29.84 |
| $P_{HX\text{-}2\ inlet}$ in Pa | 100 916.14 | 100 905.34 |
| $P_{HX\text{-}2\ inlet}$ in bar | 1.01 | 1.01 |
| $P_{HX\text{-}2\ outlet}$ in Pa | 99 854.72 | 99 843.78 |
| $P_{HX\text{-}2\ outlet}$ in bar | 1.00 | 1.00 |
| $\eta_{cycle}$ in % | 175.82 | 143.95 |

Table C.18: Tests 72-73

## C.9 Test results and diagrams with 65 °C heat source temperature, 1.8 kg/min $CO_2$ mass flow at the expander loop and 42.5 bar condensation pressure

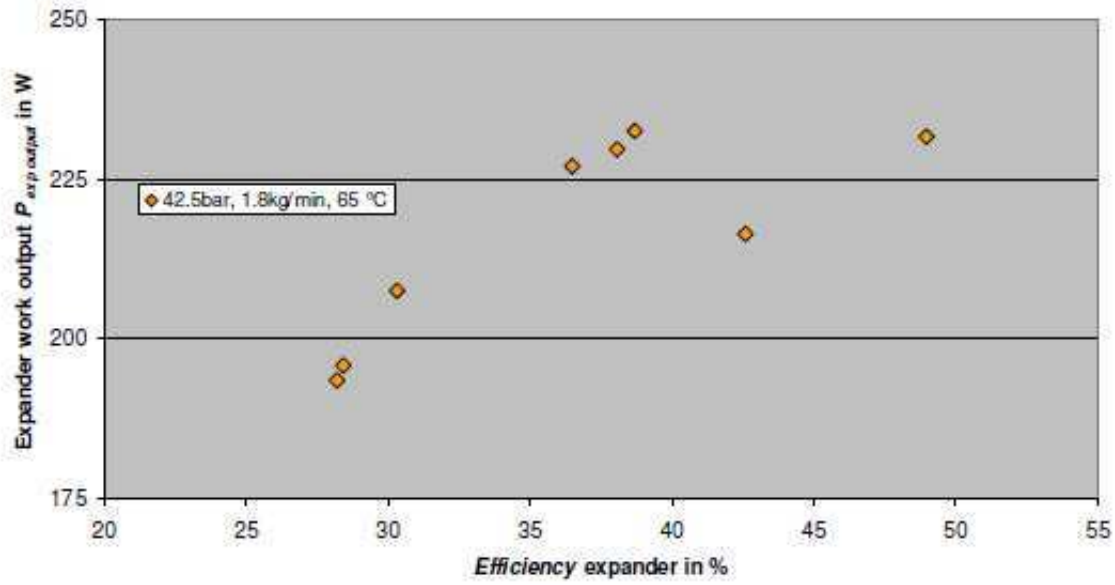


Figure C.9: Expander power output and efficiency, for tests with condensation conditions of 42.5 bar, 18 °C, with heat source temperature 65 °C and 1.8 $\frac{kg}{min}$ $CO_2$ mass flow at the expander loop

| Test number | Test 74 | Test 75 | Test 76 | Test 77 | Test 78 |
|---|---|---|---|---|---|
| $P_{exp\ output}$ in W | 192.76 | 191.87 | 188.41 | 182.79 | 170.69 |
| $M_{exp\ torque}$ in Nm | 0.64 | 0.64 | 0.70 | 0.87 | 0.94 |
| $rpm_{exp}$ in $min^{-1}$ | 2 864.07 | 2 850.58 | 2 559.74 | 1 998.28 | 1 727.58 |
| $\dot{m}_{CO2}$ in kg/min | 1.81 | 1.80 | 1.79 | 1.82 | 1.82 |
| $P_{pump\ inlet}$ in Pa | 4 094 843.89 | 4 044 238.01 | 4 068 998.72 | 4 067 836.63 | 4 067 987.27 |
| $P_{pump\ inlet}$ in bar | 40.95 | 40.44 | 40.69 | 40.68 | 40.68 |
| $t_{pump\ inlet}$ in °C | 1.51 | 1.84 | 2.12 | 2.22 | 2.23 |
| $s_{pump\ inlet}$ in J/kg*K | 1 009.12 | 1 012.63 | 1 015.03 | 1 015.96 | 1 016.02 |
| $h_{pump\ inlet}$ in J/kg | 203 157.84 | 204 066.08 | 204 754.75 | 205 009.09 | 205 025.77 |
| $h_{S\ pump\ outlet}$ in J/kg*K | 206 212.79 | 207 126.91 | 207 954.73 | 208 636.51 | 208 699.94 |
| $P_{pump\ outlet}$ in Pa | 6 928 606.76 | 6 875 235.60 | 7 023 742.56 | 7 417 238.49 | 7 460 650.32 |
| $P_{pump\ outlet}$ in bar | 69.29 | 68.75 | 70.24 | 74.17 | 74.61 |
| $t_{pump\ outlet}$ in °C | 4.40 | 4.79 | 5.22 | 5.65 | 5.72 |
| $s_{pump\ outlet}$ in J/kg*K | 1 013.60 | 1 017.37 | 1 020.00 | 1 020.89 | 1 021.19 |
| $h_{pump\ outlet}$ in J/kg | 207 456.08 | 208 444.20 | 209 335.98 | 210 008.48 | 210 140.95 |
| $\pi_{press\ ratio\ pump}$ | 1.69 | 1.70 | 1.73 | 1.82 | 1.83 |
| $P_{pump}$ in W | 129.32 | 131.07 | 136.30 | 151.60 | 155.12 |
| $\eta_{pump}$ in % | 71.07 | 69.91 | 69.85 | 72.56 | 71.83 |
| $P_{exp\ outlet}$ in Pa | 4 277 782.15 | 4 227 505.33 | 4 248 284.78 | 4 250 587.38 | 4 250 407.69 |
| $P_{exp\ outlet}$ in bar | 42.78 | 42.28 | 42.48 | 42.51 | 42.50 |
| $t_{exp\ outlet}$ in °C | 34.06 | 33.51 | 33.96 | 30.83 | 29.98 |
| $s_{exp\ outlet}$ in J/kg*K | 1 947.77 | 1 949.33 | 1 949.67 | 1 935.35 | 1 931.41 |
| $h_{exp\ outlet}$ in J/kg*K | 468 779.72 | 468 728.18 | 469 052.66 | 464 701.57 | 463 505.13 |
| $h_{S\ exp\ outlet}$ in J/kg | 456 530.46 | 456 242.77 | 455 768.82 | 448 971.88 | 447 264.06 |
| $P_{exp\ inlet}$ in Pa | 6 739 090.95 | 6 689 688.92 | 6 842 549.82 | 7 242 424.87 | 7 289 225.36 |
| $P_{exp\ inlet}$ in bar | 67.39 | 66.90 | 68.43 | 72.42 | 72.89 |
| $t_{exp\ inlet}$ in °C | 61.11 | 60.65 | 62.01 | 61.85 | 61.21 |
| $s_{exp\ inlet}$ in J/kg*K | 1 907.32 | 1 908.01 | 1 905.73 | 1 882.66 | 1 876.84 |
| $h_{exp\ inlet}$ in J/kg | 476 508.13 | 476 398.96 | 476 682.04 | 471 544.60 | 469 883.55 |
| $\pi_{press\ ratio\ exp}$ | 1.58 | 1.58 | 1.61 | 1.70 | 1.71 |
| $P_{exp}$ in W | 232.52 | 229.64 | 226.98 | 207.51 | 193.43 |
| $\eta_{exp}$ in % | 38.69 | 38.06 | 36.48 | 30.32 | 28.20 |
| $\overline{x}\ t_{HX\text{-}2\ inlet}$ in °C | 73.10 | 72.52 | 74.07 | 73.73 | 73.24 |
| $t_{HX\text{-}2\ inlet\text{-}1}$ in °C | 66.15 | 65.51 | 66.90 | 66.79 | 66.49 |
| $t_{HX\text{-}2\ inlet\text{-}2}$ in °C | 72.68 | 72.05 | 73.41 | 73.34 | 72.58 |
| $t_{HX\text{-}2\ inlet\text{-}3}$ in °C | 78.82 | 78.24 | 79.96 | 79.43 | 78.92 |
| $t_{HX\text{-}2\ inlet\text{-}4}$ in °C | 74.75 | 74.28 | 76.02 | 75.36 | 74.97 |
| $\overline{x}\ t_{HX\text{-}2\ outlet}$ in °C | 28.83 | 28.67 | 30.18 | 30.65 | 30.25 |
| $t_{HX\text{-}2\ outlet\text{-}1}$ in °C | 29.32 | 29.07 | 30.76 | 30.70 | 30.41 |
| $t_{HX\text{-}2\ outlet\text{-}2}$ in °C | 29.16 | 29.03 | 30.48 | 31.00 | 30.56 |
| $t_{HX\text{-}2\ outlet\text{-}3}$ in °C | 30.32 | 30.18 | 31.93 | 32.74 | 32.18 |
| $t_{HX\text{-}2\ outlet\text{-}4}$ in °C | 31.18 | 31.00 | 32.71 | 33.50 | 32.96 |
| $t_{HX\text{-}2\ outlet\text{-}5}$ in °C | 27.50 | 27.34 | 28.70 | 28.57 | 28.36 |
| $t_{HX\text{-}2\ outlet\text{-}6}$ in °C | 27.52 | 27.35 | 28.84 | 29.19 | 28.88 |
| $t_{HX\text{-}2\ outlet\text{-}7}$ in °C | 28.44 | 28.35 | 29.80 | 30.36 | 29.96 |
| $t_{HX\text{-}2\ outlet\text{-}8}$ in °C | 27.19 | 27.06 | 28.23 | 29.17 | 28.71 |
| $P_{HX\text{-}2\ inlet}$ in Pa | 100 649.85 | 100 609.00 | 100 578.65 | 100 570.80 | 100 548.01 |
| $P_{HX\text{-}2\ inlet}$ in bar | 1.01 | 1.01 | 1.01 | 1.01 | 1.01 |
| $P_{HX\text{-}2\ outlet}$ in Pa | 99 588.50 | 99 547.69 | 99 522.36 | 99 513.14 | 99 486.55 |
| $P_{HX\text{-}2\ outlet}$ in bar | 1.00 | 1.00 | 1.00 | 1.00 | 0.99 |
| $\eta_{cycle}$ in % | 179.80 | 175.21 | 166.54 | 136.88 | 124.70 |

Table C.19: Tests 74-78

| Test number | Test 79 | Test 80 | Test 81 |
|---|---|---|---|
| $P_{exp\ output}$ in W | 170.38 | 174.95 | 176.53 |
| $M_{exp\ torque}$ in Nm | 0.94 | 0.52 | 0.44 |
| $rpm_{exp}$ in $min^{-1}$ | 1 724.14 | 3 220.99 | 3 821.98 |
| $\dot{m}_{CO2}$ in kg/min | 1.81 | 1.78 | 1.80 |
| $P_{pump\ inlet}$ in Pa | 4 069 500.62 | 4 036 545.49 | 4 041 350.93 |
| $P_{pump\ inlet}$ in bar | 40.70 | 40.37 | 40.41 |
| $t_{pump\ inlet}$ in °C | 2.21 | 1.66 | 1.77 |
| $s_{pump\ inlet}$ in J/kg*K | 1 015.88 | 1 010.97 | 1 011.99 |
| $h_{pump\ inlet}$ in J/kg | 204 987.83 | 203 601.48 | 203 888.89 |
| $h_{S\ pump\ outlet}$ in J/kg*K | 208 666.16 | 206 057.02 | 206 137.55 |
| $P_{pump\ outlet}$ in Pa | 7 466 437.11 | 6 308 114.74 | 6 119 168.72 |
| $P_{pump\ outlet}$ in bar | 74.66 | 63.08 | 61.19 |
| $t_{pump\ outlet}$ in °C | 5.73 | 4.27 | 4.22 |
| $s_{pump\ outlet}$ in J/kg*K | 1 021.25 | 1 017.01 | 1 017.96 |
| $h_{pump\ outlet}$ in J/kg | 210 162.07 | 207 731.40 | 207 789.61 |
| $\pi_{press\ ratio\ pump}$ | 1.83 | 1.56 | 1.51 |
| $P_{pump}$ in W | 156.41 | 122.65 | 117.03 |
| $\eta_{pump}$ in % | 71.09 | 59.46 | 57.65 |
| $P_{exp\ outlet}$ in Pa | 4 251 412.33 | 4 224 330.26 | 4 235 871.50 |
| $P_{exp\ outlet}$ in bar | 42.51 | 42.24 | 42.36 |
| $t_{exp\ outlet}$ in °C | 30.77 | 39.97 | 41.88 |
| $s_{exp\ outlet}$ in J/kg*K | 1 934.99 | 1 977.17 | 1 984.14 |
| $h_{exp\ outlet}$ in J/kg*K | 464 601.75 | 477 321.26 | 479 639.47 |
| $h_{S\ exp\ outlet}$ in J/kg | 448 290.66 | 467 496.36 | 471 587.70 |
| $P_{exp\ inlet}$ in Pa | 7 294 279.42 | 6 108 742.29 | 5 914 208.47 |
| $P_{exp\ inlet}$ in bar | 72.94 | 61.09 | 59.14 |
| $t_{exp\ inlet}$ in °C | 61.96 | 61.67 | 62.11 |
| $s_{exp\ inlet}$ in J/kg*K | 1 880.31 | 1 945.41 | 1 958.33 |
| $h_{exp\ inlet}$ in J/kg | 471 078.04 | 484 607.76 | 487 359.88 |
| $\pi_{press\ ratio\ exp}$ | 1.72 | 1.45 | 1.40 |
| $P_{exp}$ in W | 195.77 | 216.39 | 231.63 |
| $\eta_{exp}$ in % | 28.42 | 42.58 | 48.95 |
| $\overline{x}\ t_{HX\text{-}2\ inlet}$ in °C | 73.87 | 74.12 | 74.53 |
| $t_{HX\text{-}2\ inlet\text{-}1}$ in °C | 67.15 | 67.21 | 67.35 |
| $t_{HX\text{-}2\ inlet\text{-}2}$ in °C | 73.43 | 73.38 | 73.54 |
| $t_{HX\text{-}2\ inlet\text{-}3}$ in °C | 79.48 | 79.96 | 80.43 |
| $t_{HX\text{-}2\ inlet\text{-}4}$ in °C | 75.43 | 75.95 | 76.81 |
| $\overline{x}\ t_{HX\text{-}2\ outlet}$ in °C | 30.90 | 28.88 | 28.73 |
| $t_{HX\text{-}2\ outlet\text{-}1}$ in °C | 30.98 | 28.52 | 28.33 |
| $t_{HX\text{-}2\ outlet\text{-}2}$ in °C | 31.22 | 29.14 | 28.96 |
| $t_{HX\text{-}2\ outlet\text{-}3}$ in °C | 32.95 | 31.14 | 30.88 |
| $t_{HX\text{-}2\ outlet\text{-}4}$ in °C | 33.74 | 31.76 | 31.62 |
| $t_{HX\text{-}2\ outlet\text{-}5}$ in °C | 28.88 | 27.28 | 26.72 |
| $t_{HX\text{-}2\ outlet\text{-}6}$ in °C | 29.50 | 27.34 | 27.01 |
| $t_{HX\text{-}2\ outlet\text{-}7}$ in °C | 30.61 | 28.61 | 28.52 |
| $t_{HX\text{-}2\ outlet\text{-}8}$ in °C | 29.34 | 27.23 | 27.81 |
| $P_{HX\text{-}2\ inlet}$ in Pa | 100 543.19 | 100 469.62 | 100 457.03 |
| $P_{HX\text{-}2\ inlet}$ in bar | 1.01 | 1.00 | 1.00 |
| $P_{HX\text{-}2\ outlet}$ in Pa | 99 489.68 | 99 411.49 | 99 399.69 |
| $P_{HX\text{-}2\ outlet}$ in bar | 0.99 | 0.99 | 0.99 |
| $\eta_{cycle}$ in % | 125.16 | 176.43 | 197.92 |

Table C.20: Tests 79-81

# D Results and input datas from the simulations

## D.1 Input datas and results of the simulation for the heat transfer coefficient times area of HX-2

| Test number | Test 5 | Test 34 | Test 42 | Test 45 | Test 56 |
|---|---|---|---|---|---|
| $P_{exp\ output}$ in W | 94.72 | 144.92 | 192.36 | 156.76 | 120.09 |
| $M_{exp\ torque}$ in Nm | 0.37 | 1.12 | 0.50 | 0.49 | 0.30 |
| $rpm_{exp}$ in $min^{-1}$ | 2477.36 | 1232.50 | 3676.77 | 3080.86 | 3831.03 |
| $\dot{m}_{CO2}$ in kg/min | 1.81 | 1.78 | 1.81 | 2.50 | 2.99 |
| $P_{pump\ inlet}$ in bar | 58.48 | 58.30 | 58.54 | 57.74 | 57.33 |
| $t_{pump\ inlet}$ in °C | 18.22 | 18.11 | 18.05 | 18.04 | 17.90 |
| $P_{pump\ outlet}$ in bar | 76.90 | 95.57 | 81.21 | 79.24 | 76.23 |
| $t_{pump\ outlet}$ in °C | 21.18 | 23.53 | 21.58 | 21.41 | 20.71 |
| $\eta_{pump}$ in % | 72.41 | 86.25 | 75.44 | 76.96 | 93.17 |
| $P_{exp\ outlet}$ in bar | 59.81 | 59.64 | 60.04 | 60.04 | 60.59 |
| $t_{exp\ outlet}$ in °C | 48.48 | 60.68 | 87.64 | 35.20 | 30.05 |
| $P_{exp\ inlet}$ in bar | 75.24 | 94.09 | 79.24 | 76.89 | 73.25 |
| $t_{exp\ inlet}$ in °C | 63.32 | 88.24 | 106.12 | 52.00 | 42.83 |
| $\eta_{exp}$ in % | 40.36 | 28.72 | 56.38 | 46.84 | 42.46 |
| $\overline{X}\ t_{HX\text{-}2\ inlet}$ in °C | 72.22 | 101.42 | 123.54 | 72.87 | 74.30 |
| $\overline{X}\ t_{HX\text{-}2\ outlet}$ in °C | 35.54 | 56.56 | 67.05 | 29.22 | 26.38 |
| $P_{HX\text{-}2\ inlet}$ in bar | 1.01 | 1.01 | 1.00 | 1.00 | 1.01 |
| $P_{HX\text{-}2\ outlet}$ in bar | 0.99 | 1.00 | 0.99 | 0.99 | 1.00 |
| $\dot{m}_{air\ loop}$ in $m^3/h$ | 569.23 | 545.82 | 531.74 | 568.20 | 567.83 |
| $\dot{m}_{air\ loop}$ in $m^3/min$ | 9.49 | 9.10 | 8.86 | 9.47 | 9.46 |
| *Simulation of* | Test 5 | Test 34 | Test 42 | Test 45 | Test 56 |
| heat transfer coefficient times area of HX-2 | Result | Result | Result | Result | Result |
| $UA$ in kW/K | 4 455.42 | 2 606.74 | 2 288.70 | 4 234.68 | 3 922.99 |

Figure D.1: Simulation input datas and results for the UA value

| Test number | Test 63 | Test 64 | Test 70 | Test 75 |
|---|---|---|---|---|
| $P_{exp\ output}$ in W | 195.69 | 116.59 | 125.52 | 191.87 |
| $M_{exp\ torque}$ in Nm | 0.37 | 0.56 | 1.00 | 0.64 |
| $rpm_{exp}$ in $min^{-1}$ | 5001.05 | 1970.82 | 1197.70 | 2850.58 |
| $\dot{m}_{CO2}$ in kg/min | 3.06 | 1.80 | 1.79 | 1.80 |
| $P_{pump\ inlet}$ in bar | 56.12 | 54.16 | 48.25 | 40.44 |
| $t_{pump\ inlet}$ in °C | 16.66 | 12.49 | 7.85 | 1.84 |
| $P_{pump\ outlet}$ in bar | 81.19 | 75.48 | 81.93 | 68.75 |
| $t_{pump\ outlet}$ in °C | 20.31 | 15.12 | 11.59 | 4.79 |
| $\eta_{pump}$ in % | 80.51 | 82.44 | 77.61 | 69.91 |
| $P_{exp\ outlet}$ in bar | 60.85 | 55.29 | 49.63 | 42.28 |
| $t_{exp\ outlet}$ in °C | 65.37 | 44.46 | 32.78 | 33.51 |
| $P_{exp\ inlet}$ in bar | 77.05 | 73.81 | 80.39 | 66.90 |
| $t_{exp\ inlet}$ in °C | 80.85 | 62.80 | 62.08 | 60.65 |
| $\eta_{exp}$ in % | 49.31 | 39.28 | 25.20 | 38.06 |
| $\overline{X}\ t_{HX\text{-}2\ inlet}$ in °C | 106.79 | 72.52 | 72.94 | 72.52 |
| $\overline{X}\ t_{HX\text{-}2\ outlet}$ in °C | 32.51 | 33.59 | 34.10 | 28.67 |
| $P_{HX\text{-}2\ inlet}$ in bar | 1.01 | 1.01 | 1.01 | 1.01 |
| $P_{HX\text{-}2\ outlet}$ in bar | 1.00 | 1.00 | 1.00 | 1.00 |
| $\dot{m}_{air\ loop}$ in $m^3/h$ | 543.26 | 576.18 | 580.88 | 581.05 |
| $\dot{m}_{air\ loop}$ in $m^3/min$ | 9.05 | 9.60 | 9.68 | 9.68 |
| *Simulation of* | Test 63 | Test 64 | Test 70 | Test 75 |
| heat transfer coefficient times area of HX-2 | Result | Result | Result | Result |
| *UA* in kW/K | 4 607.95 | 4132,2837 | 3 761.05 | 3 990.99 |

Figure D.2: Simulation input datas and results for the UA value

## D.2 Simulation results of the needed air-volume flow in the air loop and the work output at the expander

### D.2.1 Simulation results for the simulation for an UA value of 2 000 $\frac{kW}{K}$, heat source temperature 65 °C and $CO_2$massflow of 3.5 $\frac{kg}{min}$

| $P_{exp\ output}$ in W | 151.93 | 155.15 | 174.80 | 179.45 | 179.45 | 220.71 | 234.54 | 246.89 | 246.89 |
|---|---|---|---|---|---|---|---|---|---|
| Liquid facation $_{R744}$ | | | | | | | | | |
| exp $_{outlet}$ in % | 0.00 | 0.00 | 0.00 | 0.00 | 0.00 | 0.00 | 0.00 | 0.00 | 0.00 |
| $\dot{m}_{air\ loop}$ in $m^3/h$ | 991.16 | 1244.70 | 1226.30 | 1216.70 | 1047.00 | 1171.60 | 1145.00 | 1126.40 | 1148.90 |
| $P_{pump\ inlet}$ in bar | 57.00 | 57.00 | 57.00 | 57.00 | 57.00 | 57.00 | 57.00 | 57.00 | 57.00 |
| $P_{pump\ outlet}$ in bar | 70.00 | 72.00 | 74.00 | 76.00 | 78.00 | 80.00 | 82.00 | 84.00 | 86.00 |
| $t_{pump\ inlet}$ in °C | 18.00 | 18.00 | 18.00 | 18.00 | 18.00 | 18.00 | 18.00 | 18.00 | 18.00 |
| $t_{pump\ outlet}$ in °C | 20.85 | 21.27 | 21.69 | 22.12 | 22.54 | 22.96 | 23.38 | 23.79 | 24.20 |
| $P_{exp\ inlet}$ in bar | 70.00 | 72.00 | 74.00 | 76.00 | 78.00 | 80.00 | 82.00 | 84.00 | 86.00 |
| $P_{exp\ outlet}$ in bar | 60.00 | 60.00 | 60.00 | 60.00 | 60.00 | 60.00 | 60.00 | 60.00 | 60.00 |
| $t_{exp\ outlet}$ in °C | 24.00 | 42.76 | 40.79 | 40.30 | 40.30 | 35.52 | 33.66 | 31.84 | 31.84 |
| $t_{exp\ inlet}$ in °C | 49.74 | 55.00 | 55.00 | 55.15 | 52.55 | 55.08 | 55.00 | 55.06 | 55.75 |
| $\overline{X}\ t_{HX\text{-}2\ inlet}$ in °C | 72.00 | 72.00 | 72.00 | 72.00 | 72.00 | 72.00 | 72.00 | 72.00 | 72.00 |
| $\overline{X}\ t_{HX\text{-}2\ outlet}$ in °C | 40.98 | 46.53 | 46.59 | 46.81 | 44.08 | 46.84 | 46.81 | 46.92 | 47.74 |

| $P_{exp\ output}$ in W | 269.54 | 272.27 | 282.89 | 282.89 | 293.82 | 293.82 | 299.52 | 300.46 |
|---|---|---|---|---|---|---|---|---|
| Liquid facation $_{R744}$ | | | | | | | | |
| exp $_{outlet}$ in % | 0.00 | 0.00 | 0.00 | 0.00 | 0.00 | 0.00 | 2.35 | 3.14 |
| $\dot{m}_{air\ loop}$ in $m^3/h$ | 1073.00 | 1073.00 | 1025.40 | 1005.60 | 997.76 | 950.33 | 934.31 | 928.15 |
| $P_{pump\ inlet}$ in bar | 57.00 | 57.00 | 57.00 | 57.00 | 57.00 | 57.00 | 57.00 | 57.00 |
| $P_{pump\ outlet}$ in bar | 88.00 | 90.00 | 92.00 | 94.00 | 96.00 | 98.00 | 98.50 | 99.00 |
| $t_{pump\ inlet}$ in °C | 18.00 | 18.00 | 18.00 | 18.00 | 18.00 | 18.00 | 18.00 | 18.00 |
| $t_{pump\ outlet}$ in °C | 24.61 | 25.02 | 25.43 | 25.83 | 26.23 | 26.63 | 26.73 | 26.83 |
| $P_{exp\ inlet}$ in bar | 88.00 | 90.00 | 92.00 | 94.00 | 96.00 | 98.00 | 98.50 | 99.00 |
| $P_{exp\ outlet}$ in bar | 60.00 | 60.00 | 60.00 | 60.00 | 60.00 | 60.00 | 60.00 | 60.00 |
| $t_{exp\ outlet}$ in °C | 27.99 | 27.68 | 25.30 | 25.30 | 22.65 | 22.65 | 21.73 | 21.73 |
| $t_{exp\ inlet}$ in °C | 54.95 | 55.34 | 55.00 | 55.11 | 55.93 | 55.12 | 54.98 | 55.00 |
| $\overline{X}\ t_{HX\text{-}2\ inlet}$ in °C | 72.00 | 72.00 | 72.00 | 72.00 | 72.00 | 72.00 | 72.00 | 72.00 |
| $\overline{X}\ t_{HX\text{-}2\ outlet}$ in °C | 46.93 | 47.40 | 47.09 | 47.27 | 47.39 | 47.40 | 47.26 | 47.30 |

Figure D.3: Simulation results for the simulation for an UA value of 2 000 $\frac{kW}{K}$, heat source temperature 65 °C and $CO_2$massflow of 3.5 $\frac{kg}{min}$

### D.2.2 Simulation results for the simulation for an UA value of 2 000 $\frac{kW}{K}$, heat source temperature 90 °C and $CO_2$massflow of 3.5 $\frac{kg}{min}$

| $P_{exp\ output}$ in W | 153.29 | 157.99 | 174.79 | 188.47 | 188.47 | 217.01 | 231.21 | 231.21 | 231.21 | 269.70 |
|---|---|---|---|---|---|---|---|---|---|---|
| Liquid facation $_{R744}$ | | | | | | | | | | |
| exp $_{outlet}$ in % | 0.00 | 0.00 | 0.00 | 0.00 | 0.00 | 0.00 | 0.00 | 0.00 | 0.00 | 0.00 |
| $\dot{m}_{air\ loop}$ in $m^3/h$ | 1025.80 | 1046.30 | 503.20 | 497.18 | 485.42 | 482.61 | 473.72 | 469.78 | 447.66 | 441.07 |
| $P_{pump\ inlet}$ in bar | 70.00 | 72.00 | 74.00 | 76.00 | 78.00 | 80.00 | 82.00 | 84.00 | 86.00 | 88.00 |
| $P_{pump\ outlet}$ in bar | 57.00 | 57.00 | 57.00 | 57.00 | 57.00 | 57.00 | 57.00 | 57.00 | 57.00 | 57.00 |
| $t_{pump\ inlet}$ in °C | 70.00 | 72.00 | 74.00 | 76.00 | 78.00 | 80.00 | 82.00 | 84.00 | 86.00 | 88.00 |
| $t_{pump\ outlet}$ in °C | 60.00 | 60.00 | 60.00 | 60.00 | 60.00 | 60.00 | 60.00 | 60.00 | 60.00 | 60.00 |
| $P_{exp\ inlet}$ in bar | 72.41 | 72.41 | 40.78 | 39.33 | 39.33 | 35.99 | 34.12 | 34.12 | 34.12 | 28.07 |
| $P_{exp\ outlet}$ in bar | 18.00 | 18.00 | 18.00 | 18.00 | 18.00 | 18.00 | 18.00 | 18.00 | 18.00 | 18.00 |
| $t_{exp\ outlet}$ in °C | 20.85 | 21.27 | 21.69 | 22.12 | 22.54 | 22.96 | 23.38 | 23.79 | 24.20 | 24.61 |
| $t_{exp\ inlet}$ in °C | 80.41 | 81.15 | 55.00 | 55.18 | 54.87 | 55.38 | 55.37 | 56.54 | 55.09 | 55.03 |
| $\overline{X}\ t_{HX\text{-}2\ inlet}$ in °C | 104.42 | 104.42 | 104.42 | 104.42 | 104.42 | 104.42 | 104.42 | 104.42 | 104.42 | 104.42 |
| $\overline{X}\ t_{HX\text{-}2\ outlet}$ in °C | 67.12 | 68.05 | 42.54 | 42.80 | 42.68 | 43.19 | 43.31 | 43.21 | 42.78 | 43.40 |

| $P_{exp\ output}$ in W | 277.89 | 282.71 | 290.55 | 293.82 | 295.96 | 299.67 | 300.48 |
|---|---|---|---|---|---|---|---|
| Liquid facation $_{R744}$ | | | | | | | |
| exp $_{outlet}$ in % | 0.00 | 0.00 | 0.00 | 0.00 | 0.00 | 2.30 | 3.14 |
| $\dot{m}_{air\ loop}$ in $m^3/h$ | 430.39 | 430.24 | 409.34 | 400.11 | 402.19 | 382.45 | 379.43 |
| $P_{pump\ inlet}$ in bar | 90.00 | 92.00 | 94.00 | 96.00 | 98.00 | 98.50 | 99.00 |
| $P_{pump\ outlet}$ in bar | 57.00 | 57.00 | 57.00 | 57.00 | 57.00 | 57.00 | 57.00 |
| $t_{pump\ inlet}$ in °C | 90.00 | 92.00 | 94.00 | 96.00 | 98.00 | 98.50 | 99.00 |
| $t_{pump\ outlet}$ in °C | 60.00 | 60.00 | 60.00 | 60.00 | 60.00 | 60.00 | 60.00 |
| $P_{exp\ inlet}$ in bar | 26.45 | 25.28 | 23.64 | 22.65 | 22.07 | 21.73 | 21.73 |
| $P_{exp\ outlet}$ in bar | 18.00 | 18.00 | 18.00 | 18.00 | 18.00 | 18.00 | 18.00 |
| $t_{exp\ outlet}$ in °C | 25.02 | 25.43 | 25.83 | 26.23 | 26.63 | 26.73 | 26.83 |
| $t_{exp\ inlet}$ in °C | 55.00 | 55.82 | 55.05 | 55.28 | 56.21 | 55.00 | 55.00 |
| $\overline{X}\ t_{HX\text{-}2\ inlet}$ in °C | 104.42 | 104.42 | 104.42 | 104.42 | 104.42 | 104.42 | 104.42 |
| $\overline{X}\ t_{HX\text{-}2\ outlet}$ in °C | 43.50 | 44.24 | 43.78 | 43.94 | 44.89 | 44.01 | 44.04 |

Figure D.4: Simulation results for the simulation for an UA value of 2 000 $\frac{kW}{K}$, heat source temperature 90 °C and $CO_2$massflow of 3.5 $\frac{kg}{min}$

### D.2.3 Simulation results for the simulation for an UA value of 2 000 $\frac{kW}{K}$, heat source temperature 110 °C and $CO_2$massflow of 3.5 $\frac{kg}{min}$

| $P_{exp\ output}$ in W | 147.99 | 155.11 | 165.17 | 188.47 | 197.00 | 217.01 | 217.01 | 249.81 | 258.05 | 267.68 |
|---|---|---|---|---|---|---|---|---|---|---|
| Liquid facation $_{R744}$ | | | | | | | | | | |
| exp $_{outlet}$ in % | 0.00 | 0.00 | 0.00 | 0.00 | 0.00 | 0.00 | 0.00 | 0.00 | 0.00 | 0.00 |
| $\dot{m}_{air\ loop}$ in $m^3/h$ | 580.61 | 391.36 | 385.32 | 379.32 | 372.08 | 368.20 | 363.81 | 352.07 | 353.58 | 339.05 |
| $P_{pump\ inlet}$ in bar | 57.00 | 57.00 | 57.00 | 57.00 | 57.00 | 57.00 | 57.00 | 57.00 | 57.00 | 57.00 |
| $P_{pump\ outlet}$ in bar | 70.00 | 72.00 | 74.00 | 76.00 | 78.00 | 80.00 | 82.00 | 84.00 | 86.00 | 88.00 |
| $t_{pump\ inlet}$ in °C | 18.00 | 18.00 | 18.00 | 18.00 | 18.00 | 18.00 | 18.00 | 18.00 | 18.00 | 18.00 |
| $t_{pump\ outlet}$ in °C | 20.85 | 21.27 | 21.69 | 22.12 | 22.54 | 22.96 | 23.38 | 23.79 | 24.20 | 24.61 |
| $P_{exp\ inlet}$ in bar | 70.00 | 72.00 | 74.00 | 76.00 | 78.00 | 80.00 | 82.00 | 84.00 | 86.00 | 88.00 |
| $P_{exp\ outlet}$ in bar | 60.00 | 60.00 | 60.00 | 60.00 | 60.00 | 60.00 | 60.00 | 60.00 | 60.00 | 60.00 |
| $t_{exp\ outlet}$ in °C | 72.41 | 42.73 | 41.77 | 39.33 | 38.32 | 35.99 | 35.99 | 31.42 | 30.13 | 28.44 |
| $t_{exp\ inlet}$ in °C | 75.59 | 54.98 | 54.96 | 55.00 | 55.09 | 56.06 | 55.61 | 54.99 | 56.46 | 55.24 |
| $\overline{X}\ t_{HX\text{-}2\ inlet}$ in °C | 122.35 | 122.35 | 122.35 | 122.35 | 122.35 | 122.35 | 122.35 | 122.35 | 122.35 | 122.35 |
| $\overline{X}\ t_{HX\text{-}2\ outlet}$ in °C | 58.32 | 41.50 | 41.62 | 41.78 | 41.67 | 41.54 | 42.61 | 42.32 | 42.89 | 42.77 |

| $P_{exp\ output}$ in W | 277.89 | 283.05 | 290.24 | 290.24 | 295.96 | 299.66 | 300.49 |
|---|---|---|---|---|---|---|---|
| Liquid facation $_{R744}$ | | | | | | | |
| exp $_{outlet}$ in % | 0.00 | 0.00 | 0.00 | 0.00 | 0.00 | 2.30 | 3.14 |
| $\dot{m}_{air\ loop}$ in $m^3/h$ | 329.15 | 320.90 | 312.37 | 308.00 | 296.78 | 292.13 | 289.83 |
| $P_{pump\ inlet}$ in bar | 57.00 | 57.00 | 57.00 | 57.00 | 57.00 | 57.00 | 57.00 |
| $P_{pump\ outlet}$ in bar | 90.00 | 92.00 | 94.00 | 96.00 | 98.00 | 98.50 | 99.00 |
| $t_{pump\ inlet}$ in °C | 18.00 | 18.00 | 18.00 | 18.00 | 18.00 | 18.00 | 18.00 |
| $t_{pump\ outlet}$ in °C | 25.02 | 25.43 | 25.83 | 26.23 | 26.63 | 26.73 | 26.83 |
| $P_{exp\ inlet}$ in bar | 90.00 | 92.00 | 94.00 | 96.00 | 98.00 | 98.50 | 99.00 |
| $P_{exp\ outlet}$ in bar | 60.00 | 60.00 | 60.00 | 60.00 | 60.00 | 60.00 | 60.00 |
| $t_{exp\ outlet}$ in °C | 26.45 | 25.33 | 23.60 | 23.60 | 22.07 | 21.73 | 21.73 |
| $t_{exp\ inlet}$ in °C | 55.00 | 55.07 | 55.00 | 55.62 | 55.31 | 55.00 | 55.00 |
| $\overline{X}\ t_{HX\text{-}2\ inlet}$ in °C | 122.35 | 122.35 | 122.35 | 122.35 | 122.35 | 122.35 | 122.35 |
| $\overline{X}\ t_{HX\text{-}2\ outlet}$ in °C | 42.74 | 42.78 | 43.01 | 43.27 | 43.34 | 43.32 | 43.35 |

Figure D.5: Simulation results for the simulation for an UA value of 2 000 $\frac{kW}{K}$, heat source temperature 110 °C and $CO_2$massflow of 3.5 $\frac{kg}{min}$

### D.2.4 Simulation results for the simulation for an UA value of 4 000 $\frac{kW}{K}$, heat source temperature 65 °C and $CO_2$massflow of 3.5 $\frac{kg}{min}$

| $P_{exp\ output}$ in W | 121.93 | 139.33 | 174.77 | 184.01 | 205.35 | 224.45 | 231.25 | 240.99 | 240.99 |
|---|---|---|---|---|---|---|---|---|---|
| Liquid facation $_{R744}$ | | | | | | | | | |
| exp $_{outlet}$ in % | 0.00 | 0.00 | 0.00 | 0.00 | 0.00 | 0.00 | 0.00 | 0.00 | 0.00 |
| $\dot{m}_{air\ loop}$ in $m^3/h$ | 1470.30 | 1258.30 | 1225.50 | 1212.60 | 1215.80 | 1169.20 | 1144.90 | 1162.40 | 1086.30 |
| $P_{pump\ inlet}$ in bar | 57.00 | 57.00 | 57.00 | 57.00 | 57.00 | 57.00 | 57.00 | 57.00 | 57.00 |
| $P_{pump\ outlet}$ in bar | 70.00 | 72.00 | 74.00 | 76.00 | 78.00 | 80.00 | 82.00 | 84.00 | 86.00 |
| $t_{pump\ inlet}$ in °C | 18.00 | 18.00 | 18.00 | 18.00 | 18.00 | 18.00 | 18.00 | 18.00 | 18.00 |
| $t_{pump\ outlet}$ in °C | 20.85 | 21.27 | 21.69 | 22.12 | 22.54 | 22.96 | 23.38 | 23.79 | 24.20 |
| $P_{exp\ inlet}$ in bar | 70.00 | 72.00 | 74.00 | 76.00 | 78.00 | 80.00 | 82.00 | 84.00 | 86.00 |
| $P_{exp\ outlet}$ in bar | 60.00 | 60.00 | 60.00 | 60.00 | 60.00 | 60.00 | 60.00 | 60.00 | 60.00 |
| $t_{exp\ outlet}$ in °C | 24.00 | 44.25 | 40.77 | 39.81 | 37.41 | 35.11 | 34.13 | 32.77 | 32.77 |
| $t_{exp\ inlet}$ in °C | 57.79 | 55.44 | 54.99 | 55.19 | 55.49 | 55.04 | 55.09 | 55.69 | 54.83 |
| $\overline{X}\ t_{HX\text{-}2\ inlet}$ in °C | 72.00 | 72.00 | 72.00 | 72.00 | 72.00 | 72.00 | 72.00 | 72.00 | 72.00 |
| $\overline{X}\ t_{HX\text{-}2\ outlet}$ in °C | 49.58 | 46.71 | 46.57 | 46.71 | 47.17 | 46.80 | 46.78 | 47.50 | 46.67 |

| $P_{exp\ output}$ in W | 262.92 | 275.87 | 284.59 | 284.59 | 293.57 | 293.57 | 299.49 | 299.49 |
|---|---|---|---|---|---|---|---|---|
| Liquid facation $_{R744}$ | | | | | | | | |
| exp $_{outlet}$ in % | 0.00 | 0.00 | 0.00 | 0.00 | 0.00 | 0.00 | 2.36 | 2.36 |
| $\dot{m}_{air\ loop}$ in $m^3/h$ | 1115.00 | 1077.90 | 1025.40 | 978.84 | 975.88 | 995.40 | 934.04 | 934.04 |
| $P_{pump\ inlet}$ in bar | 57.00 | 57.00 | 57.00 | 57.00 | 57.00 | 57.00 | 57.00 | 57.00 |
| $P_{pump\ outlet}$ in bar | 88.00 | 90.00 | 92.00 | 94.00 | 96.00 | 98.00 | 98.50 | 99.00 |
| $t_{pump\ inlet}$ in °C | 18.00 | 18.00 | 18.00 | 18.00 | 18.00 | 18.00 | 18.00 | 18.00 |
| $t_{pump\ outlet}$ in °C | 24.61 | 25.02 | 25.43 | 25.83 | 26.23 | 26.63 | 26.73 | 26.83 |
| $P_{exp\ inlet}$ in bar | 88.00 | 90.00 | 92.00 | 94.00 | 96.00 | 98.00 | 98.50 | 99.00 |
| $P_{exp\ outlet}$ in bar | 60.00 | 60.00 | 60.00 | 60.00 | 60.00 | 60.00 | 60.00 | 60.00 |
| $t_{exp\ outlet}$ in °C | 29.26 | 26.83 | 24.96 | 24.96 | 22.62 | 22.62 | 21.73 | 21.73 |
| $t_{exp\ inlet}$ in °C | 55.61 | 55.42 | 55.00 | 55.72 | 55.58 | 55.93 | 54.98 | 55.12 |
| $\overline{X}\ t_{HX\text{-}2\ inlet}$ in °C | 72.00 | 72.00 | 72.00 | 72.00 | 72.00 | 72.00 | 72.00 | 72.00 |
| $\overline{X}\ t_{HX\text{-}2\ outlet}$ in °C | 47.63 | 47.49 | 47.09 | 46.29 | 47.02 | 48.07 | 47.26 | 47.38 |

Figure D.6: Simulation results for the simulation for an UA value of 4 000 $\frac{kW}{K}$, heat source temperature 65 °C and $CO_2$massflow of 3.5 $\frac{kg}{min}$

### D.2.5 Simulation results for the simulation for an UA value of 4 000 $\frac{kW}{K}$, heat source temperature 90 °C and $CO_2$massflow of 3.5 $\frac{kg}{min}$

| $P_{exp\ output}$ in W | 133.84 | 155.15 | 174.80 | 192.84 | 209.34 | 224.32 | 237.84 | 249.92 | 260.60 | 269.92 |
|---|---|---|---|---|---|---|---|---|---|---|
| Liquid facation $_{R744}$ | | | | | | | | | | |
| exp $_{outlet}$ in % | 0.00 | 0.00 | 0.00 | 0.00 | 0.00 | 0.00 | 0.00 | 0.00 | 0.00 | 0.00 |
| $\dot{m}_{air\ loop}$ in $m^3/h$ | 445.63 | 440.95 | 435.63 | 429.90 | 423.67 | 416.86 | 409.51 | 401.58 | 393.08 | 383.98 |
| $P_{pump\ inlet}$ in bar | 57.00 | 57.00 | 57.00 | 57.00 | 57.00 | 57.00 | 57.00 | 57.00 | 57.00 | 57.00 |
| $P_{pump\ outlet}$ in bar | 70.00 | 72.00 | 74.00 | 76.00 | 78.00 | 80.00 | 82.00 | 84.00 | 86.00 | 88.00 |
| $t_{pump\ inlet}$ in °C | 18.00 | 18.00 | 18.00 | 18.00 | 18.00 | 18.00 | 18.00 | 18.00 | 18.00 | 18.00 |
| $t_{pump\ outlet}$ in °C | 20.85 | 21.27 | 21.69 | 22.12 | 22.54 | 22.96 | 23.38 | 23.79 | 24.20 | 24.61 |
| $P_{exp\ inlet}$ in bar | 70.00 | 72.00 | 74.00 | 76.00 | 78.00 | 80.00 | 82.00 | 84.00 | 86.00 | 88.00 |
| $P_{exp\ outlet}$ in bar | 60.00 | 60.00 | 60.00 | 60.00 | 60.00 | 60.00 | 60.00 | 60.00 | 60.00 | 60.00 |
| $t_{exp\ outlet}$ in °C | 44.74 | 42.76 | 40.79 | 38.85 | 36.94 | 35.06 | 33.22 | 31.43 | 29.70 | 28.04 |
| $t_{exp\ inlet}$ in °C | 55.00 | 55.00 | 55.00 | 55.00 | 55.00 | 55.00 | 55.00 | 55.00 | 55.00 | 55.00 |
| $\overline{X}\ t_{HX\text{-}2\ inlet}$ in °C | 104.42 | 104.42 | 104.42 | 104.42 | 104.42 | 104.42 | 104.42 | 104.42 | 104.42 | 104.42 |
| $\overline{X}\ t_{HX\text{-}2\ outlet}$ in °C | 32.15 | 32.58 | 32.92 | 33.27 | 33.57 | 33.82 | 34.03 | 34.18 | 34.29 | 34.35 |

| $P_{exp\ output}$ in W | 277.91 | 284.62 | 290.23 | 294.94 | 296.97 | 297.92 | 298.82 | 299.68 | 300.49 |
|---|---|---|---|---|---|---|---|---|---|
| Liquid facation $_{R744}$ | | | | | | | | | |
| exp $_{outlet}$ in % | 0.00 | 0.00 | 0.00 | 0.00 | 0.00 | 0.64 | 1.47 | 2.30 | 3.13 |
| $\dot{m}_{air\ loop}$ in $m^3/h$ | 374.31 | 364.09 | 353.36 | 342.18 | 336.43 | 333.53 | 330.60 | 327.67 | 324.71 |
| $P_{pump\ inlet}$ in bar | 57.00 | 57.00 | 57.00 | 57.00 | 57.00 | 57.00 | 57.00 | 57.00 | 57.00 |
| $P_{pump\ outlet}$ in bar | 90.00 | 92.00 | 94.00 | 96.00 | 97.00 | 97.50 | 98.00 | 98.50 | 99.00 |
| $t_{pump\ inlet}$ in °C | 18.00 | 18.00 | 18.00 | 18.00 | 18.00 | 18.00 | 18.00 | 18.00 | 18.00 |
| $t_{pump\ outlet}$ in °C | 25.02 | 25.43 | 25.83 | 26.23 | 26.43 | 26.53 | 26.63 | 26.73 | 26.83 |
| $P_{exp\ inlet}$ in bar | 90.00 | 92.00 | 94.00 | 96.00 | 97.00 | 97.50 | 98.00 | 98.50 | 99.00 |
| $P_{exp\ outlet}$ in bar | 60.00 | 60.00 | 60.00 | 60.00 | 60.00 | 60.00 | 60.00 | 60.00 | 60.00 |
| $t_{exp\ outlet}$ in °C | 26.45 | 24.97 | 23.59 | 22.36 | 21.79 | 21.73 | 21.73 | 21.73 | 21.73 |
| $t_{exp\ inlet}$ in °C | 55.00 | 55.00 | 55.00 | 55.00 | 55.00 | 55.00 | 55.00 | 55.00 | 55.00 |
| $\overline{X}\ t_{HX\text{-}2\ inlet}$ in °C | 104.42 | 104.42 | 104.42 | 104.42 | 104.42 | 104.42 | 104.42 | 104.42 | 104.42 |
| $\overline{X}\ t_{HX\text{-}2\ outlet}$ in °C | 34.35 | 34.31 | 34.22 | 34.10 | 34.02 | 33.98 | 33.93 | 33.89 | 33.84 |

Figure D.7: Simulation results for the simulation for an UA value of 4 000 $\frac{kW}{K}$, heat source temperature 90 °C and $CO_2$massflow of 3.5 $\frac{kg}{min}$

### D.2.6 Simulation results for the simulation for an UA value of 4 000 $\frac{kW}{K}$, heat source temperature 110 °C and $CO_2$massflow of 3.5 $\frac{kg}{min}$

| $P_{exp\ output}$ in W | 133.85 | 155.15 | 174.80 | 192.85 | 209.34 | 224.33 | 237.85 | 249.93 | 260.61 | 269.93 |
|---|---|---|---|---|---|---|---|---|---|---|
| Liquid facation $_{R744}$ | | | | | | | | | | |
| exp $_{outlet}$ in % | 0.00 | 0.00 | 0.00 | 0.00 | 0.00 | 0.00 | 0.00 | 0.00 | 0.00 | 0.00 |
| $\dot{m}_{air\ loop}$ in $m^3/h$ | 340.83 | 336.58 | 332.03 | 327.19 | 322.07 | 316.63 | 310.88 | 304.81 | 298.41 | 291.68 |
| $P_{pump\ inlet}$ in bar | 57.00 | 57.00 | 57.00 | 57.00 | 57.00 | 57.00 | 57.00 | 57.00 | 57.00 | 57.00 |
| $P_{pump\ outlet}$ in bar | 70.00 | 72.00 | 74.00 | 76.00 | 78.00 | 80.00 | 82.00 | 84.00 | 86.00 | 88.00 |
| $t_{pump\ inlet}$ in °C | 18.00 | 18.00 | 18.00 | 18.00 | 18.00 | 18.00 | 18.00 | 18.00 | 18.00 | 18.00 |
| $t_{pump\ outlet}$ in °C | 20.85 | 21.27 | 21.69 | 22.12 | 22.54 | 22.96 | 23.38 | 23.79 | 24.20 | 24.61 |
| $P_{exp\ inlet}$ in bar | 70.00 | 72.00 | 74.00 | 76.00 | 78.00 | 80.00 | 82.00 | 84.00 | 86.00 | 88.00 |
| $P_{exp\ outlet}$ in bar | 60.00 | 60.00 | 60.00 | 60.00 | 60.00 | 60.00 | 60.00 | 60.00 | 60.00 | 60.00 |
| $t_{exp\ outlet}$ in °C | 44.75 | 42.76 | 40.79 | 38.85 | 36.94 | 35.06 | 33.23 | 31.44 | 29.70 | 28.04 |
| $t_{exp\ inlet}$ in °C | 55.00 | 55.00 | 55.00 | 55.00 | 55.00 | 55.00 | 55.00 | 55.00 | 55.00 | 55.00 |
| $\overline{X}\ t_{HX\text{-}2\ inlet}$ in °C | 122.35 | 122.35 | 122.35 | 122.35 | 122.35 | 122.35 | 122.35 | 122.35 | 122.35 | 122.35 |
| $\overline{X}\ t_{HX\text{-}2\ outlet}$ in °C | 27.91 | 28.28 | 28.60 | 28.91 | 29.20 | 29.45 | 29.67 | 29.86 | 30.02 | 30.15 |

| $P_{exp\ output}$ in W | 277.93 | 284.63 | 290.25 | 294.95 | 296.99 | 297.94 | 298.84 | 299.70 | 300.51 |
|---|---|---|---|---|---|---|---|---|---|
| Liquid facation $_{R744}$ | | | | | | | | | |
| exp $_{outlet}$ in % | 0.00 | 0.00 | 0.00 | 0.00 | 0.00 | 0.63 | 1.46 | 2.29 | 3.13 |
| $\dot{m}_{air\ loop}$ in $m^3/h$ | 284.62 | 277.23 | 269.54 | 261.57 | 257.49 | 255.43 | 253.36 | 251.27 | 249.18 |
| $P_{pump\ inlet}$ in bar | 57.00 | 57.00 | 57.00 | 57.00 | 57.00 | 57.00 | 57.00 | 57.00 | 57.00 |
| $P_{pump\ outlet}$ in bar | 90.00 | 92.00 | 94.00 | 96.00 | 97.00 | 97.50 | 98.00 | 98.50 | 99.00 |
| $t_{pump\ inlet}$ in °C | 18.00 | 18.00 | 18.00 | 18.00 | 18.00 | 18.00 | 18.00 | 18.00 | 18.00 |
| $t_{pump\ outlet}$ in °C | 25.02 | 25.43 | 25.83 | 26.23 | 26.43 | 26.53 | 26.63 | 26.73 | 26.83 |
| $P_{exp\ inlet}$ in bar | 90.00 | 92.00 | 94.00 | 96.00 | 97.00 | 97.50 | 98.00 | 98.50 | 99.00 |
| $P_{exp\ outlet}$ in bar | 60.00 | 60.00 | 60.00 | 60.00 | 60.00 | 60.00 | 60.00 | 60.00 | 60.00 |
| $t_{exp\ outlet}$ in °C | 26.46 | 24.97 | 23.60 | 22.36 | 21.79 | 21.73 | 21.73 | 21.73 | 21.73 |
| $t_{exp\ inlet}$ in °C | 55.01 | 55.01 | 55.01 | 55.01 | 55.01 | 55.01 | 55.01 | 55.01 | 55.01 |
| $\overline{X}\ t_{HX\text{-}2\ inlet}$ in °C | 122.35 | 122.35 | 122.35 | 122.35 | 122.35 | 122.35 | 122.35 | 122.35 | 122.35 |
| $\overline{X}\ t_{HX\text{-}2\ outlet}$ in °C | 30.25 | 30.32 | 30.37 | 30.40 | 30.41 | 30.42 | 30.42 | 30.42 | 30.43 |

Figure D.8: Simulation results for the simulation for an UA value of 4 000 $\frac{kW}{K}$, heat source temperature 110 °C and $CO_2$massflow of 3.5 $\frac{kg}{min}$

## D.3 Simulation results of the heat transfer coefficient times area of HX-2 for the increased air-volume flow

### D.3.1 Zone analysis results for the simulation for an UA value of 2 000 $\frac{kW}{K}$, a heat source temperature 65 °C and a $CO_2$massflow of 3.5 $\frac{kg}{min}$

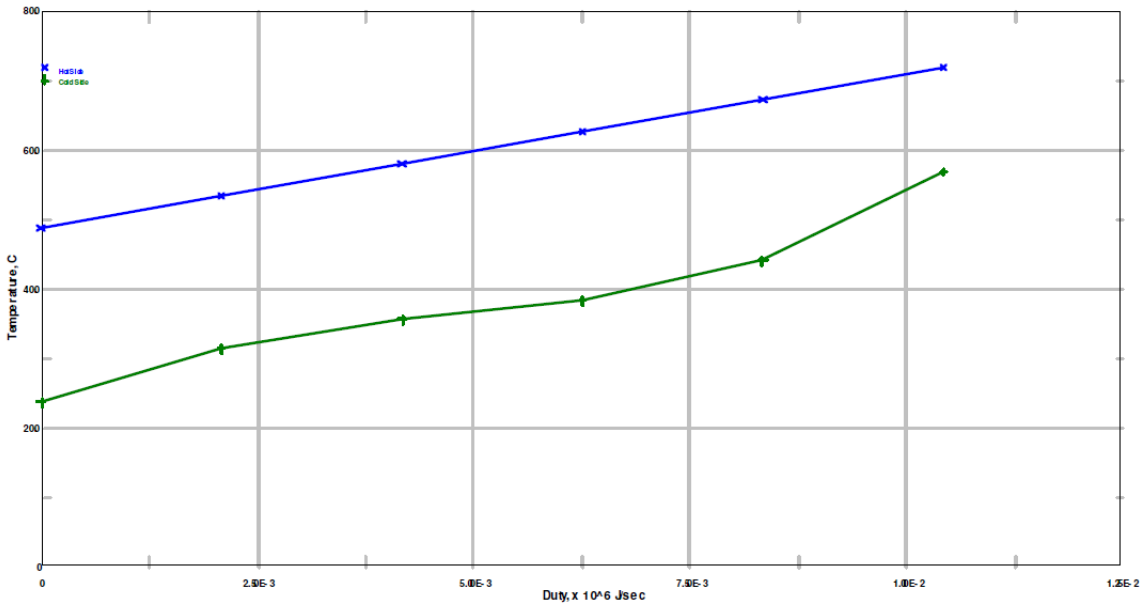


| | t hot inlet | t hot outlet | t cold inlet | t cold outlet | UA -value |
|---|---|---|---|---|---|
| Zones | in °C | in °C | in °C | in °C | in kW/K |
| 1 | 53.63 | 79.04 | 23.79 | 31.46 | 332.75 |
| 2 | 58.23 | 53.63 | 31.46 | 35.73 | 352.77 |
| 3 | 62.82 | 58.23 | 35.73 | 38.40 | 336.11 |
| 4 | 67.41 | 62.82 | 38.40 | 44.15 | 330.58 |
| 5 | 72.00 | 67.41 | 44.15 | 56.97 | 418.07 |
| Total | | | | | 1770.28 |

**Simulation set-point:**

**UA at 2 000 kW/K**
**$CO_2$ massflow 3.5 kg/min**
**Volume flow air loop 1 260 $m^3/h$**
**Heat source temperatue 65 °C**

Figure D.9: Results and Pro/II plot from the zone analysis model of the increased air-volume flow

### D.3.2 Zone analysis results for the simulation for an UA value of 2 000 $\frac{kW}{K}$, a heat source temperature 90 °C and a $CO_2$massflow of 3.5 $\frac{kg}{min}$

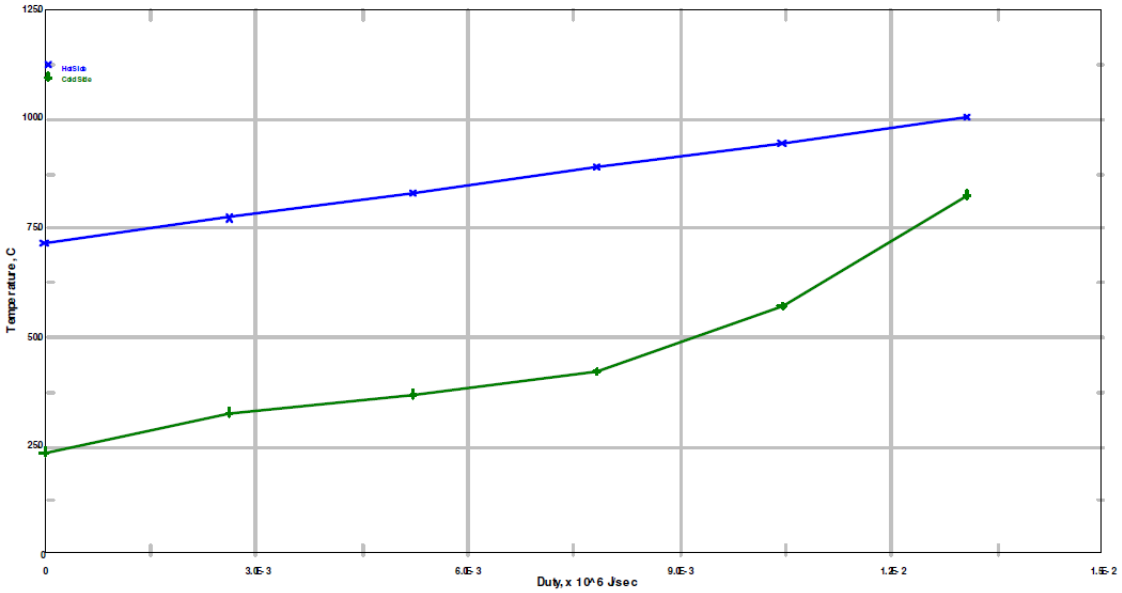


| | $t_{hot\ inlet}$ | $t_{hot\ outlet}$ | $t_{cold\ inlet}$ | $t_{cold\ outlet}$ | UA -value |
|---|---|---|---|---|---|
| Zones | in °C | in °C | in °C | in °C | in kW/K |
| 1 | 77.46 | 77.71 | 23.79 | 32.83 | 564.65 |
| 2 | 83.20 | 77.46 | 32.83 | 37.04 | 575.40 |
| 3 | 88.94 | 83.20 | 37.04 | 42.19 | 562.15 |
| 4 | 94.68 | 88.94 | 42.19 | 57.13 | 622.01 |
| 5 | 100.42 | 94.68 | 57.13 | 82.76 | 990.37 |
| Total | | | | | 3314.58 |

**Simulation set-point:**

**UA at 2 000 kW/K**
**$CO_2$ massflow 3.5 kg/min**
**Volume flow air loop 1 260 $m^3/h$**
**Heat source temperatue 90 °C**

Figure D.10: Results and Pro/II plot from the zone analysis model of the increased air-volume flow

### D.3.3 Zone analysis results for the simulation for an UA value of 2 000 $\frac{kW}{K}$, a heat source temperature 110 °C and a $CO_2$massflow of 3.5 $\frac{kg}{min}$

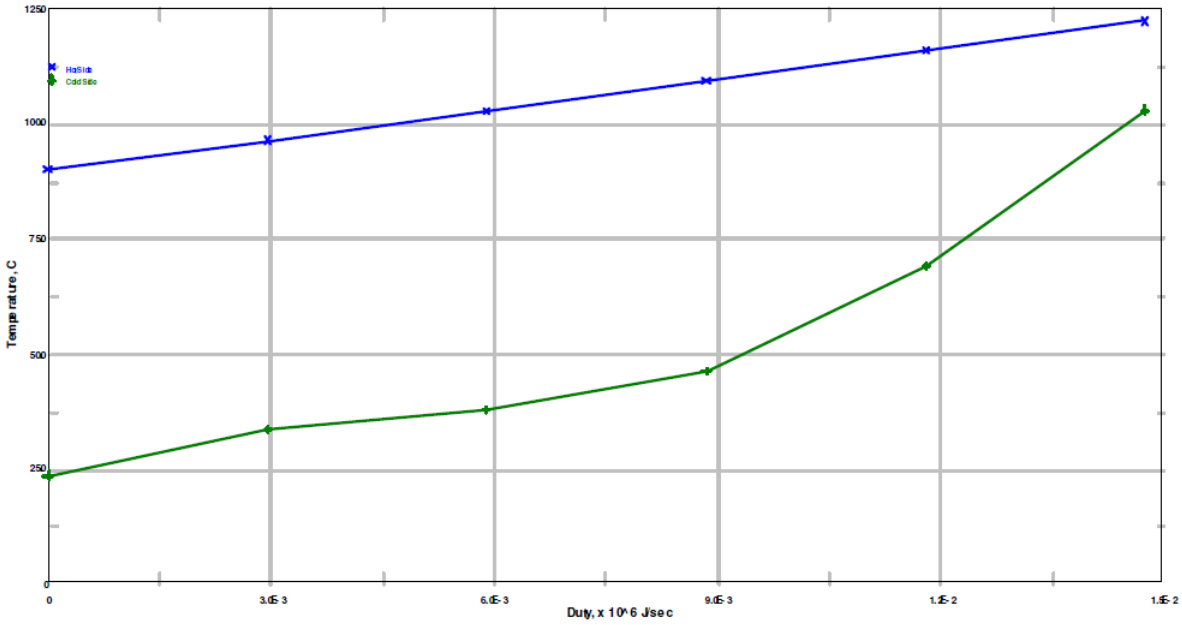


| | $t_{hot\ inlet}$ | $t_{hot\ outlet}$ | $t_{cold\ inlet}$ | $t_{cold\ outlet}$ | UA -value |
|---|---|---|---|---|---|
| Zones | in °C | in °C | in °C | in °C | in kW/K |
| 1 | 96.64 | 90.15 | 23.79 | 33.60 | 235.96 |
| 2 | 103.12 | 96.64 | 33.60 | 37.88 | 238.01 |
| 3 | 109.59 | 103.12 | 37.88 | 46.57 | 238.02 |
| 4 | 116.06 | 109.59 | 46.57 | 69.32 | 280.16 |
| 5 | 122.53 | 116.06 | 69.32 | 103.17 | 491.27 |
| Total | | | | | 1483.42 |

**Simulation set-point:**

**UA at 2 000 kW/K**
**$CO_2$ massflow 3.5 kg/min**
**Volume flow air loop 1 260 $m^3/h$**
**Heat source temperatue 110 °C**

Figure D.11: Results and Pro/II plot from the zone analysis model of the increased air-volume flow

### D.3.4 Zone analysis results for the simulation for an UA value of 4 000 $\frac{kW}{K}$, a heat source temperature 65 °C and a $CO_2$massflow of 3.5 $\frac{kg}{min}$

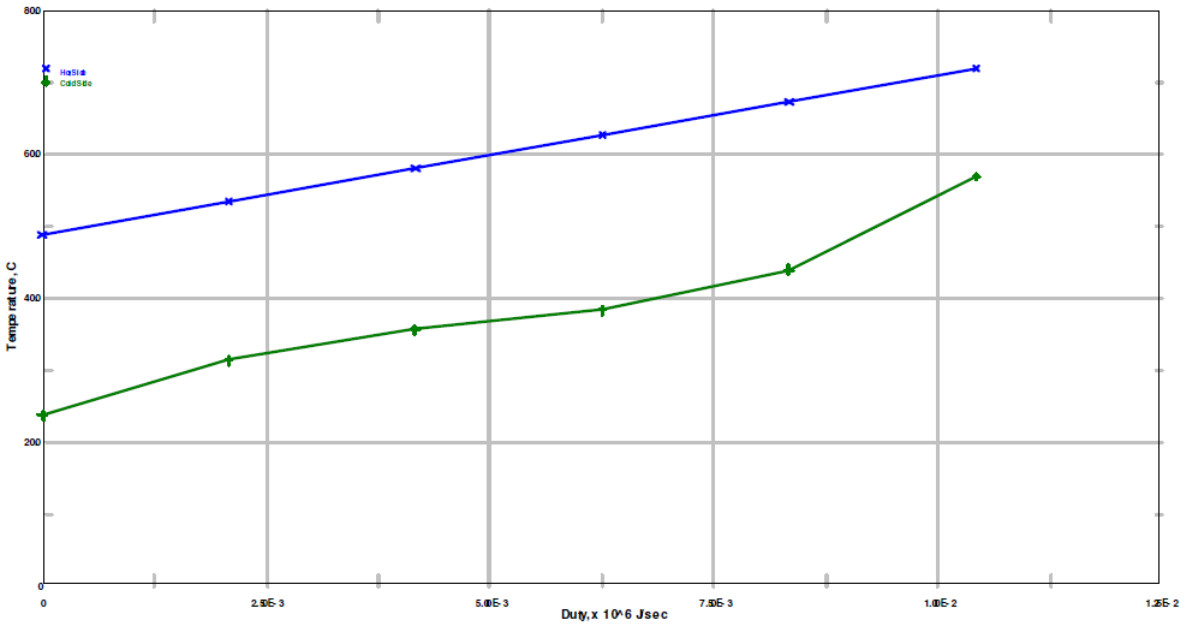


| | $t_{hot\ inlet}$ | $t_{hot\ outlet}$ | $t_{cold\ inlet}$ | $t_{cold\ outlet}$ | *UA -value* |
|---|---|---|---|---|---|
| Zones | in °C | in °C | in °C | in °C | in kW/K |
| 1 | 53.64 | 49.05 | 23.79 | 31.45 | 666.01 |
| 2 | 58.23 | 53.64 | 31.45 | 35.73 | 706.08 |
| 3 | 62.82 | 58.23 | 35.73 | 38.40 | 672.78 |
| 4 | 67.41 | 62.82 | 38.40 | 44.13 | 661.60 |
| 5 | 72.00 | 67.41 | 44.13 | 56.94 | 836.00 |
| Total | | | | | 3542.47 |

**Simulation set-point:**

**UA at 4 000 kW/K**
**$CO_2$ massflow 3.5 kg/min**
**Volume flow air loop 1 260 $m^3/h$**
**Heat source temperatue 65 °C**

Figure D.12: Results and Pro/II plot from the zone analysis model of the increased air-volume flow

### D.3.5 Zone analysis results for the simulation for an UA value of 4 000 $\frac{kW}{K}$, a heat source temperature 90 °C and a $CO_2$massflow of 3.5 $\frac{kg}{min}$

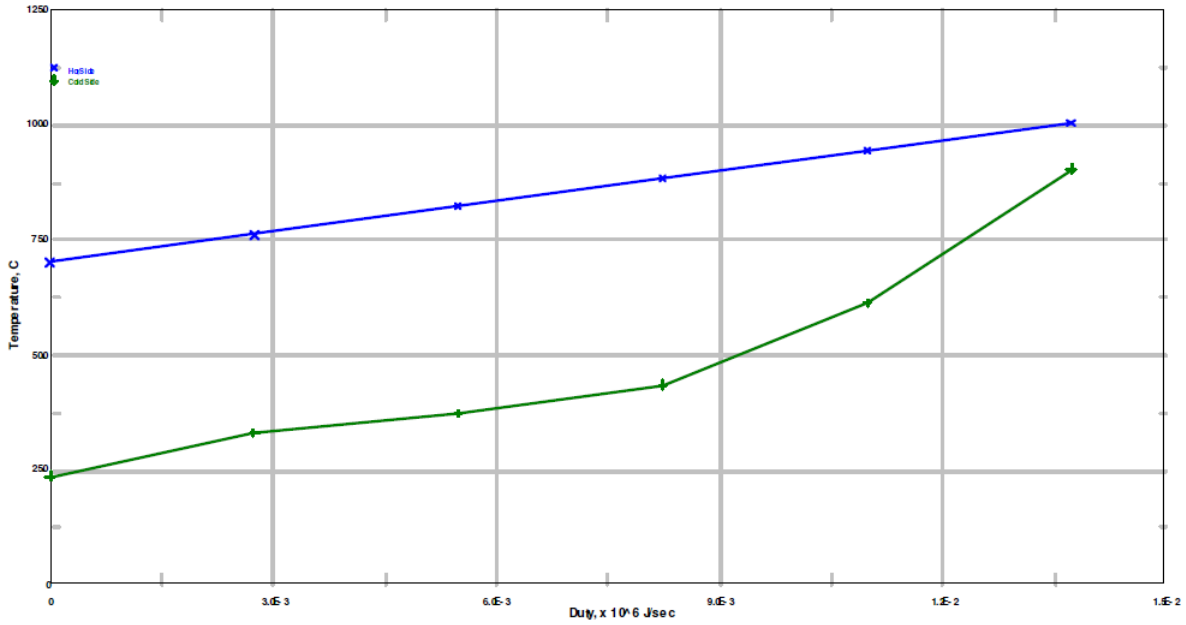


| | t hot inlet | t hot outlet | t cold inlet | t cold outlet | UA -value |
|---|---|---|---|---|---|
| Zones | in °C | in °C | in °C | in °C | in kW/K |
| 1 | 77.28 | 70.24 | 23.79 | 33.15 | 613.06 |
| 2 | 82.32 | 76.28 | 33.15 | 37.36 | 623.22 |
| 3 | 88.36 | 82.32 | 37.36 | 43.70 | 612.56 |
| 4 | 94.39 | 88.36 | 43.70 | 61.61 | 714.59 |
| 5 | 100.42 | 94.39 | 61.61 | 90.52 | 1436.47 |
| Total | | | | | 3999.90 |

**Simulation set-point:**

**UA at 4 000 kW/K**
**$CO_2$ massflow 3.5 kg/min**
**Volume flow air loop 1 260 $m^3/h$**
**Heat source temperatue 90 °C**

Figure D.13: Results and Pro/II plot from the zone analysis model of the increased air-volume flow

### D.3.6 Zone analysis results for the simulation for an UA value of 4 000 $\frac{kW}{K}$, a heat source temperature 110 °C and a $CO_2$massflow of 3.5 $\frac{kg}{min}$

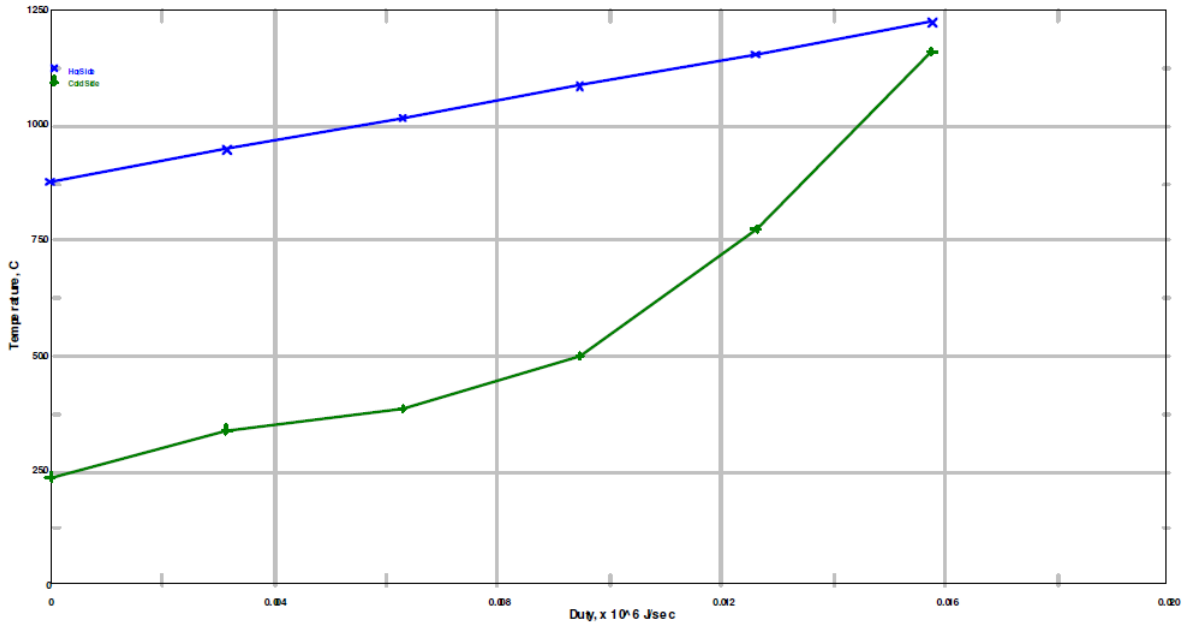


| | $t$ hot inlet | $t$ hot outlet | $t$ cold inlet | $t$ cold outlet | UA -value |
|---|---|---|---|---|---|
| Zones | in °C | in °C | in °C | in °C | in kW/K |
| 1 | 94.85 | 87.92 | 23.79 | 34.03 | 504.81 |
| 2 | 101.78 | 94.85 | 34.03 | 38.48 | 508.14 |
| 3 | 108.70 | 101.78 | 38.48 | 50.07 | 517.48 |
| 4 | 115.62 | 108.70 | 50.07 | 77.80 | 664.32 |
| 5 | 122.53 | 115.62 | 77.80 | 116.35 | 1805.24 |
| Total | | | | | 3999.99 |

**Simulation set-point:**

**UA at 4 000 kW/K**
**$CO_2$ massflow 3.5 kg/min**
**Volume flow air loop 1 260 $m^3/h$**
**Heat source temperatue 110 °C**

Figure D.14: Results and Pro/II plot from the zone analysis model of the increased air-volume flow

# Bibliography


[1] Dr. Kammer C.: Aluminium-Taschenbuch. Aluminium-Verlag GmbH. Düsseldorf Germany. (1995) 18 - 24

[2] Polmear I.: Light Alloys - Metallurgy of the Light Metals 2nd edition, Edward Arnold the educational academic and medical publishing division of Hodder and Stroughton Limited. London England. (1989) 10

[3] Turns S.: Thermal-Fluid sciences. Cambridge University Press. New York USA. (2006); 532, 952

[4] Mills D.: Advances in solar thermal electricity technology. In: Solar Energy 76 (2004), Nr. 1-3, S. 19–31. http://dx.doi.org/doi:10.1016/S0038-092X(03) 00102-6. – DOI doi:10.1016/S0038–092X(03)00102–6

[5] Kongtragool B., Wongwises S.: A review of solar-powered Stirling engines and low temperature differential Stirling engines. In: Renewable and Sustainable Energy Reviews 7 (2003), Nr. 2, S. 131–154. http://dx.doi.org/doi:10.1016/ S1364-0321(02)00053-9. – DOI doi:10.1016/S1364–0321(02)00053–9

[6] Larjola J.: Electricity from industrial waste heat using high-speed organic Rankine cycle (ORC). In: International Journal of Production Economics 41 (1995), Nr. 1- 3, S. 227–335. http://dx.doi.org/doi:10.1016/0925-5273(94)00098-0. – DOI doi:10.1016/0925–5273(94)00098–0

[7] DiPippo R.: Geothermal power plants. Elsevier Ltd. .Oxford Great Britain. (2005); 182 - 184

[8] DiPippo R.: Second Law assessment of binary plants generating power from low-temperature geothermal fluids. In: Geothermics 33 (2004), Nr. 5, S. 565– 586. http://dx.doi.org/doi:10.1016/j.geothermics.2003.10.003. – DOI doi:10.1016/j.geothermics.2003.10.003

[9] Maier W.: VDI-Berichte 377 Capturing energy from waste heat. The use of industial waste heat by means of the Organic Rankine Cycle (ORC). VDI-Verlag GmbH. Düsseldorf Germany. (1980); 17

[10] Boles M. and Cengel Y.: Thermodynamics - An engineering approach 5th edition, McGraw-Hill Companies Inc.. New York USA. (2006); 504

[11] Chen K., Elliot T., Swanekamp R.: Standard handbook of powerplat engineering 2nd edition, McGraw-Hill Companies Inc.. New York USA. (1997); 2.8 - 2.9

[12] Hsieh J.:Engineering thermodynamics, Prentice Hall. New Jersey USA. (1993) 172 - 176, 425

[13] Shavit A., Gutfinger C.: Thermodynamics from concepts to applications 2nd edition, CRC Press. Boca Rayton USA. (2009); 281

[14] Sonntag R., Borgnakke C.: Introduction to engineering thermodynamics 2nd edition, John Wiley & Sons, Inc.. New York USA. (2007); 349-350

[15] Moisseytsev A., Sienicki J.: Investigation of alternative layouts for the supercritical carbon dioxide Brayton cycle for a sodium-cooled fast reactor. In: Nuclear Engineering ans design (2009) 1362 - 1371

[16] Xue L., Wei W., Zhongyue H.: Investigations of Cycle Combined Brayton and Ambient Preesure Gas Turbines. In: International Conference on Power Engineering (2007) 69 - 72

[17] Bitterlich W., Kestner D.: VDI-Berichte 539 ORC - HP - Technology working fluid problems. A contribution to the optimum design of an ORC-plant. VDI-Verlag GmbH. Düsseldorf Germany. (1984); 357 - 358

[18] Ladam Y., Skaugen G.: $CO_2$ as working fluid in a Rankine cycle for electricity production from waste heat sources on fishing boats. Summary report TR A6570. Sintef Energy. (October 2007) 6 - 7

[19] OBRIST Engineering GmbH, Manual compressor unit CU-01-01. 4 - 6

[20] Lorenz Messtechnik GmbH, Technical Manual Two-Channel digital Display Type DD-2002; 1

[21] Chen D.:Untersuchungen zur Optimierung eines solaren Niedertemperatur-Stirlingmotors. Dissertation Fakultät Maschinenwesen der Technischen Universität Dresden Germany. (2004); 4 - 5, 61

[22] Steinborn F.: Stirling-Motor - Stand und Perspektiven - Kongress des Bundesverband Kraft-Wärme-Kopplung 12th and 13th November 2003 in Berlin Germany. http://www.bhkw-info.de/Stirling/Stirling.pdf

[23] Gu W., Weng Y., Cao G.: Testing and Thermodynamic Analysis of Low-Grade Heat Power Generation System Using Organic Rankine Cycle. In: Challenges of Power Engineering and Environment. Zhejiang China University Press. Hangzhou China, and Springer-Verlag GmbH. Berlin and Heidelberg Germany. (2007) 93 -97. *http://www.springerlink.com/content/n688k41024r62421/fulltext.pdf*

[24] Rolle K.: Thermodynamics and Heat Power 6th edition. Pearson Education. Inc. New York USA. (2005) 607

[25] Gross C.: Electric Machines. CRC Press Taylor & Francis Group. Boca Raton USA. (2007) 339

[26] Haynes H., Sead H.: Volkswagen Beetle 1200 Owners Workshop Manual. Haynes Publishing Inc.. Newbury Park USA (1974) 143